Field perturbations in general relativity and infinite derivative gravity

Harmsen, Gerhard Erwin

DOI:
10.33612/diss.99355803

university of groningen

UNIVERSITY OF THE WITWATERSRAND, JOHANNESBURG

Field perturbations in general relativity and infinite derivative gravity

PhD thesis

to obtain the degree of PhD at the
University of Groningen
on the authority of the
Rector Magnificus Prof. T. N. Wijmenga
and in accordance with
the decision by the College of Deans.

and

to obtain the degree of PhD of the
University of the Witwatersrand
on the authority of the
Chancellor Dr. J. Dlamini
and in accordance with
the decision by faculty of science

Double PhD degree

This thesis will be defended in public on

Friday 25 October 2019 at 11:00 hours

by

Gerhard Erwin Harmsen

born on 21 August 1992
in Randburg, South Africa

Supervisors
Prof. A. S. Cornell
Prof. A. Mazumdar

Assessment Committee
Prof. B. Mellado
Prof. D. Roest
Prof. V. P. Frovol
Prof. C. Kiefer

Field perturbations in general relativity and infinite derivative gravity

Gerhard Harmsen

Abstract

In the first part of this thesis we will determine the Quasi Normal Modes (QNMs) associated to spin-3/2 fields near higher dimensional Reissner-Nodström black holes, and Schwarzschild black holes which are in higher dimensional (Anti-) de Sitter space times. In order to do this we will present the idea of QNMs, and then show how effective potentials can be obtained for the spin-3/2 fields near the black holes. Where the effective potentials will give us an indication of the fields behaviour near the black hole. We then show that using the effective potential we obtain the numerical values of the QNMs by using numerical approximations. This approach will be used for each of the space times that we are interested in. We then determine what the effects of the electrical charge and asymptotic curvature are on the emitted QNMs. In the case of the electrically charge black hole we also investigate the absorption probabilities of the QNMs.
In the second part of this thesis we investigate how the theory of Infinite Derivative Gravity (IDG) can be used to obtain linear metrics, which are singularity free. In this case we provide a motivation for why we need a modified theory of gravity, such as IDG, and then show how to obtain the action and propagator for this theory. From the action of the IDG we are able to produce a metric for an electrically charged massive point source. After which we obtain the metric for a rotating object with mass. We check that these metrics are indeed non-singular, by checking that the potentials in the metric remain finite in the entire region of the space time. We also ensure that the curvature scalars and tensors are non-singular in the entire region.

Acknowledgements

Firstly it should be noted that this PhD was funded by National Institute for Theoretical Physics (NITheP), Gauteng, South Africa, under their bursary programme. I am very thankful that NITheP has funded my studies as it would not be possible for me to visit the Netherlands without this bursary. Secondly I would like to thank SA CERN who have helped sponsored part of my trips to Europe.
I would like to thank Alan S. Cornell for all the help and guidance he has provide during my graduate studies. I appreciate all the work he has done in organising international visits as well as all the work that had to be done to organise the dual degree. Our talks have been insightful and have given me a deeper understanding of QNMs and particle physics. I would also like to thank Anupam Mazumdar, who has taught me a lot about the theory of IDG, and who has always been available for discussions when I had questions. Furthermore I would like to thank him for giving me the opportunity to study in the Netherlands, without his help this would not have been possible.
I would like to thank my friends, who have helped me get through my PhD studies and kept me motivated throughout my studies. Finally I would like to thank my family who have always believed in me throughout my PhD studies and encouraged me to keep working even when I wanted to stop.

Contents

Chapter 1

Introduction

General relativity (GR) is a geometrical theory of gravity formulated by Albert Einstein in 1915 [1] and it is still considered the most accepted interpretation of gravity. In this theory it is recognised that space time can be represented using the Lorentz group, which encodes in it the idea of causality. This can only occur if there exists a maximum limit to how fast information can propagate, a crucial idea in GR which distinguishes it from Newtonian gravity. The action that describes the dynamics of the theory are given by the Einstein-Hilbert action written as

$$S = \int \sqrt{-g}\left[\frac{1}{2\kappa}R + \mathcal{L}_M\right] d^4x, \tag{1.1}$$

where $g = det(g_{\mu\nu})$, with $g_{\mu\nu}$ the metric that describes the space time. In this thesis we will work with metrics of a space like convention, that is they have a signature of $(-, +, +, +, ...)$. R is a Ricci scalar, $\mathcal{L}_m$ is the matter Lagrangian and $\kappa = 8\pi G c^{-4}$, with G the gravitational constant and c the speed of light.[1] Applying to this the principal of least action we obtain the Einstein field equations, given as

$$G_{\mu\nu} + \Lambda g_{\mu\nu} = \kappa \tau_{\mu\nu}, \tag{1.2}$$

where $G_{\mu\nu}$ is the Einstein tensor which has encoded in it the curvature of the space time, Λ is the cosmological constant and $\tau_{\mu\nu}$ is the stress-energy tensor. What this equation is stating is that the curvature experienced near an object is directly related to the matter content of that object, in fact the more matter the object has the greater the object will curve space and time [2]. One of the first experimental results which showed that GR is an attractive alternative to Newtonian gravity, is that GR was able to accurately explain the precession of the perihelion of the orbit of mercury, without the need for additional correcting factors, this is shown in Refs. [1, 3]. Another prediction of GR is that light should bend as it passes near massive objects. This is due to light always travelling along a geodesic, which is the shortest path between two points. In the case of Euclidean space this is simply a straight line connecting two points, in curved space this is not necessarily the case. As indicated in Eq. (1.2), the space around a massive object is curved, and as such the light will follow a curved path, as illustrated in Fig. 1.1. This bending of the light gives the impression that the object that is producing the light is located at a different point in space compared to where it actually is. In 1912 Einstein proposed that in the theory of general relativity the magnitude of this bending of light is twice that as predicted by von Soldner in 1804 [5, 6]. During the May 29 1919 solar eclipse Dyson et al. [7] observed the bending of light as predicted by general relativity. This observation solidified GRs position as a more acceptable interpretation of gravity. There are many

[1] In this thesis we will set $c = G = 1$ unless otherwise stated.

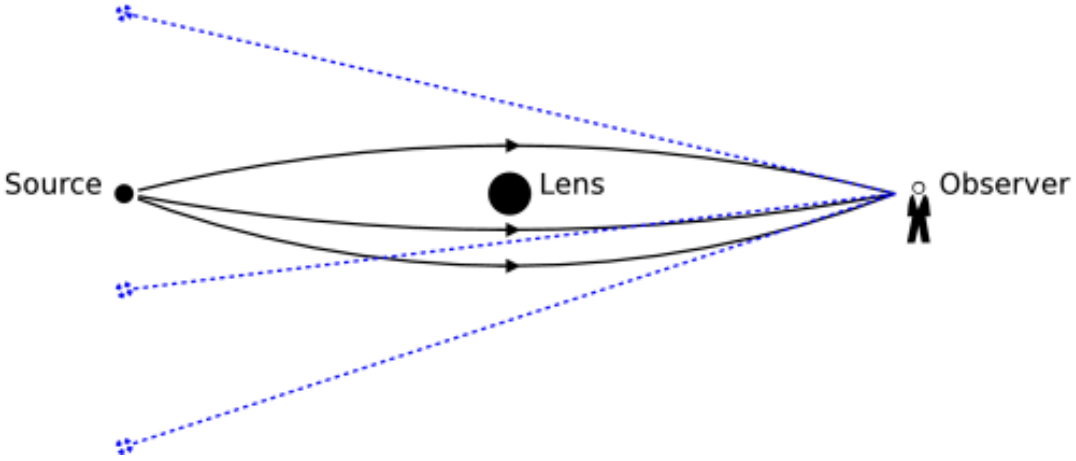

FIGURE 1.1: Image illustrating that light bends in the presence of a massive object, and that this bending of light can make it seems as if the source of light is at a different location Ref. [4].

more predictions and observations of the theory of GR, see Ref. [8] for a fuller list of observed phenomena in GR. These predictions and observations of GR are all in what is called the infrared (IR) limit of gravitational interactions, which is where the distance between interactions is large enough that quantum effects do not need to be considered.

There does, however, exist a problem with GR, and that is it cannot be incorporated into the standard theory of particle physics. As such it is not clear how the force mediator for gravity interacts with matter. This is contrary to how the other forces of nature are seen to interact. These theories come from quantum mechanical ideas, which are inherently probabilistic and do not necessarily consider large space time symmetries. They are predominantly interested in the short range interactions, that is at length scales where we need to consider the quantum nature of the interaction. These types of interactions occur at much higher energies as compared to the interaction occurring in the IR. As such, we say that these interactions occur in the Ultraviolet (UV) regime.

Due to the quantum mechanical nature of these theories, applying them to the matter part of the Einstein field equations suggests that there needs to be a quantisation of the space time part. This, however, leads to a non-renormalisable theory, meaning that there are infinities which we cannot control [9]. This non-renormalisability is indicative that the theory is only valid in the IR regime, and therefore cannot necessarily be trusted all the way up to the quantum level.

Another problem in GR is if it is applied to cosmology. In this context the theory predicts the necessary existence of singularities in any expanding universe that is spatially homogeneous and isotropic [10, 11]. This can be understood by considering an ever expanding universe with a constant matter content. If in the case of this universe we were to run the clocks backwards we would observe an ever increasingly dense universe, which would eventually become so dense as to be considered infinitely dense. Again, this would only occur in the small timescale interactions, or very early universe. This singularity is colloquially called the big bang singularity.

Our final motivation for considering theories beyond standard GR is that the Schwarzschild, Reissner-Nordström and Kerr metrics contain with in them at least one singularity. Notably there is a singularity in these metrics that cannot be removed through a coordinate transformation. As an example we consider the radial form of

the Schwarzschild metric, which describes a non-rotating electrically neutral object [12],

$$ds^2 = -f(r)dt^2 + \frac{1}{f(r)}dr^2 + r^2 d\theta^2 + r^2 sin^2\theta d\phi^2, \tag{1.3}$$

where $f(r) = 1 - 2M/r$, with m the mass. Note that in the above we have used natural units, $c = G = 1$. We see that the two singular solutions are at $f(r) = 0$ and at $r = 0$. The singularity at $f(r) = 0$ occurs at $r = 2M$ and is located at the Schwarzschild radius, its existence suggests that there are two distinct regions in the space time. The coordinate singularity that occurs at this point can be removed be a reparameterisations of coordinates, however a check of the Killing vectors shows that there still exists two distinct regions of space [13]. The singularity located at $r = 0$, cannot be removed by a change of coordinates and this singularity is predicted to exist in every black hole. The consequences of this singularity might be that the predictability of physics and many other tools of physics would not work here. Fortunately, in 1969, Roger Penrose proved, within standard GR, the cosmic censorship conjecture, which states that in GR this singularity is always hidden by the event horizon, and as such cannot be observed in the physical universe [14]. This resolves the issue of predictability from a physical point of view, but does not resolve the issue in the theoretical framework of GR, since they still remain unresolved. It should be noted that this conjecture only applies to the singularities found in black holes and does not include the cosmological singularity.

The UV completeness problems of GR have plagued scientists for many years, and as such there have been numerous approaches to solving this problem see Refs. [15–18] for some of the ideas proposed to solve the problems in GR.

One of the proposed solutions is supersymmetric gravity, usually called super gravity (SUGRA). These theories propose that there exists a supersymmetric partner to the the graviton, which in the standard model is a spin-2 gauge boson, called the gravitino, which has a 3/2 spin. A full review on the topic is given by van Nieuwenhuizen et al. in Ref. [19]. [2] Some of these SUGRA theories take inspiration from string theory and require more than four dimensions to ensure that the theory is renormalisable. Some like the 11 dimensional SUGRA are still challenging to incorporate into the standard model [19]. However the study of higher dimensions is still a topic of interest, even in non-SUGRA models of gravity, since it can give us insight into which features are unique to four dimensional gravity [22]. In this thesis we explore these higher dimensions with this motivation in mind, rather than motivating the need for the existence of higher dimensional models of gravity in order to resolve issues in the theory.

Finally, the types of modified gravity that we will explore in this thesis are those containing higher order derivatives in their field equations. These theories modify the Einstein-Hilbert action by including higher orders of the curvature scalar, and in the hopes of obtaining a non-singular theory of gravity.[3] One such theory is that of fourth order derivative gravity which, has shown that the theory can be renormalised, at the expense of introducing ghosts into the theory [23]. In Sec. 1.3 we motivate these types of theories and briefly introduce the theory of Infinite Derivative Gravity (IDG), which is ghost free.

Before looking at the modified theories of GR we will look at a prediction of GR that has only recently been detected, namely gravitational waves. These were predicted

[2] Note that to date the LHC has not detected any supersymmetric particles [20, 21]

[3] In obtaining the non-singular gravity it is hoped that the issue of renormalisablity can be resolved, although this has not yet been done.

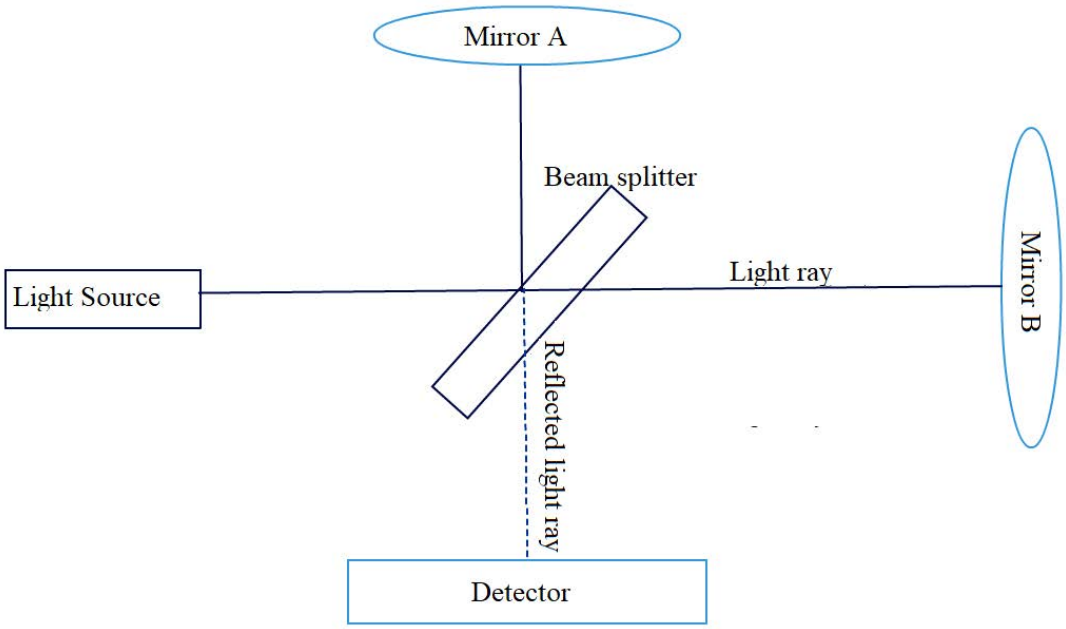

FIGURE 1.2: Diagram representing the setup of a Michealson-Morley inferometer experiment.

shortly after Einstein proposed his theory of GR, but have taken nearly a century to be observed directly [24].

1.1 Gravitational waves

Eq. (1.2) describes how the space time around an object curves due to the local energy and momentum [13]. Most importantly it ensures that the the conservation of momentum and energy are observed in GR [25]. If the object is accelerating, then these curvatures of the space time can propagate away from the object. Analogous to how an object moving through water creates a wake behind it. These propagating curvatures are called gravitational waves, and move away at the speed of light. Furthermore, the amplitude of these waves is a measure of how much they have stretched or contracted the space time as compared to the unperturbed space time. As they propagate away from the object they do carry with them some gravitational energy [26]. In fact their existence was inferred by observing the orbital decay of a binary pulsar system in 1982, since as the two objects orbited one another they slowly lost energy and thereby reduced the distance between each other, in the process increasing their orbital velocities [27].
Even though gravitational waves had long been predicted by GR they have only recently been discovered by the Laser Interferometer Gravitational-Wave Observatory (LIGO) research collaboration [28]. The first detection was on the 15th September 2015, with at least eight more detections since then. The experiment is very similar to the Michelson-Morley experiment which was used to prove that there exists no "aether" through which photons propagate, even though it was setup to try and detect this "aether" [29]. The Michealson-Morley experiment is setup as shown in Fig. 1.2, where a light source, in the case of LIGO a powerful laser, fires a light beam at a beam splitter, which sends two beams of light in perpendicular directions to each other towards two mirrors, in the case of LIGO these mirrors are 4km away from

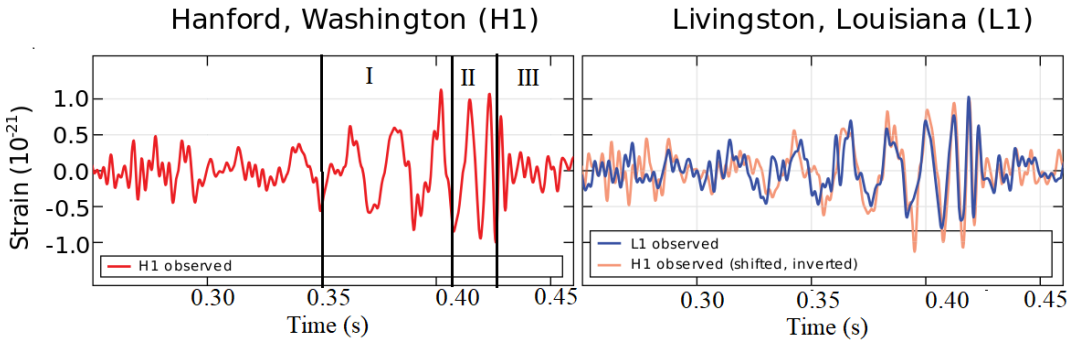

FIGURE 1.3: Gravitational wave event GW150914 detected by the LIGO Hanford, left column, and the LIGO Livingston, right column, detectors. [24]

the beam splitter. The light reflects off the mirrors and returns to the beam splitter, where the two laser beams are recombined and sent towards the detector. In recombining the two light beams interfere with each other, where in the case of LIGO the mirrors are placed such that the light beams interfere destructively, so that no photons are detected when the system is not detecting any gravitational waves. If a gravitational wave were to move through the LIGO detector, then it will cause the arms of the detector to either lengthen or contract by very small amounts. Since the arms are no longer the same length, the two light beams return to the beam splitter slightly out of phase. As such, they will no longer interact in such a way as to be completely destructively interfering with each other, i.e. the detector measures some non-zero intensity of light. The intensity of the light is directly related to the amplitude of the gravitational wave that passed through the detector.
Due to the weak nature of gravity, and a $1/r$ fall off in strength due to propagation, the gravitational waves detected had an extremely small amplitude, making them very difficult to detect. In fact, the detection by the LIGO team on the 15th of September was the detection of two black holes orbiting each other and then colliding, where the mass of one of the black holes had a mass of $35^{+5}_{-3}M_{\odot}$ and the other had a mass of $30^{+3}_{-4}M_{\odot}$ [30]. The event resulted in the lengths of the arms in the LIGO detector to change by less than the diameter of a proton [30]. Fig. 1.3 shows the gravitational wave that the LIGO team detected. Looking at the left most image in Fig. 1.3 we have labelled three regions of interest. Region I is where the two black holes are orbiting each other and are spiralling towards each other, this is called the pre-merger stage. The frequency of the gravitational wave is proportional to the orbital velocity of the two black holes. So moving from region I to II we see that the frequency increases since the two black holes are falling in towards each other and therefore increasing their orbital velocity. In region II we see that the frequency has increased drastically and the amplitude of the gravitational waves has increased. This region of the graph shows the merger phase of the two black hole systems. Here the two black holes are colliding with each other resulting in a highly perturbed black hole. Due to this highly perturbed state the new black hole will be emitting large amounts of energy as it tries to return to an almost spherical space. Note that due to rotations the black hole will be slightly elongated at its equator. This phase of large energy emission and return to a more spherical space is called the ring down phase and occurs in the region III. This ring down phase has the same form as we would see from a Quasi Normal Mode (QNM). These QNMs are of interest as they can reveal a deeper insight into black holes and GR. In fact the

first studies of QNMs were done in the 1950's by Regge and Wheeler in Ref. [31] on the QNMs on the surface of a black hole after it had been perturbed. Where they wanted to probe the stability of Schwarzschild black holes by studying the QNMs. In the 1970s Vishveshwara pointed out that these oscillations would be emitted into the surrounding space time and propagate away as gravitational waves [32], which was confirmed by the LIGO detector.

1.2 QNMs

In general terms a QNM is a normal mode with some dampening term. They occur when some object is perturbed in some way, and then emits the energy of the perturbation away from itself. For instance the tapping of a knife on a wine glass will create QNMs as at the surface of the glass resonates and emits sound waves. Extending on this thought, the allowed frequencies and the dampening terms are determined by the composition of the glass and the contents within the glass. Such that glasses of wine with different amounts of wine ring at different frequencies, and for differing lengths of time. This means that in theory if we were to measure the frequency of the ringing we could determine the amount of wine in the glass. There are a variety of ways of perturbing, or creating perturbed black holes. For instance the creation of a black hole from a collapsing star or the collision of two black holes would create these highly perturbed systems. But we need not use such massive objects to create the perturbations, which could also be created by a single field, as Regge and Wheeler suggested [31]. In all of these cases the black hole would emit QNMs as it radiated away energy to return to a none perturbed state, with the perturbation caused by a single field, possibly giving us an insight into that fields gravitational interaction. As in the case of the of the wine glass, there are certain parameters of the black hole that determine the allowed values of the emitted QNMs. Fortunately black holes are parameterised by only a few properties namely the mass of the black hole, its electric charge and the rotational speed of the black hole.
Research has been done on the allowed QNMs for spin-1/2, spin-1 and spin-2 fields [33, 34]. However there is a gap in the literature as spin-3/2 fields have not been studied to a large extent. In Ref. [35] the QNMs for spin-3/2 fields are investigated for Schwarzschild black holes. We note that in this paper we have used the results of a paper by R. Camporesi and A. Higuchi [36] where they have studied the eigenfunctions of a Dirac operator on an N dimensional sphere. Using their results we could easily expand our analysis to any arbitrary number of spatial dimensions. This means we were able to determine the effective potential for a D dimensional Schwarzschild black hole. Giving us an opportunity to not only test the limits of the numerical methods we used to obtain the QNMs, but also to check if there are any unique features in 4 dimensional gravity.
We chose to use two methods to determine the allowed QNMs, one being the well established Wentzel–Kramers–Brillouin (WKB) method, and the other being the improved Asymptotic Iterative Method (AIM). We chose these two methods since the WKB method is a well established method for determining QNMs, which has been extended to 6th order by R. Konoplya to increase the accuracy of the method [37–39]. However, obtaining this 6th order result is quite complicated, and can be computationally expensive. We therefore have used the AIM as an alternative method for calculating the numerical values of the QNMs. This method is easier to implement and it is hoped that it is computationally less expensive. It has been shown by H.

Cho et al. that this method can be used as an alternative for calculating the allowed QNMs of black holes [40–42]. In the case of the D dimensional black hole we noticed that for dimensions $D \geq 8$ our numerical methods began to breakdown. It would therefore be of interest to establish if these methods still work in the higher dimensional cases with electrically charged black holes and those that are in AdS spaces. As such the purpose of the first part of this thesis will be to determine the effective potentials and allowed QNMs in higher dimensional Reissner-Nordstöm and Anti-de Sitter (AdS) space times.

1.3 Higher order derivative theories of gravity

As stated in the opening paragraphs, of this thesis GR is a very successful theory in the IR range, but breaks down for short distances and small time scales, i.e. in the UV regime. As such, any new theory of gravity will need to only modify the UV interactions and return to the limit of GR in long range interactions. There are many theories that attempt to do exactly this, such as string theory, [43], loop quantum gravity [44, 45], causal set dynamics [46, 47], emergent gravity [48], and infinite derivative gravity [49–52].[4]
In this thesis, we will mainly focus on a class of theories known as IDG. The simplest modifications will lead to quadratic in curvature, but infinite derivative, corrections to the Ricci scalar, Ricci tensor and the Riemann tensor [50, 51]. [5] In 1962 R. Utiyama and B. De Witt showed that in order to ensure that gravity would be renormalisable we would need to consider higher order derivative terms in the action [59], and in 1977 K. Stelle showed that these higher order derivative theories are indeed renormalisable [23]. Most importantly, however, it was expected that the theories could be constructed in such away that they would introduce a new scale to the theory of gravity which would correct the gravitational behaviour in the UV, but return to GR in length scales larger than the newly introduced scale. This could then solve early universe and interior black hole singularities, while still leaving weak gravitational interactions unchanged [49]. As such the interest in these theories as possible solutions to the problems in GR has only increased, a review on the subject is given by Claus Kiefer in Refs. [44, 45].[6]
We shall briefly introduce some of the ideas in these theories, before stating why we look at the special case of IDG. One of the simplest ways of generalising the action of gravity is to consider actions of the form

$$S = \frac{1}{2\kappa}\int d^4x\sqrt{-g}f(R) + \mathcal{L}_m. \tag{1.4}$$

The simplest choice of $f(R)$ is setting it equal to R, thereby obtaining the standard Einstein-Hilbert action of GR, given in Eq. (1.1). Using the principal of least action will then give us the standard Einstein field equations as written in Eq. (1.2). These field equations have at most second order derivatives in them [62–64]. K. Stelle

[4] Note that there has been an increase in the interest in IDG [53–55].

[5] Indeed the simplest generalisation will be to include only corrections which are invariant under Ricci scalar, known as $f(R)$ theories of gravity [56]. These are not necessarily new theories, in fact they were first experimented with in 1918, however this was done more as a curiosity in determining what effects would appear when looking at higher order derivative theories of gravity [57, 58].

[6] Further reviews on the topic are given in Refs. [60, 61]

improved on this action by considering actions of the form [23],

$$S = \int d^4x\sqrt{-g}\left(\alpha R + \beta R^2 + \gamma R^{\mu\nu}R_{\mu\nu}\right), \tag{1.5}$$

where he showed for appropriate values of α, β and γ the theory can be renormalised. However for these values of the coefficients the theory has a negative energy propagating degree of freedom. This results in vacuum instabilities in the Minkowski space time as well as prevents unitary in the quantum regime. By looking at the spin-2 component of the propagator in this theory we see the signature of a Weyl ghost [23, 51]. The presence of a this Weyl ghost violates the conditions for stability and unitarity.
In fact any theory that introduces any finite number of higher derivatives (more than 2) of scalars, vectors and tensors will always end up having kinetic operators with extra poles, which could be ghost like. [7] However in 1989 Kuz'min [66] and in 1997 Tomboulis [67] showed that by considering an infinite series of higher derivatives gauge theories and gravitational theories can be made renormalisable. Using these ideas Biswas, Mazumdar and Siegel suggested that the only way to ensure a ghost free non-singular theory of gravity was to consider an action which contained within it an infinite number of derivative terms [49]. Furthermore, in Ref. [49] the authors showed that such a theory of gravity could be applied to cosmology, and provided a viable solution to the cosmological singularity problem. Where they consider a cosmological bounce scenario instead of a Big Bang singularity. The authors have argued that this theory can be made asymptotically free in the UV regime without violating fundamental idea of physics such as unitary [50]. The Lagrangian that the authors have considered in this case is of the form

$$f = R + R_{\mu_1\nu_1\alpha_1\beta_1}\mathcal{O}^{\mu_1\nu_1\alpha_1\beta_1}_{\mu_2\nu_2\alpha_2\beta_2}R^{\mu_2\nu_2\alpha_2\beta_2}, \tag{1.6}$$

where $\mathcal{O}^{\mu_1\nu_1\alpha_1\beta_1}_{\mu_2\nu_2\alpha_2\beta_2}$ is a differential operator which contains within it covariant derivatives and $g_{\mu\nu}$ the metric of interest.

Outline

This thesis is split into two parts. Part one of this thesis will investigate the allowed QNMs for spin-3/2 fields near GR metrics describing electrically charged black holes and black holes in a universe with a none zero cosmological constant. Part 1 is set out as follows, in Ch. 2 we provide the background information necessary to construct the effective potential describing our spin-3/2 fields in the relevant black hole backgrounds. We also provide the tools necessary to calculate the allowed QNMs using the effective potentials. In Ch. 3 we obtain the effective potential for the spin-3/2 fields in a D dimensional space-time with an electrically charged black hole. Using this potential we calculate and present the numerical values for the QNMs for various dimensions and electrical charges of the black hole. Finally we present the absorption probabilities associated with the QNMs, before concluding and beginning our investigation of black holes in (A)dS in Ch. 4. Again we will investigate the effect of dimension and in this case curvature on the allowed QNMs.
In part 2 of the thesis we investigate the modified theory of gravity called IDG. In

[7] Note also that Ostrogradsky showed that any non-degenerate Lagrangian dependent on time derivatives higher than the second order corresponds to a linearly unstable Hamiltonian [65].

Ch. 5 we provide the necessary background material for understanding IDG, as well as show that it is in fact a ghost free theory of gravity by constructing the fields equations and the propagator using a modified Einstein-Hilbert action. Then in Ch. 6 we construct and test the metric for an electrically charged object in the theory of IDG. Finally we construct the rotational metric for IDG. In Ch. 7 we show that this metric is indeed singularity free and can be reduced to the GR rotational metric in the appropriate limit.
In Ch. 8 we present our final concluding statements remarking on both the works from part 1 and part 2.

Part I

Quasi normal modes in black hole backgrounds

Chapter 2

Introduction to QNMs

In this chapter we will introduce the ideas and tools necessary to study the QNMs of black holes due to spin-3/2 perturbations. We begin by introducing a more mathematical definition of QNMs, and what the general procedure is for obtaining the numerical values of QNMs. We then introduce spin-3/2 fields, by giving the appropriate equation of motion describing these types of fields, note that due to the space times we wish to study we will need to modify our covariant derivative. Finally, we provide an overview of the numerical methods we shall use to calculate our QNMs.

2.1 A Mathematical description of QNMs

To build on the intuitive picture described in Ch. 1, we will use a more mathematical formalism to describe QNMs. We begin by considering the formula for standing waves, since as stated previously, QNMs are damped standing waves which, crucially, obey the boundary conditions given in Ref. [38]. We can represent standing waves in one dimension as [32]

$$\frac{d^2}{dr^2}\Psi(r,t) - \frac{d^2}{dt^2}\Psi(r,t) - V(r)\Psi(r,t) = 0\,, \tag{2.1}$$

with Ψ describing some wavelike function, where r and t denote space and time coordinates respectively, and V is some r-dependent potential. We can solve this equation by assuming the form of the standing wave as [68]

$$\Psi(r,t) = e^{-i\omega t}\phi(r)\,. \tag{2.2}$$

In the case of an undamped wave ω has a purely real value, in the case of a damped wave, however, the parameter ω complex values, where the real part represents frequency and the imaginary part represents the damping that the wave experiences. Plugging Eq. (2.2) into our wave equation we get

$$\frac{d^2\phi(r)}{dr^2} - \Big(\omega^2 + V(r)\Big)\phi(r) = 0\,. \tag{2.3}$$

This is the general form of the equations that we will be using to determine the numerical values of our QN frequencies. Note that we will be solving for the QN frequencies. In the chapters that follow our task will be to take an appropriate equation of motion and obtain the above equation. Once we have this we need to impose the appropriate boundary conditions to ensure that we obtain the complex value for ω. The boundary conditions that we would need to place on the equation is that the QNMs are purely ingoing at the event horizon, and purely outgoing at spacial infinity. As such the appropriate boundary conditions for the asymptotically flat case are

[38]

$$\phi(r) \sim e^{\pm i\omega r_*} \;\; ; \;\; r_* \to \pm\infty\,, \tag{2.4}$$

where r_* is the tortoise coordinate and is determined as follows

$$dr_* = \frac{dr}{f(r)}, \tag{2.5}$$

where $f(r)$ is a function specified by the metric of interest [38]. In order to determine the effective potential such that we obtain the wave equation, we must first determine the equation of motion that defines our field. As we are interested in spin-3/2 fields, we will derive their appropriate equation of motion by firstly considering their Lagrangian.

2.2 Spin-3/2 fields

Before we introduce the spin-3/2 field, we will briefly go over some points on notation. In principal we can use the SU(2) $\times$ SU(2) Lorentz group to represent different spin fields. Below is a brief overview of this:

- (0, 0) - Represents the spin-0 field.
- $(\frac{1}{2}, 0) \oplus (0, \frac{1}{2})$ - Represents the spin-1/2 fields or spinor fields.
- $(\frac{1}{2}, \frac{1}{2})$ - Represents the spin-1 or vector fields.
- $(1, 1) \oplus (0, 0)$ - Represents the spin-2 or tensor field.

Where in the above "$\oplus$" is the tensor summation operator, later we also use the tensor product denoted as "$\otimes$". Spin-3/2 fields are considered to be a combination of the spinor and vector fields, so are naively called spinor-vector fields. This means they require components from both the spinor and vector fields. The representation of these fields in the Lorentz group representation would be [69]

$$\left(\frac{1}{2}, 0\right) \oplus \left(0, \frac{1}{2}\right) \otimes \left(\frac{1}{2}, \frac{1}{2}\right) = \left[\left(\frac{1}{2}, 0\right) \otimes \left(\frac{1}{2}, \frac{1}{2}\right)\right] \oplus \left[\left(0, \frac{1}{2}\right) \otimes \left(\frac{1}{2}, \frac{1}{2}\right)\right]. \tag{2.6}$$

Further decomposition of the field yields that the field can be described as follows in the representation

$$\left((1, \frac{1}{2}) \oplus (0, \frac{1}{2})\right) \oplus \left((\frac{1}{2}, 1) \oplus (\frac{1}{2}, 0)\right). \tag{2.7}$$

So this field contains both a spin-1/2 component and a spin-3/2 component, given by $(1, \frac{1}{2})$. We require a spinor representation to show these types of fields, as this makes the notation easier. We will be using a notation first given by Rarita and Schwinger [70] where spinors are represented as Ψ_μ. Note that spinors are considered to be the simplest mathematical objects that can represent Lorentz transformations, such as boosts or rotations [71]. This makes them ideal for describing fields with spin, especially fields with half integer spin. Weinberg has shown that we can isolate the spin-3/2 component of the fields description by requiring that [69]

$$\gamma^\mu \psi_\mu = 0, \tag{2.8}$$

where γ^μ is the Dirac gamma matrix and ψ_μ is a Majorana type spinor representing the field, and μ is a spatial index running from 0 to one minus the total number of space time dimensions. Spinors can be thought of as vectors which can provide a linear representation of the rotation group of dimension n. With each spinor having 2^v components, with $n = 2v + 1$ or $n = 2v$ for the case of n odd or even respectively [72]. This makes them useful in physics, as they naturally encode within them spin (meaning they are occasionally used interchangeably when referring to fermionic particles). In physics there are three main types of spinors, the Dirac, Majorana and Weyl spinors. Majorana spinors were introduced to solve the Majorana equation, written as

$$\gamma^\mu \partial_\mu \psi_c + m\psi = 0, \tag{2.9}$$

where $\psi_c = i\psi^*$ is the charge conjugate of the field ψ. However, since the field and its charge conjugate appear in the equation, this equation cannot contain fields that have electric charge, since the charge conjugate would be negative. This means when we construct the spin-3/2 field we must assume it has no electric charge. Due to rotational invariance, Eq. (2.8) tells us that a field of momentum $q = 0$ and spin s in the z-component will satisfy the conditions

$$\langle 0|\psi_0(0)|s\rangle = 0, \tag{2.10}$$

and

$$\sum_{s=-3/2}^{3/2} \langle 0|\psi_i(0)|s\rangle \langle 0|\psi_i(0)|s\rangle^* = (2\pi)^{-3} \left(\frac{1+\beta}{2}\right) \left[\delta_{ij} - \frac{1}{3}\gamma_i\gamma_j\right]. \tag{2.11}$$

It then follows that the propagator of the spin-3/2 field should be [69]

$$\mathcal{P}^{\mu\nu} = \frac{\mathbf{P}^{\mu\nu}(q)}{q^2 + m_g^2 - i\epsilon}, \tag{2.12}$$

where $\mathbf{P}^{\mu\nu}(q)$ is a Lorentz-covariant polynomial of the four vector q. From the condition that for $q = 0$ and $q^0 = m_g$, where m_g is the mass of the spin-3/2 field, we have

$$P^{ij} = \left(\frac{1+\beta}{2}\right) \left[\delta_{ij} - \frac{1}{3}\gamma_i\gamma_j\right], \tag{2.13}$$

with $P^{i0} = P^{0i} = P^{00} = 0$. The unique covariant function that can describe this behaviour is given as [69]

$$\mathbf{P}^{\mu\nu}(q) = \left(\eta^{\mu\nu} + \frac{q^\mu q^\nu}{m_g^2}\right)(-i\not{q} + m_g) - \frac{1}{3}\left(\gamma^\mu - i\frac{q^\mu}{m_g}\right)(i\not{q} + m_g)\left(\gamma^\nu - i\frac{q^\nu}{m_g}\right). \tag{2.14}$$

As such, a Lagrangian that can correctly describe this type of field must have the form

$$\mathcal{L} = -\frac{1}{2}\left(\bar{\psi}^\mu D_{\mu\nu}(-i\partial)\psi^\nu\right), \tag{2.15}$$

where

$$\mathcal{P}^{\mu\nu}(q) D_{\nu\lambda}(q) = \delta^\mu_\lambda. \tag{2.16}$$

Weinberg has shown that the relationship in Eq. (2.16) implies that [69]

$$D_{\nu\lambda}(q) = -\epsilon_{\nu\mu\kappa\lambda}\gamma_5\gamma^\mu q_\kappa - \frac{1}{2}m_g\left[\gamma^\nu, \gamma^\lambda\right]. \tag{2.17}$$

As such the Lagrangian for the massive spin-3/2 field is written as [69]

$$\mathcal{L} = -\frac{1}{2} i\epsilon^{\nu\mu\kappa\lambda} \left(\bar{\psi}_\nu \gamma_5 \gamma_\mu \partial_\kappa \psi_\lambda\right) + \frac{1}{4} m_g \left(\bar{\psi}_\nu \left[\gamma^\nu, \gamma^\lambda\right] \psi_\lambda\right). \tag{2.18}$$

In this thesis we work with only the massless form of the fields, in which case we can simplify the Lagrangian to its massless form,

$$\mathcal{L} = -\frac{1}{2} i\epsilon^{\nu\mu\kappa\lambda} \left(\bar{\psi}_\nu \gamma_5 \gamma_\mu \partial_\kappa \psi_\lambda\right). \tag{2.19}$$

It can be shown straight forwardly, using the gamma matrix identities, that this Lagrangian can be rewritten as

$$\mathcal{L} = \bar{\psi}_\nu \gamma^{\mu\nu\lambda} \partial_\kappa \psi_\lambda, \tag{2.20}$$

where $\gamma^{\mu\nu\alpha} = \gamma^\mu \gamma^\nu \gamma^\alpha + \gamma^\mu g^{\nu\alpha} - \gamma^\nu g^{\mu\alpha} + \gamma^\alpha g^{\mu\nu}$ is the anti-symmetric gamma matrix relation. Using the principal of least action to determine the equations of motion, the result of varying the above Lagrangian gives

$$\delta\mathcal{L} = \delta\bar{\psi}_\mu \gamma^{\mu\nu\lambda} \partial_\kappa \psi_\lambda - \partial_\kappa \bar{\psi}_\mu \gamma^{\mu\nu\lambda} \delta\psi_\lambda. \tag{2.21}$$

as shown in Ref. [69] using the "Majorana-flip property" this can be simplified to

$$\delta\mathcal{L} = 2\delta\bar{\psi}_\mu \gamma^{\mu\nu\lambda} \partial_\kappa \psi_\lambda, \tag{2.22}$$

which by the principal of least action, $\delta\mathcal{L} = 0$, implies that

$$\gamma^{\mu\nu\lambda} \nabla_\nu \psi_\lambda = 0. \tag{2.23}$$

This is the Rarita-Schwinger equation, as given by Rarita and Schwinger in Ref. [70]. This form of the equation of motion, however, is not necessarily gauge invariant in all space times. If we perform the following gauge transformation

$$\psi'_\lambda = \psi_\lambda + \nabla_\lambda \varphi, \tag{2.24}$$

where φ is some spinor, and plug this into Eq. (B.10) and then require that

$$\gamma^{\mu\nu\lambda} \nabla_\nu \nabla_\lambda \varphi = 0, \tag{2.25}$$

then our Lagrangian is invariant [73]. In the purely gravitational case this equation can be written as

$$\begin{aligned} \gamma^{\mu\nu\lambda} \nabla_\nu \nabla_\lambda \varphi &= \frac{1}{2} \gamma^{\mu\nu\lambda} \left[\nabla_\nu, \nabla_\lambda\right] \varphi \\ &= \frac{1}{8} \gamma^{\mu\nu\lambda} R_{\nu\lambda\rho\sigma} \gamma^\rho \gamma^\sigma \varphi. \end{aligned} \tag{2.26}$$

Using the Bianchi identity we can show that

$$\gamma^\mu \gamma^\nu \gamma^\lambda R_{\nu\lambda\rho\sigma} = -2\gamma^\lambda R_{\rho\sigma}, \tag{2.27}$$

furthermore $\gamma^\mu \gamma^\nu \gamma^\rho \gamma^\sigma R_{\mu\nu\rho\sigma} = -2R$. Using these identities we have that

$$\gamma^{\mu\nu\lambda} \nabla_\nu \nabla_\lambda \varphi = \frac{1}{8} \gamma^{\mu\nu\lambda} R_{\nu\lambda\rho\sigma} \gamma^\rho \gamma^\sigma \varphi = \frac{1}{4} \left(2\gamma^\lambda R^\mu_\lambda - \gamma^\mu R\right) \varphi. \tag{2.28}$$

The expression on the far right is only zero if we are working in Ricci flat space times, such as the Schwarzschild space time [74]. This is not the case when introducing

charge or when introducing asymptotic curvature to the space time (as in the case of AdS space times). So for both the AdS space time and the Reissner-Nordstöm black hole we will need to modify this equation. We therefore need to modify the derivative function such that it is applicable in the cases that we are interested in. In the next section we show how we have constructed a so called "super covariant derivative", since it is a modified covariant derivative for spin-3/2 fields.

2.3 Super covariant derivative

In constructing the "super covariant derivative" we need to ensure that

$$\gamma^{\lambda\mu\nu}\left[\mathbb{D}_\mu, \mathbb{D}_\nu\right]\varphi = 0, \tag{2.29}$$

as alluded to in Eq. (2.26), where here we have used the "super covariant derivative" $\mathbb{D}_\mu$ instead of the ordinary covariant derivative. This new covariant derivative takes into account the electrical charge and the curvature, due to the cosmological constant. The most general derivative we can construct is of the form

$$\mathbb{D}_\mu = \widetilde{\mathbb{D}}_\mu + a\sqrt{\Lambda}\gamma_\mu + b\gamma^\rho F_{\mu\rho} + c\gamma_{\mu\rho\sigma}F^{\rho\sigma}, \tag{2.30}$$

where $\widetilde{\mathbb{D}}_\mu = \nabla_\mu - ieA_\mu$, with A_μ the D dimensional form of the four potential, $F_{\mu\nu}$ is the stress tensor and Λ is the cosmological constant. We are then left to determine the values of a, b and c. Plugging this into Eq. (2.29) we have

$$\begin{aligned}0 =&\gamma\lambda\mu\nu\left[\widetilde{\mathbb{D}}_\mu, \widetilde{\mathbb{D}}_\nu\right]\varphi + 2b\gamma^{\lambda\mu\nu}\left[\widetilde{\mathbb{D}}_\mu, \gamma^\rho F_{\nu\rho}\right]\varphi + 2c\gamma^{\lambda\mu\nu}\left[\widetilde{\mathbb{D}}_\mu, \gamma_{\nu\rho\sigma}F^{\rho\sigma}\right]\varphi \\ &+ a^2\Lambda\gamma^{\lambda\mu\nu}\left[\gamma_\mu, \gamma_\nu\right]\varphi + 2ab\sqrt{\Lambda}\gamma^{\lambda\mu\nu}\left[\gamma_\mu, \gamma^\rho F_{\nu\rho}\right] + 2ac\sqrt{\Lambda}\gamma^{\lambda\mu\nu}\left[\gamma_\mu, \gamma_{\nu\rho\sigma}F^{\rho\sigma}\right]\varphi \\ &+ b^2\gamma^{\lambda\mu\nu}\left[\gamma^\alpha F_{\mu\alpha}, \gamma^\rho F_{\nu\rho}\right]\varphi + 2bc\gamma^{\lambda\mu\nu}\left[\gamma^\alpha F_{\mu\alpha}, \gamma_{\nu\rho\sigma}F^{\rho\sigma}\right] + c^2\gamma^{\lambda\mu\nu}\left[\gamma_{\mu\alpha\beta}F^{\alpha\beta}, \gamma_{\nu\rho\sigma}F^{\rho\sigma}\right]\varphi.\end{aligned} \tag{2.31}$$

We first look at the commutation relation of the differential operator,

$$\begin{aligned}\gamma^{\lambda\mu\nu}\left[\mathbb{D}_\mu, \mathbb{D}_\nu\right]\varphi &= -\frac{1}{8}\gamma^{\lambda\mu\nu}(R_{\mu\nu}{}^{ab}\left[\gamma_a, \gamma_b\right])\varphi - ie\gamma^{\lambda\mu\nu}F_{\mu\nu}\varphi \\ &= -\frac{1}{4}\gamma^{\lambda\mu\nu}(R_{\mu\nu}{}^{ab}\left(\gamma_a\gamma_b - g_{ab}\right))\varphi - ie\gamma^{\lambda\mu\nu}F_{\mu\nu}\varphi \\ &= \gamma^\mu G_\mu{}^\lambda\varphi - ie\gamma^{\lambda\mu\nu}F_{\mu\nu}\varphi,\end{aligned} \tag{2.32}$$

Where $G_\mu{}^\lambda$ is the Einstein tensor. Next consider the commutation relation between the differential operator and the $F_{\mu\nu}$ operator,

$$\begin{aligned}\gamma^{\lambda\mu\nu}\left[\mathbb{D}_\mu, \gamma^\rho F_{\nu\rho}\right]\varphi &= \gamma^{\lambda\mu\nu}\gamma^\rho\mathbb{D}_\mu F_{\nu\rho}\varphi \\ &= \left(\gamma^\lambda\gamma^\mu\gamma^\nu\gamma^\rho - \gamma^\lambda g^{\mu\nu}\gamma^\rho + \gamma^\mu g^{\lambda\nu}\gamma^\rho - \gamma^\nu g^{\lambda\mu}\gamma^\rho\right)\mathbb{D}_\mu F_{\nu\rho}\varphi.\end{aligned} \tag{2.33}$$

But $\gamma^{\mu\nu\rho}\nabla_\mu F_{\nu\rho} = 0$ by the Bianchi identities. Furthermore $g^{\mu\rho}\nabla_\mu F_{\nu\rho} = g^{\mu\nu}\nabla_\mu F_{\nu\rho} = 0$ since $\nabla_\mu F^\mu_\rho = 0$. Next $g^{\nu\rho}\nabla_\mu F_{\nu\rho} = 0$ since the tensor $F_{\mu\nu}$ is antisymmetric. Finally by using the Bianchi identities we can show that

$$\begin{aligned}\nabla_\mu F_{\nu\alpha} + \nabla_\nu F_{\alpha\mu} + \nabla_\alpha F_{\mu\nu} &= 0, \\ \gamma^{\mu\nu}(\nabla_\mu F_{\nu\alpha} + \nabla_\nu F_{\alpha\mu} + \nabla_\alpha F_{\mu\nu}) &= 0, \\ 2\gamma^{\mu\nu}(\nabla_\mu F_{\nu\alpha}) &= \gamma^{\mu\nu}\nabla_\alpha F_{\mu\nu}.\end{aligned} \tag{2.34}$$

This result implies that

$$\gamma^{\lambda\mu\nu}\left[D_\mu,\gamma^\rho F_{\nu\rho}\right]\varphi=\gamma^{\lambda\nu}D_\mu F^\mu_{\ \nu}\varphi-\frac{1}{2}\gamma^{\mu\nu}D^\lambda F_{\mu\nu}\varphi. \tag{2.35}$$

In App. A we continue in this fashion, deriving all the commutation relations as seen in Eq. (2.31), where we also provide a brief overview of the gamma matrices. Using the relations obtained above and those in App. A, we can solve for a, b and c in Eq. (2.30).
Beginning with simplest case $D=4$, Eq. (2.31) reduces to

$$\begin{aligned}&8c\nabla_\mu F^{\mu\lambda}\varphi\\&+\gamma^\mu\left(G^\lambda_\mu-12a^2\Lambda g^\lambda_\mu+8a(b+2c)\sqrt{\Lambda}F^\lambda_\mu-4(b^2+4c^2)F_{\mu\nu}F^{\nu\lambda}F_{\mu\nu}F^{\nu\lambda}-2b^2g^\lambda_\mu F_{\rho\sigma}F^{\rho\sigma}\right)\varphi\\&+\gamma^{\mu\nu}\left(b+2c\right)\left(2g^\lambda_\mu\nabla F^\alpha_\nu-\nabla^\lambda F_{\mu\nu}\right)\varphi\\&+\gamma^{\mu\rho\sigma}\left(-ieg^\lambda_\mu F_{\rho\sigma}-4ab\sqrt{\Lambda}g^\lambda_\mu F_{\rho\sigma}+4(b^2-4c^2)F_{\rho\sigma}f^\lambda_\mu\right)\varphi=0.\end{aligned} \tag{2.36}$$

In order to ensure that the $\gamma^{\mu\nu}$ term is zero we set $b+2c=0$. This simplifies the equation as

$$\begin{aligned}&8c\nabla_\mu F^{\mu\lambda}\varphi+\gamma^\mu\left(G^\lambda_\mu-12a^2\Lambda g^\lambda_\mu-32c^2F_{\mu\nu}F^{\nu\lambda}-8c^2g^\lambda_\mu F_{\rho\sigma}F^{\rho\sigma}]\right)\varphi\\&+\gamma^{\mu\rho\sigma}\left(-ieg^\lambda_\mu F_{\rho\sigma}+8ac\sqrt{\Lambda}g^\lambda_\mu F_{\rho\sigma}\right)\varphi=0.\end{aligned} \tag{2.37}$$

This implies that $\nabla_\nu F^{\mu\nu}=0$, in which case

$$G^\lambda_\mu-12a^2\Lambda g^\lambda_\mu-32c^2F_{\mu\nu}F^{\nu\lambda}-8c^2g^\lambda_\mu F_{\rho\sigma}F^{\rho\sigma}=0, \tag{2.38}$$

and that

$$-ieg^\lambda_\mu F_{\rho\sigma}+8ac\sqrt{\Lambda}g^\lambda_\mu F_{\rho\sigma}=0. \tag{2.39}$$

Eq. (2.38) contains the Einstein tensor, and this implies that we need to take $12a^2=-\frac{1}{12}$ and $c^2=-\frac{1}{64}$, implying that $b^2=-\frac{1}{16}$.
Next for 5 dimensions Eq. (2.31) reduces to

$$\begin{aligned}&12c\left(\nabla_\mu F^{\mu\lambda}\right)\varphi+\gamma^\mu\left[G^\lambda_\mu-24a^2\Lambda g^\lambda_\mu+12a\left(b+4c\right)\sqrt{\Lambda}F^\lambda_\mu-4\left(b^2+8c^2\right)F_{\mu\nu}F^{\nu\lambda}\right.\\&\left.-2\left(b^2-4c^2\right)g^\lambda_\mu F_{\rho\sigma}F^{\rho\sigma}\right]\varphi+\gamma^{\mu\nu}\left[\left(b+4c\right)\left(2g^\lambda_\mu\nabla_\alpha F^\alpha_\nu-\nabla^\lambda F_{\mu\nu}\right)\right]\varphi\\&+\gamma^{\mu\rho\sigma}\left[-ieg^\lambda_\mu F_{\rho\sigma}-8a\left(b+c\right)\sqrt{\Lambda}g^\lambda_\mu F_{\rho\sigma}+4\left(b+4c\right)\left(b-c\right)F_{\rho\sigma}F^\lambda_\mu\right]\varphi\\&+\gamma^{\lambda\mu\nu\rho\sigma}\left[-2\left(b^2-4c^2\right)\right]F_{\mu\nu}F_{\rho\sigma}\varphi=0.\end{aligned} \tag{2.40}$$

Taking $b+4c=0$ we simplify the above to

$$\begin{aligned}&12c\left(\nabla_\mu F^{\mu\lambda}\right)\varphi+\gamma^\mu\left[G^\lambda_\mu-24a^2\Lambda g^\lambda_\mu-96c^2F_{\mu\nu}F^{\nu\lambda}-24c^2g^\lambda_\mu F_{\rho\sigma}F^{\rho\sigma}\right]\varphi\\&+\gamma^{\mu\rho\sigma}\left[-ieg^\lambda_\mu F_{\rho\sigma}+24ac\sqrt{\Lambda}g^\lambda_\mu F_{\rho\sigma}\right]\varphi\\&+\gamma^{\lambda\mu\nu\rho\sigma}\left[-24c^2\right]F_{\mu\nu}F_{\rho\sigma}\varphi=0.\end{aligned} \tag{2.41}$$

From the γ^μ term we get the Einstein equation

$$G^\lambda_\mu - 24a^2\Lambda g^\lambda_\mu - 96c^2 F_{\mu\nu}F^{\nu\lambda} - 24c^2 g^\lambda_\mu F_{\rho\sigma}F^{\rho\sigma} = 0, \tag{2.42}$$

and get $a = \frac{i}{2\sqrt{6}}$ and $c = \frac{i}{8\sqrt{3}}$, implying $b = -\frac{i}{2\sqrt{3}}$.
For the general case we assume $b = -2(D-3)c$, then Eq. (2.31) can be rewritten as

$$\begin{aligned}
&4c(D-2)\nabla_\mu F^{\mu\lambda}\varphi \\
&+\gamma^\mu\left[G^\lambda_\mu - 2a^2\Lambda(D-1)(D-2)g^\lambda_\mu + 16(D-2)(D-3)c^2\left(F_{\mu\nu}F^{\lambda\nu} - \frac{1}{4}g^\lambda_\mu F_{\rho\sigma}F^{\rho\sigma}\right)\right]\varphi \\
&+\gamma^{\mu\rho\sigma}\left[-ieg^\lambda_\mu F_{\rho\sigma} + 4(D-2)(D-3)ac\sqrt{\Lambda}g^\lambda_\mu F_{\rho\sigma}\right]\varphi \\
&+\gamma^{\lambda\mu\nu\rho\sigma}(-2c^2)(D-1)(D-2)F_{\mu\nu}F_{\rho\sigma}\varphi = 0.
\end{aligned} \tag{2.43}$$

The first term gives the electromagnetic field equation of motion

$$\nabla_\mu F^{\mu\lambda} = 0. \tag{2.44}$$

From the γ^μ term we get

$$G^\lambda_\mu - 2a^2\Lambda(D-1)(D-2)g^\lambda_\mu + 16(D-2)(D-3)c^2\left(F_{\mu\nu}F^{\lambda\nu} - \frac{1}{4}g^\lambda_\mu F_{\rho\sigma}F^{\rho\sigma}\right) = 0 \tag{2.45}$$

By expanding the Einstein tensor G^λ_μ, and matching terms in the above equations we find that

$$\begin{aligned}
2a^2\Lambda(D-1)(D-2) &= -1, \\
16(D-2)(D-3)c^2 &= -\frac{1}{2}.
\end{aligned} \tag{2.46}$$

This implies that $a = \frac{i}{\sqrt{2(D-1)(D-2)}}$ and $c = \frac{i}{4\sqrt{2(D-2)(D-3)}}$. So the supercovariant derivative is determined to be

$$\begin{aligned}
\mathbb{D}_\mu =& \nabla_\mu - ieA_\mu + \frac{i\sqrt{\Lambda}}{\sqrt{2(D-1)(D-2)}}\gamma_\mu - \frac{i}{2}\sqrt{\frac{D-3}{2(D-2)}}\gamma_\nu F^\nu_\mu \\
&+ \frac{i}{4\sqrt{2(D-2)(D-3)}}\gamma_{\mu\rho\sigma}F^{\rho\sigma}
\end{aligned} \tag{2.47}$$

This is the most general form of the super covariant derivative that we will use to determine our effective potential for the cases we will investigate in this thesis.

2.4 Eigenvalues on the N-Sphere

For the QNMs investigation we restrict ourselves to studying spherically symmetrical space times. As such we will need to determine the eigenvalues and eigenfunctions of our spinors and spinor-vectors on the N-sphere, S^N. In this regard we use results obtained by Camporesi and Higuchi who in Ref. [36] have shown how to obtain these eigenfunctions and values for both the S^N and for hyperbolic surfaces. This approach to using the spherical symmetric space time has the advantage that going to higher dimensions is made much simpler when compared to using the

Newman-Penrose formalism as has been used in Ref. [75–77].

2.4.1 Eigenmodes of spinors on S^N

The line element of the S^N is given as [36]

$$d\Omega_N^2 = \sin^2\theta_N d\widetilde{\Omega}_{N-1}^2 + d\theta_N^2, \tag{2.48}$$

where $d\widetilde{\Omega}_{N-1}$ is the metric of the S^{N-1}, all tilde terms will represent quantities from the S^{N-1}. The Dirac covariant derivative on this space is given as

$$\gamma^\mu \nabla_\mu \psi_\lambda = \gamma^\mu \left(\partial_\mu \psi_\lambda + \omega_\mu \psi_\lambda\right), \tag{2.49}$$

where ω_μ is the spin connection, and ψ_λ is a spinor. The spin connection is defined as

$$\omega_\mu = \frac{1}{2}\omega_{\mu ab}\sigma^{ab}, \tag{2.50}$$

with $\Sigma^{ab} = \frac{1}{4}\left[\gamma^a, \gamma^b\right]$ and $\omega_{\mu ab}$ is defined as

$$\omega_{\mu ab} = e_a^\alpha \left(\partial_\mu e_{\alpha b} - \Gamma^\rho_{\mu\alpha} e_{\rho b}\right). \tag{2.51}$$

In the above equation e_a^α is an n-bein and $\Gamma^\rho_{\mu\alpha}$ are the Christoffel symbols on a sphere with the non-zero components given as

$$\Gamma^{\theta_N}_{\theta_i\theta_j} = -\sin\theta_N \cos\theta_N \widetilde{g}_{\theta_i\theta_j}\ ;\ \Gamma^{\theta_j}_{\theta_i\theta_N} = \cot\theta_N \widetilde{g}^{\theta_j}_{\theta_i}\ ;\ \Gamma^{\theta_k}_{\theta_i\theta_j} = \widetilde{\Gamma}^{\theta_k}_{\theta_i\theta_j}. \tag{2.52}$$

Before moving on we will better define what an n-bein is. The elements in an n-bein allow us to more easily convert between a curved space and an orthonormal space. They follow the following set of relations

$$g_{\mu\nu} = e^a_\mu e^b_\nu \delta^{ab},\ e^a_\mu e^\mu_b = \delta_{ab},\ e^a_\nu e^\mu_a = \delta_{\mu\nu}. \tag{2.53}$$

Note that Greek letters represent our curved space indices, and the Latin letters represent our orthonormal indices. For the S^N the n-beins are

$$e^{\theta_N}_N = 1,\ e^{\theta_i}_i = \frac{1}{\sin\theta_i}\widetilde{e}^{\theta_i}_i. \tag{2.54}$$

By using Eqs. (2.52) and (2.53) it can be easily shown that $\gamma^{\theta_i} = \frac{1}{\sin\theta_N}\widetilde{e}^{\theta_i}_i \gamma^i$ and $\gamma^{\theta_N} = \gamma^N$, where the orthonormal gamma matrices respect the ordinary Clifford algebra. If we write the spinors as

$$\psi_\lambda = \begin{pmatrix} \psi^{(1)}_\lambda \\ \psi^{(2)}_\lambda \end{pmatrix} = \begin{pmatrix} A_\lambda(\theta_N)\widetilde{\psi}_\lambda \\ -iB_\lambda(\theta_N)\widetilde{\psi}_\lambda \end{pmatrix}, \tag{2.55}$$

where if we let the spinors on the S^{N-1} have the following eigenvalues

$$\widetilde{\lambda}^\mu \widetilde{\nabla}_\mu \widetilde{\psi}_\lambda = 0;\ \widetilde{\lambda} = \pm\left(l + \frac{N-1}{2}\right), \tag{2.56}$$

then using the Jacobi polynomial we can relate A_λ to B_λ and show that the eigenvalues of our spinors on the S^N can be written as

$$i\lambda = \pm i\left(n + \frac{N}{2}\right),\ n = 0,\ 1,\ 2,\ 3,\ ....\tag{2.57}$$

2.4.2 Eigenmodes of spinor-vectors on S^N

We construct spinors on S^N as $\psi_\mu = (\psi_{\theta_1}, \psi_{\theta_2}, \psi_{\theta_3}, ..., \psi_{\theta_{,N}})$. Then starting from the S^2 we can construct two orthogonal spinors which can be written as the linear combiniation of the basis $\gamma_\mu\psi_\lambda$ and $\nabla_\mu\psi_\lambda$. These two spinors are called the "non-Transverse and Traceless modes" (non-TT modes). In the S^2 these spinors form the complete set of eigenmodes. In higher dimensions, however we must construct more spinors in order to form the complete set of eigenmodes. For the S^N we construct the spinors using linear combinations of those that form the set of spinors on the S^{N-1}.
For instance, on the S^3 we use the two non-TT modes of the S^2 and then using a linear combination of these two spinors we construct a third spinor. This new spinor, however, does not satisfy the non-TT mode condition and is a "Transverse and Traceless eigenmode", specifically this is the TT mode I.
For spheres with N>3 we need to introduce another type of TT mode, which we call the TT mode II. In general, to describe a sphere of N>3 we need one non-TT mode, one TT mode I and $N-3$ TT mode II's.

2.5 Numerical methods

Once we have the effective potential, $V(r)$, from an equation of the form

$$\frac{d}{dr^2}\Psi(r) + V(r)\Psi(r) = \omega^2.\tag{2.58}$$

We will use known methods for solving the equations of this form, such as the WKB method. Note that this is the same form of the equation that we would have for the quantum wave equation.

2.5.1 WKB Approximation

Note that the WKB method can be used to determine the approximate solution to any second order differential equations of the Schrödinger form, and so is typically employed when solving the Schrödinger wave equation [78]. In Ref. [79] we have given an example of how we use the WKB method to solve second order differential equations, which we present in the example below. To start with we have a general second order equation

$$\epsilon^2\frac{d^2y}{dx^2} = Q(x)y\,,\tag{2.59}$$

where $\epsilon \ll 1$ and $Q(x)$ is some function dependent on x. We can solve this equation by assuming the following solution

$$y(x,\epsilon) = A(x,\epsilon)e^{iu(x)/\epsilon}\,.\tag{2.60}$$

Taking the first and second derivatives of this function we see that

$$y(x,\epsilon) = A(x,\epsilon)e^{iu(x)/\epsilon},$$

$$y'(x,\epsilon) = A'(x,\epsilon)e^{iu(x)/\epsilon} + A(x,\epsilon)\left(\frac{iu'(x)}{\epsilon}\right)e^{iu(x)/\epsilon},$$

$$\begin{aligned} y''(x,\epsilon) &= A''(x,\epsilon)e^{iu(x)/\epsilon} + A'(x,\epsilon)\left(\frac{iu'(x)}{\epsilon}\right)e^{iu(x)/\epsilon} + A'(x,\epsilon)\left(\frac{iu'(x)}{\epsilon}\right)e^{iu(x)/\epsilon} \\ &\quad - A(x,\epsilon)\left(\frac{u'(x)}{\epsilon}\right)^2 e^{iu(x)/\epsilon} \\ &= \left(A'' + 2A'\frac{iu'(x)}{\epsilon} + A(\frac{iu''(x)}{\epsilon} - \left(\frac{u'(x)}{\epsilon}\right)^2\right)e^{iu(x)/\epsilon}. \end{aligned} \tag{2.61}$$

Plugging Eq. (2.61) into Eq. (2.59) we get

$$\epsilon^2\left(A'' + 2A'\frac{iu'(x)}{\epsilon} + A(\frac{iu''(x)}{\epsilon} - \left(\frac{u'(x)}{\epsilon}\right)^2\right) - Q(x)A(x,\epsilon) = 0\,. \tag{2.62}$$

Then since ϵ is very small, we can perform a series expansion of A around the point $\epsilon = 0$;

$$\begin{aligned} A(x,\epsilon) &= A_0(x) + \epsilon A_1(x) + \epsilon^2 A_2(x) + ... \\ A'(x,\epsilon) &= A_0'(x) + \epsilon A_1'(x) + \epsilon^2 A_2'(x) + ... \\ A''(x,\epsilon) &= A_0''(x) + \epsilon A_1''(x) + \epsilon^2 A_2''(x) + ... \end{aligned} \tag{2.63}$$

so that Eq. (2.62) becomes

$$\begin{aligned} 0 =& \epsilon^2\left(\left(A_0''(x) + \epsilon A_1''(x) + \epsilon^2 A_2''(x) + ...\right) + 2\left(A_0'(x) + \epsilon A_1'(x) + \epsilon^2 A_2'(x) + ...\right)\frac{iu'(x)}{\epsilon}\right) \\ &+ \epsilon^2\Big(\left(A_0(x) + \epsilon A_1(x) + \epsilon^2 A_2(x) + ...\right)(\frac{iu''(x)}{\epsilon} - \left(\frac{u'(x)}{\epsilon}\right)^2 \\ &- Q(x)\left(A_0(x) + \epsilon A_1(x) + \epsilon^2 A_2(x) + ...\right)\Big)\,. \end{aligned} \tag{2.64}$$

Grouping in terms of powers of ϵ we can solve for $u(x)$.
This method of obtaining QNMs for black holes has been employed for many years, where it had previously been used up to 3rd order in the approximation [80]. However, Konoplya has extended the method up to 6th order [37]. This extension to the 6th order has resulted in more stable and accurate solutions for the WKB when applied to black holes, at the expense of computational time. This increase in computational time is due to the increased complexity in the functions used to solve for the QNMs, see Ref. [37] for the full form of these functions. As such we wish to use a method which could give us the same level of accuracy as the WKB to 6th order without the large computation time. In this respect we have chosen the improved AIM [39–41]. This method is hoped to produce similar results using less computational power, as compared to the WKB 6th order method. In Ch. 3 we show the comparison of results between the two methods.

2.5.2 Improved AIM

We begin by showing how the AIM can be used to solve for QNMs, as shown in Ref. [81]. We then show how this method was improved by Cho et al. in Ref. [42]. Just as for the WKB, the AIM is useful in solving second order differential equations of the form

$$y'' = \lambda_0(x)y' + s_0(x)y\,, \tag{2.65}$$

where λ_0 and s_0 are elements of $C_\infty(a,b)$ [81], and y is some function of x, with $'$ denoting derivatives in terms of x. Taking n derivatives of this equation we obtain the following result

$$y^{(n+2)} = \lambda_n y' + s_n y\,, \tag{2.66}$$

where $\lambda_n = \lambda'_{n-1} + s_{n-1} + \lambda_0\lambda_{n-1}$ and $s_n = s'_{n-1} + s_0\lambda_{n-1}$. We then divide the $n+2$ iteration with the $n+1$ iteration to get the following ratio

$$\frac{y^{(n+2)}}{y^{(n+1)}} = \frac{d}{dx}\ln(y^{(n+1)}) = \frac{\lambda_n(y' + \frac{s_n}{\lambda_n}y)}{\lambda_{n-1}(y' + \frac{s_{n-1}}{\lambda_{n-1}}y)}\,. \tag{2.67}$$

The objective of this method is to use values of n such that

$$\alpha = \frac{s_n}{\lambda_n} \cong \frac{s_{n-1}}{\lambda_{n-1}}. \tag{2.68}$$

So that we can rewrite Eq. (2.67) as

$$\frac{d}{dx}\ln(y^{(n+1)}) = \frac{\lambda_n}{\lambda_{n-1}}\,. \tag{2.69}$$

This has the solution

$$y^{(n+1)} = C_1\lambda_{n-1}\exp\left[\int^x \alpha + \lambda_0 dt\right], \tag{2.70}$$

where C_1 is some integration constant. Plugging this into Eq. (2.66) we obtain the first order equation

$$y' + \alpha y = C_1\exp\left[\int^x \alpha + \lambda_0 dt\right], \tag{2.71}$$

which yields the solution

$$y(x) = \exp\left(-\int^x \alpha dt\right)\left[C_2 + C_1\int^x \exp\left(\int^t (\lambda_0(\tau) + 2\alpha(\tau))\,d\tau\right)dt\right], \tag{2.72}$$

where C_2 is another integration constant. In our case this gives the solution of the wavefunction. By using the boundary conditions we are able to obtain the allowed QNMs.

In the case of QNMs we need to know α to a very high precision, and so in order to satisfy the condition given in Eq. (2.68) we would need to use large values of n. Taking this iterative approach would result in large computation time. Instead we use the approach given by Cho et al. in Ref. [42], where they have used a Taylor

expansion to determine the values of λ_n and s_n as follows:

$$\begin{aligned} \lambda_n(\xi) &= \sum_{i=0}^{\infty} c_n^i (x-\xi)^i \,, \\ s_n(\xi) &= \sum_{n}^{\infty} d_n^i (x-\xi)^i \,, \end{aligned} \tag{2.73}$$

where ξ is value around which the AIM is performed and c_n^i and d_n^i are our Taylor coefficients. Plugging these into the previous expressions for λ_n and s_n we have the following recursion relation:

$$\begin{aligned} c_n^i &= (i+1)c_{n-1}^{i+1} + d_{n-1}^i + \sum_{k=0}^{i} c_0^k c_{n-1}^{i-k} \,, \\ d_n^i &= (i+1)d_{n-1}^{i+1} + \sum_{k=0}^{i} d_0^k c_{n-1}^{i-k} \,. \end{aligned} \tag{2.74}$$

We calculate the values of our QNMs by solving $d_n^0 c_{n-1}^0 - d_{n-1}^0 c_n^0 = 0$, where n represents the number of iterations we wish to perform. This approach of using the Taylor expansion considerably speeds up the computation time. As we do not need to keep the full derivative of the function each time, instead keeping only the coefficients of the Taylor series. Where as stated previously this is advantageous since in order to accurately compute the QNMs we need to consider a very high number of iterations, in fact we use 200 iterations in the following work.

2.6 Absorption probabilities of a black hole

In 1974 Steven Hawking proposed that by applying quantum effects to a black hole one could show that the black hole would evaporate over time [82]. His argument was that due to the quantum fluctuations on the surface of the black hole we could expect the black hole to emit particles in the same way that a hot object radiates heat. This radiation of particles from the surface of the black hole would lead to the black hole losing mass over time, and hence would have a finite lifetime, as it would eventually evaporate away all of its mass. Furthermore Hawking showed that a black hole would have a lifetime of the order $10^{71}\,(M_\odot/M)^{-3}\,s$, where $M_\odot$ is the solar mass and M is the mass of the black hole. So a black hole with a mass of the sun would exist for a very long time indeed. However, for very small black holes the life time could be much shorter. So we may be able to put astrophysical constraints on the evaporation of these types of black holes. Unruh pointed out that an important parameter for determining the likely hood of the quantum evaporation of these small black hole is to know what the absorption probability associated to the black hole is for the various possible fields that it could emit [83]. In our case we wish to calculate the absorption probabilities as this allows us to determine the likelihood of a field with a particular quantum state being formed at the surface of the black hole, and this would give us an indication of the likely QNMs we would detect from the black hole. In Unruh's paper he provides a methodology for calculating the absorption probabilities associated with scalar fields near Schwarzschild black holes [83]. This method is only valid in the low energy regime. Instead, in this thesis, we use a method developed by Iyer and Will to obtain absorption probabilities for more general cases [80].

For the Iyer and Will approach to finding the absorption probabilities we start from Eq. (2.58) and perform a change of variables, namely $x = \omega r$, this is purely for convenience. Such that we have the following second order differential equation

$$\left(\frac{d^2}{dx_*^2} + Q\right)\Phi = 0, \tag{2.75}$$

where $Q(x) = -\omega^2 - V(x)$. The absorption probability is then determined to be [84]

$$\left|A_j(\omega)\right|^2 = \exp\left[-2\int_{x_1}^{x_2} dx\sqrt{Q(x)}\right], \tag{2.76}$$

where x_1 and x_2 are turning points in Q, namely $Q(x_{1,2}) = 0$ for the given energy ω. This method, however, is only valid for $\omega^2 \ll V$. In the case of $\omega^2 \sim V$ the exponential will go to infinity and so the method is not valid. However, Iyer and Will have shown that by taking the third order WKB approximation we can obtain solutions that are valid for all energy regimes [80]. In this case the absorption probabilities are given as

$$\left|A_j(\omega)\right|^2 = \frac{1}{1 + e^{2S(\omega)}}, \tag{2.77}$$

with

$$\begin{aligned} S(\omega) = {} & \pi k^{1/2}\left[\frac{1}{2}z_0^2 + \left(\frac{15}{64}b_3^2 - \frac{3}{16}b_4\right)z_0^4\right] \\ & + \pi k^{1/2}\left[\frac{1155}{2048}b_3^4 - \frac{315}{256}b_3^2 b_4 + \frac{35}{128}b_4^2 + \frac{35}{64}b_3 b_5 - \frac{5}{32}b_6\right]z_0^6 \\ & + \pi k^{-1/2}\left[\frac{3}{16}b_4 - \frac{7}{64}b_3^2\right] \\ & - \pi k^{-1/2}\left[\frac{1365}{2048}b_3^4 - \frac{525}{256}b_3^2 b_4 + \frac{85}{128}b_4^2 + \frac{95}{64}b_3 b_5 - \frac{25}{32}b_6\right]z_0^2. \end{aligned} \tag{2.78}$$

Note that z_0^2, b_0 and k are determined by the Taylor expansion of Q around its peak x_0, and they are determined as follows [80]

$$\begin{aligned} Q &= Q_0 + \frac{1}{2}Q_0^{(2)}z^2 + \sum_{n=3}\frac{1}{n!}\left(\frac{d^nQ}{dx^n}\right)_0 z^n \\ &\equiv k\left[z^2 - z_0^2 + \sum_{n=3} b_n z^n\right], \end{aligned} \tag{2.79}$$

and

$$\begin{aligned} & z = x - x_0; \quad z_0^2 \equiv -2\frac{Q_0}{Q_0''} \\ & k \equiv \frac{1}{2}Q_0''; \quad b_n \equiv \left(\frac{2}{n!Q_0''}\right)\left(\frac{d^nQ}{dx^n}\right)_0. \end{aligned} \tag{2.80}$$

Note that in the above equations the subscript zero denotes maximal values obtained when plugging in x_0 The notations and techniques developed in this chapter shall now be applied to obtain the QNMs for Reissner-Nordström type black holes in Ch.3, and the AdS space time in Ch. 4.

Chapter 3

Electrically charged black holes

We begin our investigation into QNMs for spin-3/2 fields by looking at the electrically charged space-time of a higher dimensional Reissner-Nordström black hole. Where our interest is in determining the effect that the electric charge has on the allowed QNMs as compared to the Schwarzschild cases as determined in Ref. [73].
The Reissner-Nordström space time is a solution to the EFE for massive objects which are non-rotating and have a non-zero electric charge. The line element for this type of black hole is given as [85],

$$ds^2 = -f(r)dt^2 + \frac{1}{f(r)}dr^2 + r^2 d\bar{\Omega}_N^2, \tag{3.1}$$

where $f = 1 - \frac{2M}{r^{D-3}} + \frac{Q^2}{r^{(2D-6)}}$, and $D = N + 2$. The term $d\bar{\Omega}_N$ denotes the metric of the S^N, and throughout the first part of the thesis we will use terms with over bars to denote terms coming from this metric. We also need to define the electromagnetic tensor $F_{\mu\nu}$, with D dimensional equivalent of the four potential [86],

$$A_t = \frac{q}{(D-3)r^{D-3}} \quad \Longrightarrow \quad F_{tr} = \frac{q}{r^{D-2}}, \tag{3.2}$$

where $Q^2 = \frac{1q^2}{2(D-2)(D-3)}$. Although the Schwarzschild metric and the Reissner-Nordström metric are very similar, the existence of two horizons, the event horizon and the Cauchy horizon, is a crucial difference between the two metrics [87]. As usual these horizons are located where the radial component of our metric diverges, that is $f(r) = 0$, and it can be easily shown that the result is

$$r_\pm = \left(M \pm \sqrt{M^2 - Q^2}\right)^{\frac{1}{D-3}}. \tag{3.3}$$

In the extremal case, $Q = M$, these two horizons are degenerate. Furthermore this result shows that it is not physical to have an object that has $Q > M$ as this would mean there exist no physical horizon to shield the singularity [88].
In the next section we will obtain the effective potential and radial equations for the spin-3/2 fields near the electrically charged black holes. To do so we use the super covariant derivative obtained in Eq. (2.47) and plug it into the Rarita-Schwinger equation as given in Eq. (B.10).

3.1 Potential function

For convenience we rewrite the Rarita-Schwinger equation as

$$\gamma^{\mu\nu\alpha}\tilde{\mathcal{D}}_\nu \psi_\alpha = 0, \tag{3.4}$$

where $\tilde{\mathcal{D}}_\nu$ is the supercovariant derivative in Eq. (2.47), with $\Lambda = 0$ such that we have

$$\mathcal{D}_\mu = \nabla_\mu - ieA_\mu - \frac{i}{2}\sqrt{\frac{D-3}{2(D-2)}}\gamma_\nu F^\nu_\mu + \frac{i}{4\sqrt{2(D-2)(D-3)}}\gamma_{\mu\rho\sigma}F^{\rho\sigma}. \tag{3.5}$$

We must solve for both the case of the non-TT eigenfunctions and the TT eigenfunctions, where we shall begin with the non-TT eigenfunctions.

3.1.1 Non-TT eigenfunctions

We can represent the spin-3/2 fields using spinor representation, where ϕ_r, ϕ_t, $\phi^{(1)}_\theta$ and $\phi^{(2)}_\theta$ represent the two-spinors of the radial, temporal and angular parts respectively. However, these two-spinors need to be projected onto the S^N. In order to do this we use the eigenspinor of the S^N, with $N = D-2$, represented as $\bar{\psi}_{(\lambda)}$ [36, 74] .[1] The eigenvalues, $i\bar{\lambda}$, of the eigenspinor $\bar{\psi}_{(\lambda)}$ are given as $\bar{\lambda} = (j + (D-3)/2)$, where $j = 3/2,\ 5/2,\ 7/2,\ \ldots$ [74]. In the case of the non-TT eigenfunctions we can write the radial, ψ_r, and temporal, ψ_t, wave functions as [74]

$$\psi_r = \phi_r \otimes \bar{\psi}_{(\lambda)} \quad \text{and} \quad \psi_t = \phi_t \otimes \bar{\psi}_{(\lambda)}. \tag{3.6}$$

Our angular wave function is written as

$$\psi_{\theta_i} = \phi^{(1)}_\theta \otimes \bar{\nabla}_{\theta_i}\bar{\psi}_{(\lambda)} + \phi^{(2)}_\theta \otimes \bar{\gamma}_{\theta_i}\bar{\psi}_{(\lambda)}, \tag{3.7}$$

where $\phi^{(1)}_\theta$, $\phi^{(2)}_\theta$ are functions of r and t, and behave like 2-spinors. We will use the Weyl gauge, such that $\phi_t = 0$, and then introduce a gauge invariant variable in order to determine the gauge invariant equations of motion using this variable.

Equations of motion

We begin by looking at the case of $\mu = t$ in Eq. (3.4), and obtain the following result

$$\begin{aligned} 0 = &-\left(i\bar{\lambda} + (D-2)\frac{\sqrt{f}}{2}i\sigma^3 + (D-2)\frac{iQ}{2r^{D-3}}\right)\phi_r \\ &+\left(i\bar{\lambda}\partial_r - \frac{1}{4}\frac{(D-2)(D-3)}{r\sqrt{f}}i\sigma^3 + (D-3)\frac{i\bar{\lambda}}{2r}\right)\phi^{(1)}_\theta \\ &+\left((D-2)\partial_r + (D-3)\frac{i\bar{\lambda}}{r\sqrt{f}}i\sigma^3 + \frac{(D-2)(D-3)}{2r}\right)\phi^{(2)}_\theta. \end{aligned} \tag{3.8}$$

[1] A detailed explanation of how this is done is given in Refs. [36, 74]. In particular see Ref. [74] where we have explained this approach.

Next we consider $\mu = r$ to get the second equation of motion as

$$0 = \left[-\frac{i\bar{\lambda}}{\sqrt{f}}\partial_t + \frac{i\bar{\lambda}f'}{4\sqrt{f}}\sigma^1 - \frac{(D-3)(D-2)}{4r}\sigma^2 + (D-3)\frac{i\bar{\lambda}\sqrt{f}}{2r}\sigma^1 \right]\phi_\theta^{(1)} + \left[-\frac{D-2}{\sqrt{f}}\partial_t + \frac{(D-2)f'}{4\sqrt{f}}\sigma^1 + (D-3)\frac{i\bar{\lambda}}{r}\sigma^2 + (D-2)(D-3)\frac{\sqrt{f}}{2r}\sigma^1 \right]\phi_\theta^{(2)}. \tag{3.9}$$

Finally we consider the case of $\mu = \theta_i$ where

$$\begin{aligned} 0 = &\left(\partial_t - \frac{f'}{4}\sigma^1 + i\bar{\lambda}\frac{\sqrt{f}}{r}\sigma^2 - (D-3)\frac{f}{2r}\sigma^1\right)\phi_r \\ &+ \left(\frac{\bar{\lambda}}{r\sqrt{f}}\sigma^3\partial_t - i\bar{\lambda}\frac{f'}{4r\sqrt{f}}\sigma^2 - i\bar{\lambda}\frac{\sqrt{f}}{r}\sigma^2\partial_r - \frac{(D-3)(D-4)}{4r^2}\sigma^1 - i\bar{\lambda}(D-4)\frac{\sqrt{f}}{2r^2}\sigma^2 \right. \\ &\left. - \bar{\lambda}(D-2)\frac{Q}{2r^{D-1}}\sigma^1\right)\phi_\theta^{(1)} \\ &+ \left(-\frac{D-3}{r\sqrt{f}}i\sigma^3\partial_t - (D-3)\frac{f'}{4r\sqrt{f}}\sigma^2 - (D-3)\frac{\sqrt{f}}{r}\sigma^2\partial_r + (D-4)\frac{i\bar{\lambda}}{r^2}\sigma^1 \right. \\ &\left. - (D-3)(D-4)\frac{\sqrt{f}}{2r^2}\sigma^2 + (D-3)(D-2)\frac{iQ}{2r^{D-1}}\sigma^1\right)\phi_\theta^{(2)}, \end{aligned} \tag{3.10}$$

$$0 = -\frac{\sqrt{f}}{r}\sigma^2\phi_r + \left(\frac{1}{r\sqrt{f}}i\sigma^3\partial_t + \frac{f'}{4r\sqrt{f}}\sigma^2 + \frac{\sqrt{f}}{r}\sigma^2\partial_r + (D-4)\frac{\sqrt{f}}{2r^2}\sigma^2 - (D-2)\frac{iQ}{2r^{D-1}}\sigma^1\right)\phi_\theta^{(1)} - \frac{D-4}{r^2}\sigma^1\phi_\theta^{(2)}. \tag{3.11}$$

Here we obtain two equations of motion. However it can be shown that these four equations of motion are not linearly independent, and one can be obtained through a combination of the other three. As such we will only use Eqs. (3.8), (3.9) and (3.11) in the following.

Effective potential

We can now introduce the gauge invariant variable, where the method is described in Ref. [74] and is repeated here for clarity. We begin by considering the transformation of $\varphi = \phi \otimes \bar{\psi}_\lambda$, then the radial and temporal parts of our field would transform as

$$\psi_t' = \psi_t + \partial_t\phi - \frac{f'}{4}\sigma^1\phi \text{ and } \psi_r' = \psi_r + \partial_r\phi. \tag{3.12}$$

The gauge transformation of the angular part however is more complicated

$$\begin{aligned}
&\psi'_{\theta_i} = \psi_{\theta_i} \mathcal{D}_{\theta_i} \varphi, \\
\Longrightarrow\ &\left(\phi_\theta^{(1)\prime} \otimes \bar{\nabla}_{\theta_i} + \phi_\theta^{(2)\prime} \otimes \bar{\gamma}_{\theta_i}\right) \bar{\psi}_\lambda = \\
&\left(\left(\phi_\theta^{(1)} + \phi\right) \otimes \bar{\nabla}_{\theta_i} + \left(\phi_\theta^{(2)} + \left(\frac{\sqrt{f}}{2} i\sigma^3 + \frac{iQ}{2r^{D-3}}\right)\varphi\right) \otimes \bar{\gamma}_{\theta_i}\right) \bar{\psi}_\lambda, \\
\Longrightarrow\ &\phi_\theta^{'(1)} = \phi_\theta^{(1)} + \phi \ ; \ \phi_\theta^{'(2)} = \phi_\theta^{(2)} + \left(\frac{\sqrt{f}}{2}(i\sigma^3)\phi + \frac{iQ}{2r^{D-3}}\right)\phi.
\end{aligned} \tag{3.13}$$

Considering these gauge transformations we can construct a gauge invariant combination, where a simple choice would be

$$\Phi = -\left(\frac{\sqrt{f}}{2} i\sigma^3 + \frac{iQ}{2r^{D-3}}\right)\phi_\theta^{(1)} + \phi_\theta^{(2)}. \tag{3.14}$$

Plugging this into Eq. (3.8), Eq. (3.9) and Eq. (3.11) we obtain the equation of motion for the gauge invariant variable Φ,

$$\begin{aligned}
&\left((D-2)\frac{\sqrt{f}}{2} + \left(\bar{\lambda} + (D-2)\frac{Q}{2r^{D-3}}\right)\sigma^3\right) \\
&\left[-\frac{D-2}{f}\sigma^1\partial_t + (D-2)\frac{f'}{4f} - \frac{(D-3)\bar{\lambda}}{r\sqrt{f}}\sigma^3 + \frac{(D-2)(D-3)}{2r}\right]\Phi = \\
&\left((D-2)\frac{\sqrt{f}}{2} - \left(\bar{\lambda} + (D-2)\frac{Q}{2r^{D-3}}\right)\sigma^3\right) \\
&\left[(D-2)\partial_r - \frac{\bar{\lambda}}{r\sqrt{f}}\sigma^3 + \frac{(2D-7)(D-2)}{2r} + (D-2)(D-4)\frac{Q}{2r^{D-2}\sqrt{f}}\sigma^3\right]\Phi.
\end{aligned} \tag{3.15}$$

We can then rewrite Φ as

$$\Phi = \begin{pmatrix} \phi_1 e^{-i\omega t} \\ \phi_2 e^{-i\omega t} \end{pmatrix}, \tag{3.16}$$

where ϕ_1 and ϕ_2 are purely radially dependent terms. Furthermore we set

$$\phi_1 = \frac{(\frac{D-2}{2})^2 f - \left(\bar{\lambda} + C\right)^2}{B r^{\frac{D-4}{2}} f^{1/4}} \tilde{\phi}_1 \ \text{ and } \ \phi_2 = \frac{(\frac{D-2}{2})^2 f - \left(\bar{\lambda} - C\right)^2}{A r^{\frac{D-4}{2}} f^{1/4}} \tilde{\phi}_2, \tag{3.17}$$

where

$$A = \frac{D-2}{2}\sqrt{f} + \left(\bar{\lambda} + C\right); \ \ B = \frac{D-2}{2}\sqrt{f} - \left(\bar{\lambda} + C\right) \ \text{ and } \ C = (D-2)\frac{Q}{2r^{D-3}}. \tag{3.18}$$

Applying Eq. (3.16) and Eq. (3.17) to Eq. (3.15) we get the following set of coupled equations

$$\left(f\partial_r - W\right)\tilde{\phi}_1 = i\omega\tilde{\phi}_2; \ \ \left(f\partial_r + W\right)\tilde{\phi}_2 = i\omega\tilde{\phi}_1, \tag{3.19}$$

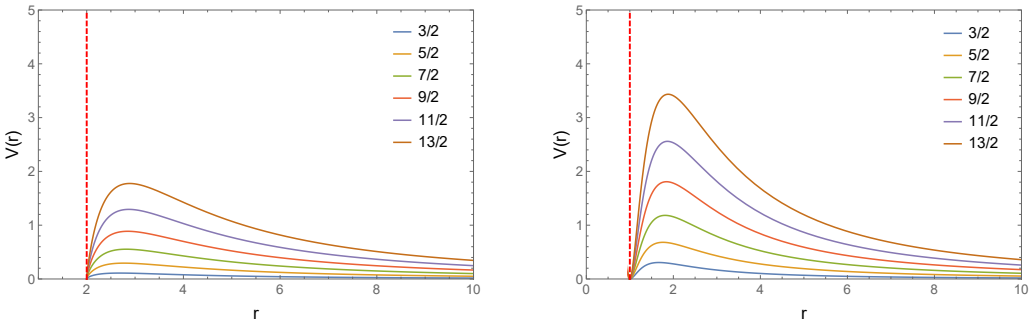

(A) Potential function with $D = 4$ and $Q = 0$ for $j = 3/2$ to $j = 13/2$.

(B) Potential function with $D = 4$ and $Q = 1$ for $j = 3/2$ to $j = 13/2$.

FIGURE 3.1: In the above plots we have shown the effective potential function, in Eq. (3.22), for the non-TT eigenspinors in 4 dimensions for $Q = 0,\ 0.1,\ 0.5, 1$,and have set $M = 1$. Furthermore, note that the red dashed line indicated the radial location of the event horizon. These figures are taken from [89].

where

$$W = \frac{(D-3)\sqrt{f}}{rAB}\left[(\bar{\lambda}+C)\frac{2}{D-2}AB + \frac{D-2}{2}\left(C+\bar{\lambda}\left(1-f\right)\right)\right] - \frac{D-4}{r(D-2)}\sqrt{f}(\bar{\lambda}+C). \tag{3.20}$$

Decoupling these two equations we obtain the following radial equations

$$-\frac{d^2}{dr_*^2}\tilde{\phi}_1 + V_1\tilde{\phi}_1 = \omega^2\tilde{\phi}_1; \quad -\frac{d^2}{dr_*^2}\tilde{\phi}_2 + V_2\tilde{\phi}_2 = \omega^2\tilde{\phi}_2, \tag{3.21}$$

where r_* is the tortoise coordinate with the definition $dr_* = \frac{1}{f(r)}dr$, and

$$V_{1,2} = \pm f(r)\frac{dW}{dr} + W^2. \tag{3.22}$$

Setting $Q = 0$ in Eqs. (3.21) we recover the Schwarzschild potential as given in Ref. [74].

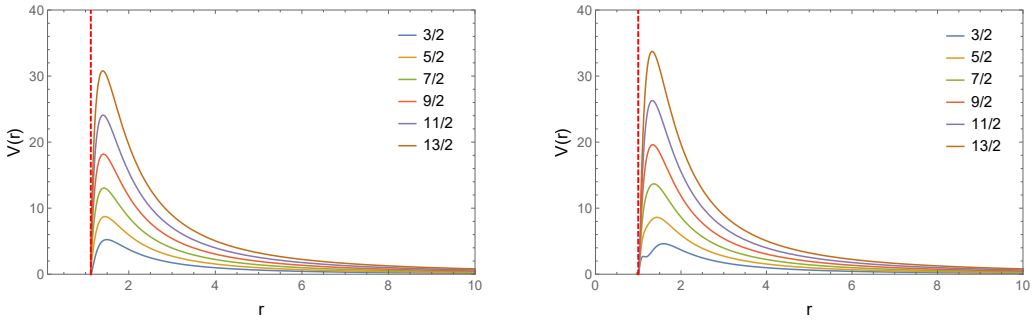

(A) Potential function with $D = 9$ and $Q = 0$ for $j = 3/2$ to $j = 13/2$.

(B) Potential function with $D = 9$ and $Q = 1$ for $j = 3/2$ to $j = 13/2$.

FIGURE 3.2: In the above plots we have shown the effective potential function, in Eq. (3.22), for the non-TT eigenspinors in 9 dimensions for $Q = 0,\ 0.1,\ 0.5, 1$,and have set $M = 1$. Furthermore, note that the red dashed line indicated the radial location of the event horizon. These figures are taken from [89].

In Fig. 3.1, panel A is the case of the Schwarzschild metric, and its values match those of Ref. [73, 74]. In Fig. 3.2 it is clear that as the value of the potential maximum is directly related to the electric charge of the black hole. This would suggest that for larger values of the electric charge we would expect to see larger frequencies for the QNM, since large potential barriers would reflect more energetic fields. As is the case with the ordinary Schwarzschild black hole the larger the value of j the larger the potential maximum, similarly the potential maximum is connected to the number of dimensions we are investigating. Note that in the extremal case, that is $Q = M$, we see a second local maximum appear inside the radial location of the event horizon. This double maximum can be seen in Ref. [89]. Although these maximums are inside the event horizon they do have an effect on the numerical calculations in determining the allowed QNMs, as discussed in Sec. 3.2. We would also like to note that the event horizon in Fig. 3.1 and 3.2 is in a different location this is due to the exponential reliance on the number of dimensions in the metric. Next we look at the effective potential for the TT eigenfunctions.

3.1.2 TT eigenfunctions

Equations of motion

The ψ_r and ψ_t components are set to be the same as in the "non-TT eigenfunctions" case given in Eq. (3.6), however in this case $\phi_r = \phi_t = 0$ [74]. The angular part is now given as

$$\psi_{\theta_i} = \phi_\theta \otimes \bar{\psi}_{\theta_i}, \tag{3.23}$$

where $\bar{\psi}_{\theta_i}$ is the TT mode eigenspinor-vector which includes the "TT mode I" and "TT mode II", as described in Ref. [74]. Following the same procedure as that of the "non-TT eigenfunctions" we obtain four equations of motion. In this case, however, we only have one non-zero solution given as

$$\left(\frac{1}{r\sqrt{f}} i\sigma^3\partial_t + \frac{\sqrt{f}}{r}\sigma^2\partial_r + \frac{f'}{4r\sqrt{f}}\sigma^2 + (D-4)\frac{\sqrt{f}}{2r^2}\sigma^2 + \frac{i\bar{\zeta}}{r^2}\sigma^1 - (D-2)\frac{iQ}{2r^{D-1}}\sigma^1\right)\phi_\theta = 0. \tag{3.24}$$

It is not necessary for us to determine the gauge invariant variable in this case as ϕ_θ is already gauge invariant. We therefore move straight into determining the effective potential.

Effective potential

We can rewrite ϕ_θ as

$$\phi_\theta = \sigma^2 \begin{pmatrix} \Psi_{\theta_1} e^{-i\omega t} \\ \Psi_{\theta_2} e^{-i\omega t} \end{pmatrix}. \tag{3.25}$$

Substituting Eq.(3.25) into Eq. (3.24) we get the following set of coupled equations

$$\begin{aligned} \left(f\partial_r + \frac{f'}{4} + (D-4)\frac{f}{2r} - \left(\frac{\bar{\zeta}\sqrt{f}}{r} - (D-2)\frac{Q\sqrt{f}}{2r^{D-2}} \right) \right) \Psi_{\theta_1} = i\omega \Psi_{\theta_2}; \\ \left(f\partial_r + \frac{f'}{4} + (D-4)\frac{f}{2r} + \left(\frac{\bar{\zeta}\sqrt{f}}{r} - (D-2)\frac{Q\sqrt{f}}{2r^{D-2}} \right) \right) \Psi_{\theta_2} = i\omega \Psi_{\theta_1}. \end{aligned} \tag{3.26}$$

Setting

$$\tilde{\Psi}_{\theta_1} = r^{\frac{D-4}{2}} f^{\frac{1}{4}} \Psi_{\theta_1} \text{ and } \tilde{\Psi}_{\theta_2} = r^{\frac{D-4}{2}} f^{\frac{1}{4}} \Psi_{\theta_2} \tag{3.27}$$

we can simplify the equations in Eq. (3.26), and get the following

$$\begin{aligned} (f\partial_r - \mathbb{W})\,\tilde{\Psi}_{\theta_1} = i\omega \tilde{\Psi}_{\theta_1}; \\ (f\partial_r + \mathbb{W})\,\tilde{\Psi}_{\theta_2} = i\omega \tilde{\Psi}_{\theta_2} \end{aligned} \tag{3.28}$$

where

$$\mathbb{W} = \frac{\bar{\zeta}\sqrt{f}}{r} - (D-2)\frac{Q\sqrt{f}}{2r^{D-2}}. \tag{3.29}$$

We now decouple the equations in Eq. (3.28) and obtain the radial equations

$$-\frac{d}{dr_*^2}\tilde{\Psi}_{\theta_1} + \mathbb{V}_1 = \omega^2 \Psi_{\theta_1} \text{ and } -\frac{d^2}{dr_*^2}\tilde{\Psi}_{\theta_2} + \mathbb{V}_2 \tilde{\Psi}_{\theta_2} = \omega^2 \tilde{\Psi}_{\theta_2}, \tag{3.30}$$

where

$$\mathbb{V}_{1,2} = \pm f(r)\frac{d\mathbb{W}}{dr} + \mathbb{W}^2 \tag{3.31}$$

and our eigenvalue $\bar{\zeta}$ is given as $\bar{\zeta} = j + (D-3)/2$ with $j = 3/2, 5/2, 7/2, ...$ As noted in Ref. [74] the Schwarzschild case of this potential is the same as for Dirac particles in a general dimensional Schwarzschild black hole [90], this however is not true for the Reissner-Nordström case. For the spin-3/2 field one needs to use the supercovariant derivative in the charged black hole space-time. Whereas for the Dirac field one would still use the ordinary covariant derivative. The extra terms in the supercovariant derivative would render the effective potential of the spin-3/2 field in the TT mode to be different from that of the Dirac field in the same space-time.

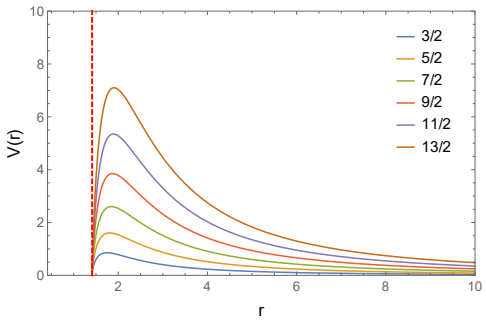

(A) Potential function with $D = 4$ and $Q = 0$ for $j = 3/2$ to $j = 13/2$.

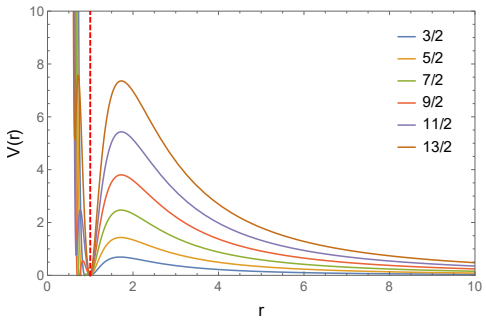

(B) Potential function with $D = 4$ and $Q = 0.1$ for $j = 3/2$ to $j = 13/2$.

FIGURE 3.3: In the above plots we have shown the effective potential function, in Eq. (3.31), for the TT eigenspinors in 4 dimensions for $Q = 0,\ 0.1,\ 0.5, 1$,and have set $M = 1$. Furthermore, note that the red dashed line indicated the radial location of the event horizon. These figures are taken from [89]

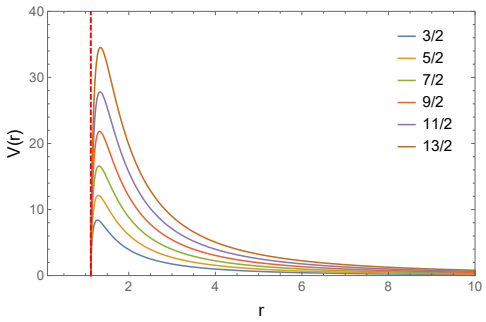

(A) Potential function with $D = 4$ and $Q = 0.5$ for $j = 3/2$ to $j = 13/2$.

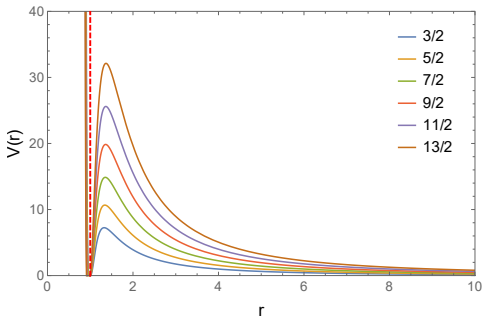

(B) Potential function with $D = 4$ and $Q = 1$ for $j = 3/2$ to $j = 13/2$.

FIGURE 3.4: In the above plots we have shown the potential function, in Eq.(3.31), for the TT eigenspinors in 9 dimensions for $Q = 0,\ 0.1,\ 0.5, 1$,and have set $M = 1$. Furthermore, note that the red dashed line indicated the radial location of the event horizon. These figures are taken from [89].

In Fig. 3.4 we see the same behaviour of the potential function as we did for the non-TT eigenfunction case. As such we expect the same behaviour from our QNMs.

3.2 QNMs

In order to obtain the QNMs we have chosen to use the WKB, to 3rd and 6th order, and the AIM methods in order to determine them. Our interest in generating the numerical values of the allowed QNMs is that we would like to see how the electric charge, Q, changes the values of the QNMs. A particularly interesting case of the Reissner-Nordström black hole would be the extremal case with $Q = M$. We will present the results for the allowed QNMs in the cases of $Q = 0.1$, $Q = 0.5$, and $Q = 1$ for both “non-TT eigenfunction related" and “TT eigenfunction related" potentials from $D = 4$ to $D = 7$.

3.2.1 non-TT eigenfunctions related QNMs

The potentials V_1 and V_2 in Eq. (3.21) are isospectral and so we need choose only one and generate the QNMs as described by the procedure given in Ch. 2, we shall use V_1 to generate our results. In Fig. 3.6 we have plotted the values for the allowed QNMs for the spin-3/2 fields for varying values of the dimension D, as well as for varying values of the electric charge Q. Note that in obtaining these values we have set $M = 1$, as was done for the case of the Schwarzschild black hole in Ref. [74]. We note that as the value of n increases, for fixed values of l and D, the real part of the QNM decreases and the magnitude of the imaginary part increases, this is the same result as we have seen for the Schwarzschild black hole. This result suggests that the lower modes are easier to detect compared to the higher less energetic modes, plus they decay the slowest. We also note that an increase in the number of dimensions results in the QNM being emitted more energetically. This can be understood by considering the change in the potentials as the dimension is increased, as shown in Fig. 3.2. From $D = 4$ to $D = 7$ the maximum value of the potential increases as D is increased. Hence, the real part of the QNM frequency would also increase. Lastly, when the charge Q is increased, the real part of the frequency for the same mode increases while the magnitude of the imaginary part also increases. This is consistent with the change of the effective potentials as Q is increased as shown in Fig. 3.2. As Q is increased from 0 to 1 (in units of M), the maximum value of the potential increases, hence the real part of the QNM frequency increases. On the other hand, the potential tends to sharpen as Q is increased, this implies that the field can decay faster, giving a large decay constant or a large absolute value of the imaginary part of the frequency.
In the figures below we have omitted certain values for the QNMs, this is due to the values being physically inconsistent. We can see from Fig. 3.2 that we obtain spurious results for our potential functions inside of the event horizon as the black holes space time dimensions is 9 and when the charge of the black hole has a charge of $Q = 1$. This is a case where the mass is equal to the charge and so we are at the limits of what is allowed in GR.
We also find that there is a strong disagreement for the WKB methods in the cases of $Q = M$, with the dimension higher than 7. The reason of the disagreement is two-folds. The first one is again the problem with the WKB series expansion mentioned above. The second one is due to the peculiar behaviour of the effective potential.
As shown in Fig.3.2, it is clear that for the $j = 3/2$ potentials in the cases $D > 7$,

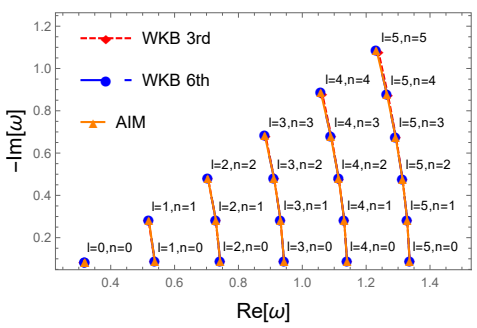

(A) QNMs for D=4 and Q=0.1.

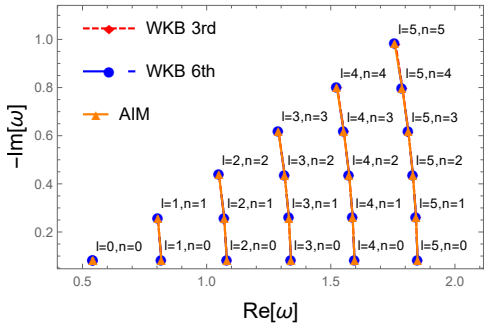

(B) QNMs for D=4 and Q=1.

FIGURE 3.5: In the above plot we have shown the relation between the QNMs for the non-TT eigenspinors for differing values of the dimension, D, as well as the electric charge Q, note that in the above $M = 1$. The values of l and n are the angular and principal quantum number respectively. These figures are taken from [89].

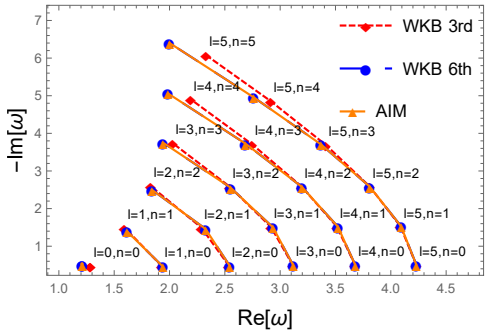

(A) QNMs for D=7 and Q=0.1.

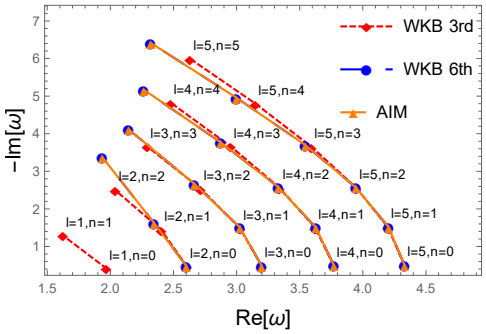

(B) QNMs for D=7 and Q=0.5.

FIGURE 3.6: In the above plot we have shown the relation between the QNMs for the non-TT eigenspinors for differing values of the dimension, D, as well as the electric charge Q, note that in the above $M = 1$. The values of l and n are the angular and principal quantum number respectively. Note that in the higher dimensions some of the labels have been removed to make the figures easier to read. These figures are taken from [89].

a second local maximum will develop. This happens not just for the $j = 3/2$ cases but also for potentials with other j values. For larger values of j, the dimension at which the potential will have this behaviour gets higher. The presence of a second maximum renders the WKB approximation and the AIM to be not reliable so we have only listed the results up to $D = 7$.

3.2.2 TT eigenfunctions related QNMs

For the “TT eigenfunction related" cases, both WKB and AIM present reasonable results. We have to note that there is no “TT eigenfunction related" case in the 4-dimensional Reissner-Nordström spacetime because of the absent of the TT eigenmodes on 2-sphere. In Fig. 3.8, we present the TT QNMs for $Q = 0.1$, $Q = 0.5$, and $Q = 1$ from $D = 5$ to $D = 7$. The change in QNM frequencies is similar to that for non-TT cases when either n or D is changed. The result indicates that when Q gets larger, the real part decreases and the absolute value of imaginary part also increases. This is consistent with the change of the TT potential with Q, which is

plotted in Fig. 3.4. We can see that when Q is increased, the maximum value of the potential decreases. This implies that the real part of the QNM frequency decreases accordingly. In addition to this the potential broadens when Q is increased so the mode decays slower which implies that the absolute value of the imaginary part of the frequency becomes smaller. Note that this trend is just the opposite to that for the non-TT cases for $D < 7$.

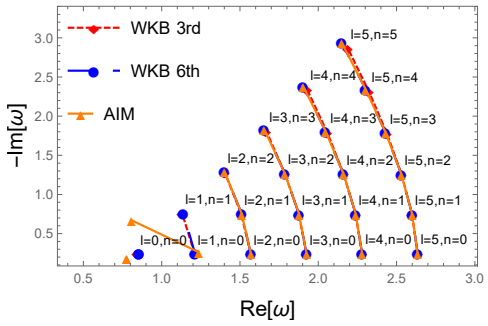

(A) QNMs for D=5 and Q=0.1.

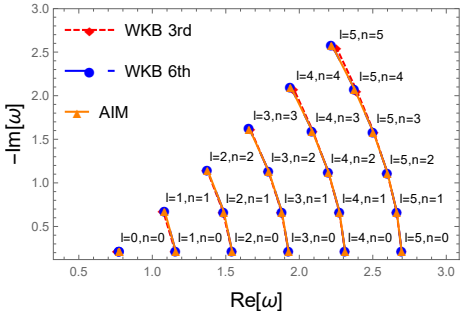

(B) QNMs for D=5 and Q=1.

FIGURE 3.7: In the above plot we have shown the relation between the QNMs for the TT eigenspinors for differing values of the dimension, D, as well as the electric charge Q, note that in the above $M = 1$. The values of l and n are the angular and principal quantum number respectively. Note that in the higher dimensions some of the labels have been removed to make the figures easier to read. These figures are taken from [89]

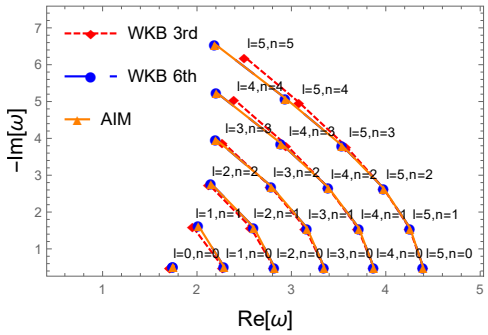

(A) QNMs for D=7 and Q=0.1.

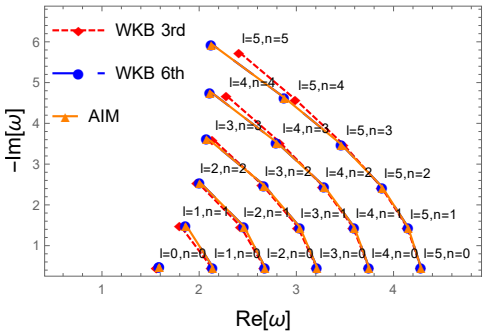

(B) QNMs for D=7 and Q=1.

FIGURE 3.8: In the above plot we have shown the relation between the QNMs for the TT eigenspinors for differing values of the dimension, D, as well as the electric charge Q, note that in the above $M = 1$. The values of l and n are the angular and principal quantum number respectively. Note that in the higher dimensions some of the labels have been removed to make the figures easier to read. These figures are taken from [89]

3.3 Absorption probabilities

Finally we investigate the absorption probabilities associated with the spin-3/2 fields near the Reissner-Nordström black hole. We use the method as described in Ch. 2.

3.3.1 Non-TT eigenmodes related absorption probabilities

In Figs. 3.9 and 3.10 we see that for specific values of Q and D, the behaviour of the absorption probability shifts from lower energy to higher energy as j increases, and this trend is similar to the Schwarzschild case. For fixed j and Q, we can compare the scale of each subplot and realise a lower energy to higher energy shift as D increase. For a fixed j and D, the absorption probability also shifts from left to right as Q increases. This is because the maximum value of the corresponding potential increases as Q increases, as shown in Fig. 3.4 for the case $D = 5$, $j = 5/2$. An exception is in $j = 3/2$, $D = 7$, where the curve shifts to the left instead. This is because the maximum value of the potential decreases instead of increasing as Q is increased. Moreover, we have left out the absorption probability in the case of $j = 3/2$, $D = 7$, and $Q = 1$. We could not obtain a satisfactory curve for this case and we believe this is due to the fact that the effective potential has two local maxima rather than one in this case, thus rendering the WKB approximation inapplicable.

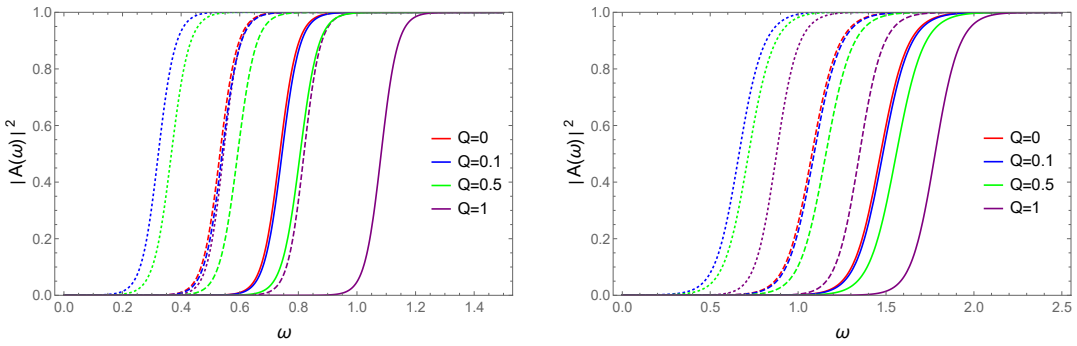

(A) $D = 4$ (B) $D = 5$

FIGURE 3.9: Spin-3/2 field absorption probabilities with various dimensions and $j = 3/2$ (left most) to $j = 7/2$ (right most). These figures are taken from [89].

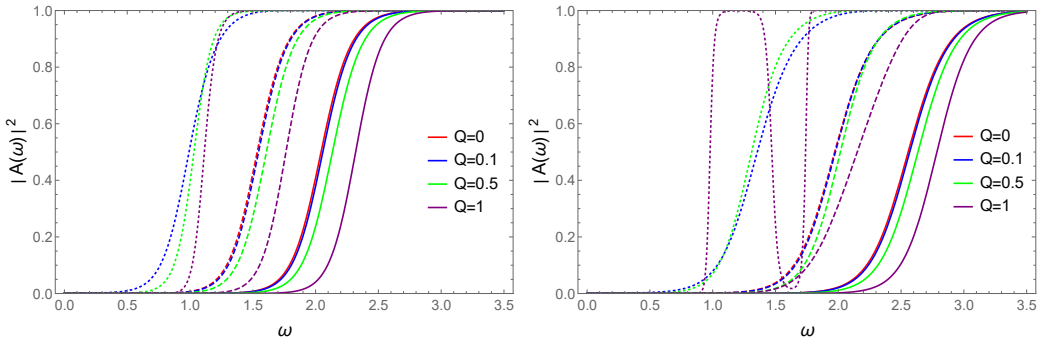

(A) $D = 6$ (B) $D = 7$

FIGURE 3.10: Spin-3/2 field absorption probabilities with various dimensions and $j = 3/2$ (left most) to $j = 7/2$ (right most). These figures are taken from [89].

3.3.2 TT eigenmodes related

The absorption probabilities associated with the "TT eigenmodes" are present in Fig. 3.11. It is clear that the absorption probabilities shift from lower energy to higher energy when we increase j (with fixed Q and D), and when we increase D (with fixed Q and j). However, when Q is increased but with fixed D and j, the absorption probabilities shift from higher energy to lower energy, This is because the maximum value of effective potential decreases when Q increases, as shown in Fig. 3.4 with the typical case of $D = 5$, $j = 5/2$.

To briefly conclude this chapter we have shown that we an use the idea of eigenvalues on a sphere to obtain the effective potential for spin-3/2 fields near electrically charged black holes in 4 or more dimensions. We have also shown that in the appropriate limits this reduces to the non-charged case and produces results consistent with the results shown in Ref. [74]. In terms of the charge we see that as the charge of the black hole is increased so does the frequency of the emitted QNMs. Furthermore as is consistent with the non-charged case higher dimensional black holes emit more energetic QNMs, but these QNMs also experience larger dampening terms. As such we would be unlikely to detect these modes due to their short existence. We now move onto the case of non-asymptotically flat space times.

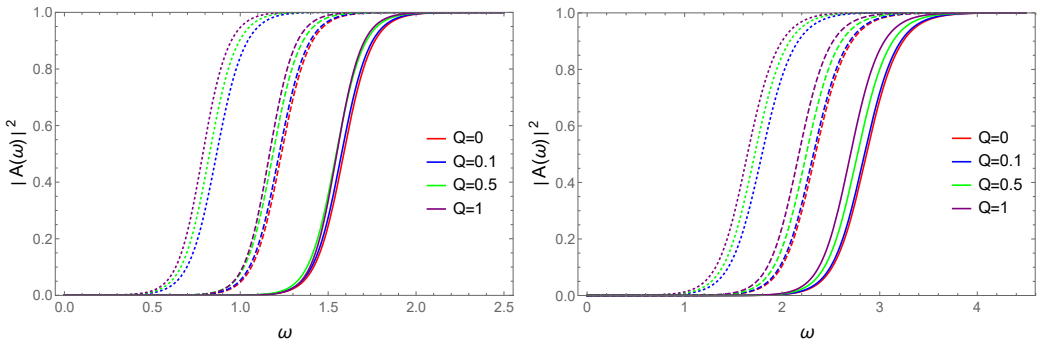

(A) $D = 5$ (B) $D = 7$

FIGURE 3.11: Spin-3/2 field absorption probabilities with various dimensions and $j = 3/2$ (left most) to $j = 7/2$ (right most). This figure is taken from [89].

Chapter 4

Black holes in (A)dS space

QNMs in asymptotically flat space times have been studied for many years, as the boundary conditions are rather simple. In this case the perturbations can only fall into the black hole or propagate outwards to infinity. Motivated by the study of inflation there has been an increased interest in studying QNMs in dS space, and in this space the boundary conditions are very similar to those of the asymptotically flat case [91–93]. In fact the asymptotically flat case can be thought of as a limit of the dS space time [94].
The case of the AdS space, however, is vastly different since the space acts almost as a potential box confining the QNMs. As such in the case of no black hole the QNMs take on a purely real value, as they can't leave the system [91]. Introducing the black hole to the system allows for the dampening of the QNMs as it acts almost like a drain for the QNMs. In order to obtain the different space time we introduce to the metric a constant curvature term called the cosmological constant. The line element for the (A)dS space time is given then given as

$$ds^2 = -f(r)dt^2 + \frac{1}{f(r)}dr^2 + r^2 d\bar{\Omega}_N^2, \tag{4.1}$$

where $f(r) = 1 - \frac{2M}{r^{D-2}} - \frac{2r^2\Lambda}{(D-2)(D-3)}$, and Λ is the cosmological constant. The case of $\Lambda = 0$ gives the Minkowski metric, $\Lambda > 0$ is the dS space time and $\Lambda < 0$ is the AdS space. Recall that $d\Omega_N^2$ is the metric of the S^N, and is given in Eq. (2.48).

4.1 The effective potential

Using the metric in Eq. (4.1) and the same convention of using over bars to denote terms from the S^N as we have in the previous chapter we will derive the effective potential below. Note that the "non-TT eigenmodes" and "TT eigenmodes" on S^N are constructed in the same manner as in the previous chapter. Furthermore in the following derivation we make no assumptions on the size of the cosmological constant. We will determine the most general form of the potential function and then study black holes of varying size in the dS space time.

4.1.1 Potential function for the non-TT eigenfunctions

We use the same definition of the radial and temporal wave functions as we have used in the previous chapter, and simply rewrite them here for convenience,

$$\psi_t = \phi_r \otimes \bar{\psi}_{(\lambda)} \quad \text{and} \quad \psi_t = \phi_t \otimes \bar{\psi}_{(\lambda)}, \tag{4.2}$$

where $\bar{\psi}_{(\lambda)}$ is an eigenspinor on S^N, with eigenvalues $i\bar{\lambda}$. As before the angular wave functions are defined to be

$$\psi_{\theta_i} = \phi_\theta^{(1)} \otimes \bar{\nabla}_{\theta_i} \bar{\psi}_{(\lambda)} + \phi_\theta^{(2)} \otimes \bar{\gamma}_{\theta_i} \bar{\psi}_{(\lambda)}, \tag{4.3}$$

where $\phi_\theta^{(1)}$ and $\phi_\theta^{(2)}$ are functions of r and t that behave like 2-spinors. The eigenvalue $\bar{\lambda}$ are given in the previous chapter. Working in the Weyl gauge we will first develop the non-gauge invariant form of the equations of motion and then add a gauge invariant variable just before we construct the potential function.

Equations of motion

As before we derive our equations of motion from the Rarita-Schwinger equation, rewritten here for convenience,

$$\gamma^{\mu\nu\alpha} \mathcal{D}_\nu \psi_\alpha = 0. \tag{4.4}$$

In this case

$$\mathcal{D}_\mu = \nabla_\mu + \frac{i\sqrt{\Lambda}}{\sqrt{2(D-1)(D-2)}} \gamma_\mu. \tag{4.5}$$

We obtain the first equation of motion by setting $\mu = t$ in Eq. (4.4) we obtain the first of our equations of motion

$$\begin{aligned} 0 = &\left(i\bar{\lambda}\partial_r + (D-3)\frac{i\bar{\lambda}}{2r} - \frac{(D-2)(D-3)}{4r\sqrt{f}} i\sigma^3 - \frac{\bar{\lambda}}{\sqrt{f}}\sqrt{\frac{\Lambda(D-2)}{2(D-1)}}\sigma^2 \right) \phi_\theta^{(1)} \\ &+ \left((D-2)\partial_r + (D-3)\frac{i\bar{\lambda}}{r\sqrt{f}} i\sigma^3 + \frac{(D-2)(D-3)}{2r} + (D-2)\frac{i}{\sqrt{f}}\sqrt{\frac{\Lambda(D-2)}{2(D-1)}}\sigma^2 \right) \phi_\theta^{(2)} \\ &- \left(i\bar{\lambda} + \frac{D-2}{2}\sqrt{f} i\sigma^3 + ir\sqrt{\frac{\Lambda(D-2)}{2(D-1)}}\sigma^1 \right) \phi_r. \end{aligned} \tag{4.6}$$

The second equation of motion is obtained by setting $\mu = r$, and is written as

$$\begin{aligned} &\left(-\frac{i\bar{\lambda}}{\sqrt{f}}\partial_t + (D-3)\frac{i\bar{\lambda}\sqrt{f}}{2r}\sigma^1 + \frac{i\bar{\lambda}f'}{4\sqrt{f}}\sigma^1 - \frac{(D-2)(D-3)}{4r}\sigma^2 - \frac{\bar{\lambda}}{r} ir\sqrt{\frac{\Lambda(D-2)}{2(D-1)}}\sigma^3 \right) \phi^{(1)} \\ &+ \Big(-\frac{D-2}{\sqrt{f}}\partial_t + \frac{(D-3)(D-2)}{2r}\sqrt{f}\sigma^1 + \frac{(D-2)f'}{4\sqrt{f}}\sigma^1 + (D-3)\frac{i\bar{\lambda}}{r}\sigma^2 \\ &- (D-2)\sqrt{\frac{\Lambda(D-2)}{2(D-1)}}\sigma^3 \Big) \phi_\theta^{(2)} = 0. \end{aligned} \tag{4.7}$$

Finally by setting $\mu = \theta$ we obtain the third and fourth equations of motion. As in the case of the Reissner-Nordstöm black hole these four equations are not linearly independent as such we work with only the simpler of the two equations obtained

when setting $\mu = \theta$

$$\left(\frac{i}{r\sqrt{f}}\sigma^3\partial_t + \frac{\sqrt{f}}{r}\sigma^2\partial_r + \frac{f'}{4r\sqrt{f}}\sigma^2 + (D-4)\frac{\sqrt{f}}{2r^2}\sigma^2 + \frac{1}{r^2}\frac{D-2}{2}\sqrt{f}\right)\phi_\theta^{(1)} - \frac{D-4}{r^2}\sigma^1\phi_\theta^{(2)} - \frac{\sqrt{f}}{r}\sigma^2\phi_r = 0. \tag{4.8}$$

Effective potential

We now need to perform the transformation to a gauge invariant variable. We use the same approach as we have used in the Ch. 3, and have that the simplest form of the gauge invariant variable is

$$\Phi = -\left(\frac{\sqrt{f}}{2}i\sigma^3 + \frac{ir}{D-2}\sqrt{\frac{\Lambda(D-2)}{2(D-1)}}\sigma^1\right)\phi_\theta^{(1)} + \phi_\theta^{(2)}. \tag{4.9}$$

Applying this variable to Eqs. (4.6), (4.7) and (4.8) and then simplifying we obtain the following gauge invariant form of the equations of motion

$$\begin{aligned}&(i\bar{\lambda} + \frac{D-2}{2}\sqrt{f}i\sigma^3 - ir\sqrt{\frac{\Lambda(D-2)}{2(D-1)}}\sigma^1)\Big[\sigma^1\partial_t - \frac{(D-3)f}{2r} - \frac{f'}{4}\\ &-\frac{D-3}{D-2}\frac{\sqrt{f}i\bar{\lambda}}{r}i\sigma^3 - i\sqrt{\frac{\Lambda f(D-2)}{2(D-1)}}\sigma^2\Big]\Phi =\\ &(i\bar{\lambda} - \frac{D-2}{2}\sqrt{f}i\sigma^3 - ir\sqrt{\frac{\Lambda(D-2)}{2(D-1)}}\sigma^1)\Big[f\partial_r + i\frac{\bar{\lambda}\sqrt{f}}{(D-2)r}i\sigma^3 + \frac{(2D-7)f}{2r}\\ &+\frac{2i}{D-2}\sqrt{\frac{\Lambda f(D-2)}{2(D-1)}}\sigma^2\Big]\Phi.\end{aligned} \tag{4.10}$$

If we take $\Psi = (i\lambda - \frac{D-2}{2}\sqrt{f}i\sigma^3 - ir\sqrt{\frac{\Lambda(D-2)}{2(D-1)}})\Phi$ then we can rewrite the equations as

$$f\partial_r\Psi + \left(\mathcal{A} + \mathcal{B}i\sigma^3 + \mathcal{D}\sigma^2\right)\Psi = \sigma^1\partial_t\Psi \tag{4.11}$$

where

$$\begin{aligned}\mathcal{A} &= \frac{1}{-\bar{\lambda}^2 + \frac{(D-2)^2}{4}f + r^2\frac{\Lambda(D-2)}{2(D-1)}}\Bigg[-\bar{\lambda}^2\left(\frac{f'}{4} + \frac{D-4}{2r}f\right) + \frac{(D-2)^2}{4}f\left(-\frac{3}{4}f' + \frac{D-4}{2r}f\right)\\ &\quad - r^2\frac{\Lambda(D-2)}{2(D-1)}\left(-\frac{f'}{4} - \frac{(D-8)f}{2r}\right)\Bigg],\\ \mathcal{B} &= \frac{i\bar{\lambda}\sqrt{f}}{r}\left[1 + \frac{1}{-\bar{\lambda}^2 + \frac{(D-2)^2}{4}f + r^2\frac{\Lambda(D-2)}{2(D-1)}}\left(\frac{(D-2)(D-3)M}{r^{D-3}}\right)\right],\\ \mathcal{D} &= -i\sqrt{\frac{\Lambda f(D-2)}{2(D-1)}}\left[\frac{D-4}{D-2} + \frac{(D-3)(D-2)}{-\bar{\lambda}^2 + \frac{(D-2)^2}{4}f + r^2\frac{\Lambda(D-2)}{2(D-1)}}\frac{M}{r^{D-3}}\right].\end{aligned} \tag{4.12}$$

By setting $\Psi - \mathcal{K}(r) = \widetilde{\Psi}$, and where $\mathcal{K}(r)$ satisfies the partial equation

$$f\frac{\partial \mathcal{K}(r)}{\mathcal{K}(r)} + \mathcal{A} = 0, \tag{4.13}$$

we can remove the $\mathcal{A}$ term and rewrite Eq. (4.11) as

$$f\partial_r\widetilde{\Psi} + \left(\mathcal{B}i\sigma^3 + \mathcal{D}\sigma^2\right)\widetilde{\Psi} = \sigma^1\partial_t\widetilde{\Psi}. \tag{4.14}$$

Finally we can separate the spinor Ψ into its components, the choice we make is

$$\widetilde{\Psi} = \left(\sin\left(\frac{\theta}{2}\right)\sigma^3 + \cos\left(\frac{\theta}{2}\right)\sigma^2\right)e^{i\omega t}\begin{pmatrix}\phi_1\\ \phi_2\end{pmatrix} \tag{4.15}$$

where $\phi_{1,2}$ are functions of the radial coordinate only, and

$$\theta = \tan^{-1}\left(\frac{i\mathcal{D}}{\mathcal{B}}\right). \tag{4.16}$$

Plugging this into Eq. (4.14) and simplifying we get

$$\left(f\partial_r + \frac{f}{2}\left[\frac{\partial}{\partial r}\left(\frac{-\mathcal{D}}{i\mathcal{B}}\right)\right]\left(\frac{\mathcal{B}^2}{\mathcal{B}^2-\mathcal{D}^2}\right)i\sigma^1 + \sqrt{\mathcal{D}^2-\mathcal{B}^2}\sigma^3\right)\begin{pmatrix}\phi_1\\ \phi_2\end{pmatrix} = i\omega\sigma^1\begin{pmatrix}\phi_1\\ \phi_2\end{pmatrix}. \tag{4.17}$$

Which can be expanded to give

$$\begin{aligned}\left(f\partial_{r_*} + W\right)\phi_1 &= i\omega\phi_2,\\ \left(f\partial_{r_*} - W\right)\phi_2 &= i\omega\phi_1,\end{aligned} \tag{4.18}$$

where $dr_* = f(r)dr$ is the tortoise coordinate and

$$W = \sqrt{\mathcal{D}^2-\mathcal{B}^2}\left[1 + \frac{f}{2\omega}\left(\frac{\partial}{\partial r}\frac{\mathcal{D}}{i\mathcal{B}}\right)\left(\frac{\mathcal{B}^2}{\mathcal{B}^2-\mathcal{D}^2}\right)\right]^{-1}. \tag{4.19}$$

Then decoupling the equations in Eq. (4.18) we obtain the following

$$\begin{aligned}\left(f^2\partial_{r_*}^2 - V_{eff_1}\right)\phi_1 &= -\omega^2\phi_1,\\ \left(f^2\partial_{r_*}^2 - V_{eff_2}\right)\phi_2 &= -\omega^2\phi_2,\end{aligned} \tag{4.20}$$

where

$$V_{eff_{1,2}} = \pm f\frac{dW}{dr} - W^2 \tag{4.21}$$

is the effective potential. There is a notable difference here for the effective potential, in that the potential does have some reliance on the QNM value ω. In our previous works we have only had to work with potentials reliant on the radial coordinate only [73, 74]. It is possible to remove this reliance on the QNM value by looking at the limit where Λ is very small, however this is simply the Schwarzschild limit and tells us nothing new about the cosmological constants. As such we will avoid such cases as this makes the solutions trivial extensions of the work in Ref. [74].
In the above we have made no assumption on the value of Λ, however as stated in the introduction to this chapter the cases of $\Lambda > 0$ or $\Lambda < 0$ are vastly different from each other. As such we investigate the potentials in each case separately below.

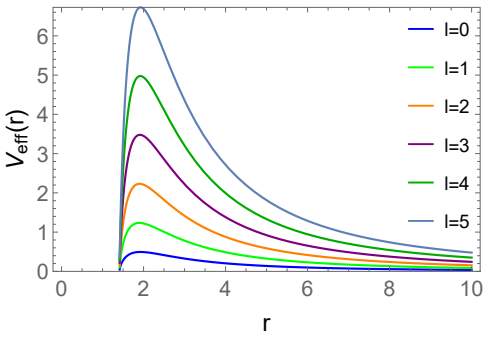

(A) Effective potential function for $l = 0$ to 5 with $\Lambda = 0.0001$, $M = 1$ and $D = 5$.

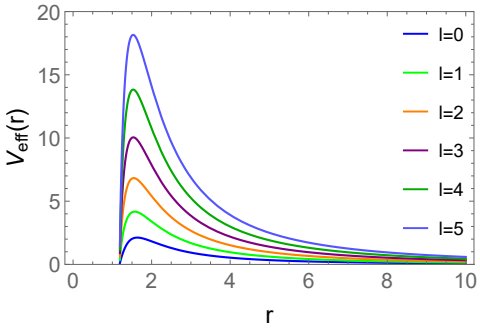

(B) Effective potential function for $l = 0$ to 5 with $\Lambda = 0.01$, $M = 1$ and $D = 7$.

FIGURE 4.1: In the above we have plotted the effective potential functions, in Eq. (4.21), for the effective potential for the case of the dS space time. Comparing how the change in modes affects the values of the potential function. Note that in the above we have chosen $\omega = 1$.

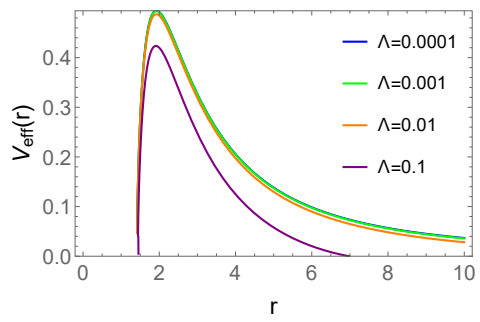

(A) Effective potential function for $\Lambda = 0.0001,\ 0.001,\ 0.01, 0.1$ for $l = 0$, $M = 1$ and $D = 5$.

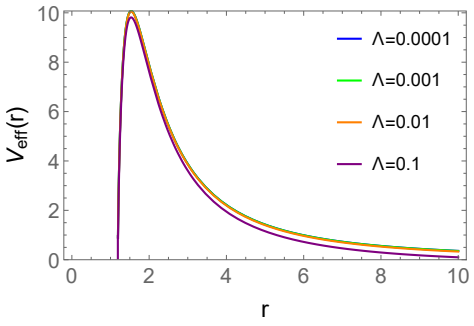

(B) Effective potential function for $\Lambda = 0.0001,\ 0.001,\ 0.01, 0.1$ for $l = 3$, $M = 1$ and $D = 7$.

FIGURE 4.2: In the above we have plotted the effective potential functions, in Eq. (4.21), for the effective potential for the case of the dS space time. Comparing how the value of λ affects the value of the potential function. Note that in the above we have chosen $\omega = 1$.

The dS space time potentials

In Figs. 4.1 and 4.2 we have plotted the effective potential to show how the values of l and Λ affect the effective potential.

From Figs. 4.1 and 4.2 we can see that the potential still behaves similarly as it did in the previous cases, in that increasing the number of dimensions and the value of l both results in increasing the maximum value of the potential function. As was seen in the Schwarzschild case in Ref. [74] we see that the potential goes to zero at the event horizon. From the plots it would appear that the potential functions also go to zero as $r \to \infty$. This however does not actually happen, by testing the potential in this limit we find that for dimensions greater than 4 the potential diverges in this limit. For the 4 dimensional case the potential does not blow up but instead tends to some non-zero finite value. This suggests that the 4 dimensional case is a special case of the the dS space.

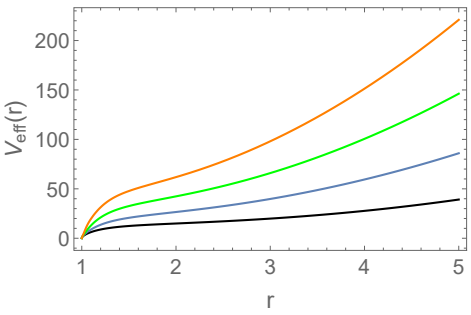

(A) Effective potential function for the AdS case of the space time. In this case $\Lambda = -\frac{(D-1)(D-2)}{2}$, $M = 1$ and $\omega = 10$

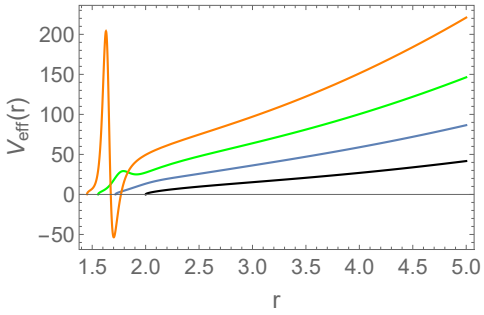

(B) Effective potential function for the AdS case of the space time. In this case $\Lambda = -\frac{(D-1)(D-2)}{2}$, $M = 10$ and $\omega = 10$.

FIGURE 4.3: In the above we have plotted the potential functions for the effective potential, in Eq.(4.21), for the case of the AdS space time. In the above the black, blue, green and orange lines represent the $D = 5, 6, 7, 8$ case respectively.

AdS space time potentials

In the case of the AdS space time the potential is very different to that of the flat case or the dS case. As can be seen in Fig. 4.3 the potential function in the AdS case does not act as a potential barrier. In the case of the AdS space we can relate the cosmological constant Λ to some curvature radius R_{AdS} as [91]

$$\Lambda = -\frac{(D-1)(D-2)}{2R_{AdS}^2}. \tag{4.22}$$

This gives us a different approach to investigating the relationship between the QNMs, and effective potential, and the cosmological constant. Since we can we can compare the radius of the black hole r_+ with that of the AdS radius R_{AdS}. Following the procedure of Ref.[91] we set $R_{AdS} = 1$ and change the radial location of the event horizon, by choosing different masses as done in Fig. 4.3. Note that for $r_+ > R_{AdS}$ we would be investigating large black hole, and for $r_+ < R_{AdS}$ we would be studying the equivalent of very small black holes [91]. Note that in the higher dimensional cases shown above the potential tends to infinity as $r \to \infty$. In the 4 dimensional case this is not true however and as such requires a different approach to solving for the QNMs.

4.1.2 TT eigenspinor potential functions

We set ψ_r and ψ_t in the same manner as we did for the "non-TT eigenfunctions". Our angular component changes and is now written as

$$\psi_{\theta_i} = \phi_\theta \otimes \bar{\psi}_{\theta_i}, \tag{4.23}$$

where $\bar{\psi}_{\theta_i}$ is the TT mode eigenspnionr-vector which includes the "TT mode I" and "TT mode II", as described in Ref. [74], and ϕ_θ behaves like a 2-spinor. We again use the Weyl gauge, for the TT case this means $\phi_r = \phi_t = 0$ [73]. Our only non-zero

equation of motion is

$$\left(\frac{1}{r\sqrt{f}}i\sigma^3\partial_t+\frac{\sqrt{f}}{r}\sigma^2\partial_r+\frac{f'}{4r\sqrt{f}}\sigma^2+\frac{\sqrt{f}}{2r^2}(D-4)\sigma^2+\frac{i\zeta}{r^2}\sigma^1+\frac{i\sqrt{\Lambda}}{r}\sqrt{\frac{D-2}{2(D-1)}}\right)\phi_\theta=0. \tag{4.24}$$

In this case the function ϕ_θ is already gauge invariant. We set

$$\phi_\theta=\sigma^2 e^{-i\omega t}\begin{pmatrix}\phi_1\\ \phi_2\end{pmatrix}, \tag{4.25}$$

and apply it to Eq. (4.24) to obtain

$$\begin{pmatrix} f\partial_r+\frac{f'}{4}+\frac{f}{2r}(D-4)-\frac{\bar{\zeta}\sqrt{f}}{r} & -i\omega+\sqrt{\Lambda f}\sqrt{\frac{D-2}{2(D-1)}} \\ -i\omega-\sqrt{\Lambda f}\sqrt{\frac{D-2}{2(D-1)}} & f\partial_r+\frac{f'}{4}+\frac{f}{2r}(D-4)+\frac{\bar{\zeta}\sqrt{f}}{r}\end{pmatrix}\begin{pmatrix}\phi_1\\ \phi_2\end{pmatrix}=0. \tag{4.26}$$

Redefining

$$\widetilde{\phi}_1=r^{\frac{D-4}{2}}f^{\frac{1}{4}}\phi_1 \text{ and } \widetilde{\phi}_2=r^{\frac{D-4}{2}}f^{\frac{1}{4}}\phi_2, \tag{4.27}$$

we obtain two coupled equations

$$\begin{aligned}\left(f\partial_r-\frac{\bar{\zeta}\sqrt{f}}{r}\right)\phi_1+\left(\sqrt{\Lambda f}\sqrt{\frac{D-2}{2(D-1)}}\right)\phi_2&=i\omega\phi_2,\\ \left(f\partial_r+\frac{\bar{\zeta}\sqrt{f}}{r}\right)\phi_2-\left(\sqrt{\Lambda f}\sqrt{\frac{D-2}{2(D-1)}}\right)\phi_1&=i\omega\phi_1.\end{aligned} \tag{4.28}$$

Decoupling the equations and refining the wave functions as $\phi_{1,2}\to H\Phi_{1,2}$ we obtain the following

$$\left[f^2\partial_r^2H+\left[-f^2\frac{(i\omega-B)'}{i\omega-B}+ff'\right]\partial_rH+\left(f\frac{(i\omega-B)'}{i\omega-B}-fA'-A^2+B^2+\omega^2\right)\right]\Phi_1=0 \tag{4.29}$$

Setting $H=\sqrt{i\omega-B}$ and converting to toroise coordinates we have

$$\partial_{r_*}^2\Psi_1+\left[-\mathcal{V}_{eff}+\omega^2\right]\Psi_1=0 \tag{4.30}$$

where

$$\begin{aligned}A&=\frac{\bar{\zeta}\sqrt{f}}{r}\\ B&=f\sqrt{\frac{\Lambda(D-2)}{2(D-1)}}\\ \mathcal{V}_{eff}&=-f^2\frac{H''}{H}+f^2\frac{(i\omega-B)'}{i\omega-B}\frac{H'}{H}-ff'\frac{H'}{H}-f\frac{(i\omega-B)'}{i\omega-B}A+fA'+A^2-B^2\end{aligned} \tag{4.31}$$

We again have the same issue as with the non-TT eigenspinor solution, in that we have a reliance on the ω value of the QNMs. So we cannot guarantee that the potential is real at all parts in all cases of the Λ value. However looking at the Schwarzschild limit, i.e $\Lambda\to 0$, we can ensure that the potential is always real.
Therefore in order to obtain the QNMs for black holes in this space time we would

need to use some other method to obtain their numerical values.

4.2 QNMs

4.2.1 QNMs for the non-TT spinors

Due to the reliance on the ω in the potential function we cannot use directly the numerical methods to solve for the QNMs. Instead we need to perform an expansion on the potential function to obtain the QNMs. Horowitz and Hubeny in Ref. [91] have developed a method that allows for determining the QNMs of of AdS Schwarzschild black holes. We will use their method to obtain the allowed QNMs for our case. In order to use their method we convert back the radial equations to radial coordinate form, Eq. (4.20) given below as

$$\left[f\frac{d^2}{dr^2}+\left(f'-2i\omega\right)\frac{d}{dr}-\left(\frac{\omega^2+V_{eff}}{f}\right)\right]\Phi(r)=0. \tag{4.32}$$

Note that here we have dropped the subscript of the effective potential as both give the same results. We need to perform this conversion as the Horowitz-Hubeny method works by taking a Taylor expansion at the event horizon of the black hole and then imposing that the field should vanish at infinity. So we would want to map the entire region of space into some finite parameter range, a simple choice is $r=1/x$, then x_+ is the location of the event horizon and $x=0$ is infinity. Then due to the radius of convergence of our expansion our solution will be valid for the entire region of $x=0\rightarrow x=x_+$, as so we would be able to ensure the QNMs obey the requirement of vanishing at infinity. Next the mass of the black hole can be redefined to be $M=\frac{1}{2}\left[\frac{1+x_+^2}{x_+^{(D-1)}}\right]$. The radial equation then becomes

$$\left[s(x)\frac{d^2}{dx^2}+\frac{t(x)}{(x-x_+)}\frac{d}{dx}+\frac{u(x)}{(x-x_+)^2}\right]\Phi(x)=0, \tag{4.33}$$

with [91]

$$\begin{aligned}
s(x)&=\frac{x_+^2+1}{x_+^{D-1}}x^D+\cdots+\frac{x_+^2+1}{x_+^3}x^4+\frac{1}{x_+^2}x^3+\frac{1}{x_+}x^2,\\
t(x)&=(D-1)r_0^{D-3}x^D-2x^3-2x^2i\omega\\
u(x)&=(x-x_+)\left(\frac{\omega^2+V_{eff}}{f(x)}\right).
\end{aligned} \tag{4.34}$$

We can take a series expansion of these functions such that for instance $s(x)=\sum_{n=0}^{d}s_n(x-x_+)^n$, similarly for $u(x)$ and $t(x)$. To determine the behaviour of the solutions near the horizon we assume that the wave function is satisfied by $\psi(x)=(x-x_+)^\alpha$. This can be plugged into Eq. (4.33) such that to leading order we have

$$\alpha(\alpha-1)s_0+\alpha t_0=0. \tag{4.35}$$

This implies that $\alpha=0$ and $\alpha=-(t_0+s_0)/(s_0)$ are both solutions, however the solution of $\alpha=0$ corresponds to the case of in going QNMs at the horizon. Since these are the modes we would actually be able to detect we focus on this solution.

Which it turns out means we are looking for a solution of the form [91]

$$\psi(x) = \sum_{n=0}^{\infty} a_n (x - x_+)^n, \tag{4.36}$$

Plugging this into the Eq. (4.33) gives us that the a_n can be obtained by the following recursion relation [91]

$$a_n = \frac{1}{P_n} \sum_{k=0}^{n-1} \left[k(k-1)s_{n-k} + kt_{n-k} + u_{n-k} \right] a_k \tag{4.37}$$

with

$$P_n = n(n-1)s_0 + nt_0. \tag{4.38}$$

Note for $n > D$ $s_n = t_n = 0$ therefore the a_n terms are determined by fewer and fewer parameters for higher iterations. Once we have the expressions for a_n we simply solve for $\psi(x) = 0$.
Using the method developed by Horowitz and Hubeny we are able to determine the numerical values of the allowed QNMs. The relationship we would be most interested in is the allowed value for the QNMs in relation to the radius of curvature. In the plots below we have done exactly this and considered the cases of $r = 0.1,\ 0.8333,\ 10,\ 40,\ 100$. Note that in the plots below the r values represent the location of the event horizon. So the larger the value of r the bigger the black holes is.

In Fig. 4.4 we have plotted the real and imaginary values of the QNMs of a Schwarzschild black hole in a dS space time. The values were obtained by using the Horowitz and Hubeny method to an iteration depth of 24 iterations as most values to this level of iteration converge to a stable result. Higher order iterations will provide more precise results but the computational time increases very rapidly, and as such the small corrections obtain in these cases does not justify the increased computation time. The r values given is not the radial location but instead the radial value of the event horizon. So larger values of r represent larger black holes. As has been shown in Ref. [91] the QNMs associated with black holes scale with the value of the radial value of the event horizon. We see the same behaviour in our results, these results are also seen in Ref. [34]. For values of $r = 10$ and smaller we see that there are some divergences from the linear trend seen for results from larger values of r, this may be down to the the method not converging to a stable solution fast enough in these cases. It should be noted that in these cases the asymptotic curvature will play a bigger role as its value as compared to the mass will become more significant. In these case it would be worth looking at higher order iterations. This results in QNMs modes that are far larger than the ones we have previously seen in the case of the Schwarzschild and Reissner-Nordström black holes. Note that this choice of values of M much larger than those chosen in the previous cases is the fact that here we have set the radius of curvature to one and are showing values for when the black holes would be very large compared to this curvature, in staying with the procedure taken by Horowitz and Hubeny. We note that the higher dimensional black holes produce more energetic QNMs, but that these QNMs are also less likely to be detected since they decay very quickly. This is the same behaviour that we have seen in the previous cases and as such is not of much note other than suggesting that the behaviour of the QNMs does not change drastically by adding the asymptotic curvature. We also see that fields with larger l modes are more energetic, this is the same as for the results that we see when considering the QNMs of the purely

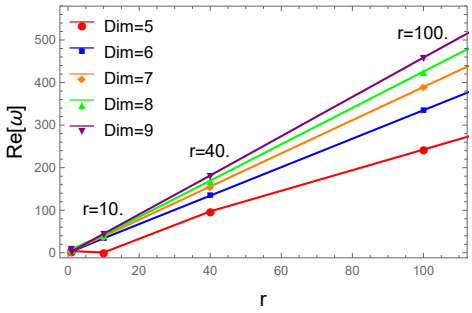

(A) Real values of the QNMs for $l = 0$.

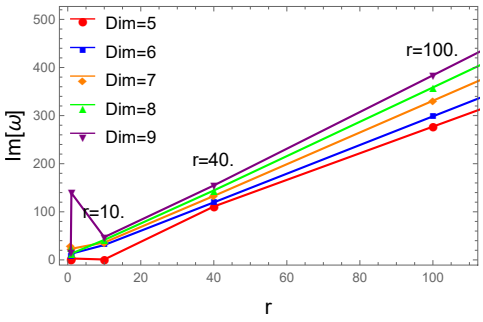

(B) Negative of imaginary values of the QNMs for $l = 0$.

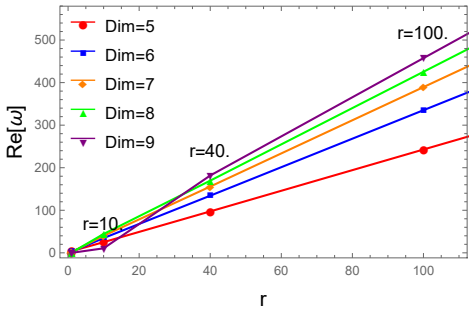

(C) Real values of the QNMs for $l = 1$.

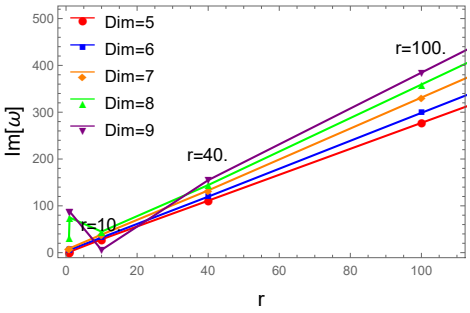

(D) Negative of imaginary values of the QNMs for $l = 1$.

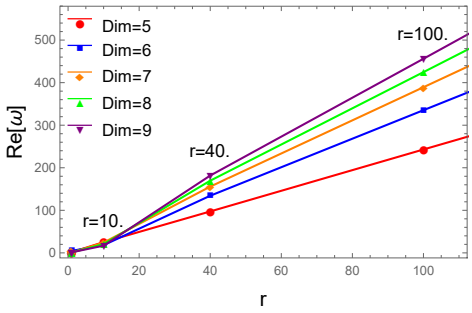

(E) Real values of the QNMs for $l = 2$.

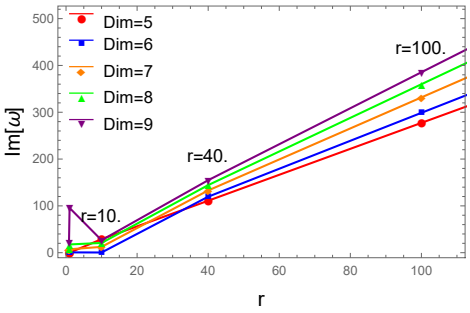

(F) Negative of imaginary values of the QNMs for $l = 2$.

FIGURE 4.4: In the above figures we have plotted both the real and imaginary values for the QNMs obtained for selected values of r. The dimensions for the results are also given.

Schwarzschild black holes.
To briefly conclude we have shown that the approach of using the eigenvalues of the S^N can be used to derive the effective potential for spin-3/2 fields near higher dimensional (A)dS Schwarzschild black holes. We also note that this effective potential is directly affected by the QNMs of the spin-3/2 fields as they are functions of these values. We can also use the method developed by Horowitz and Hubeny in Ref. [91] to determine the numerical values of the allowed QNMs.

Part II

Infinite derivative Gravity

Chapter 5

Infinite derivative gravity

In this chapter we develop the theoretical idea behind IDG. In this process we will show how to obtain the propagator for IDG as well as derive the field equations that we will use later in this thesis to derive the modified metrics that describe space times in the theory of IDG. In order to do this we begin by considering a modified version of the Einstein-Hilbert action, one which considers all orders of the curvatures, which allows us to construct the Lagrangian and propagator for quadratic gravity. We then show that by a careful choice of parameters we can obtain a theory that is singularity free and ghost free.

5.1 The linearised action

We wish to produce some flat space propagator that we can then modify in some way to create a singularity free theory of gravitational interactions. As such the best approach would be to study the Minkowski space with some small perturbation applied to it. A metric of this type would be written as

$$g_{\mu\nu} = \eta_{\mu\nu} + h_{\mu\nu}, \tag{5.1}$$

where $\eta_{\mu\nu}$ is the flat Minkowski space, with signature (-1, 1, 1, 1), and $h_{\mu\nu}$ is some small perturbation. Such that the values of $h_{\mu\nu} < \eta_{\mu\nu}$, allowing higher order terms of $h_{\mu\nu}$ to be ignored. As these fluctuations are very small we need only concern ourselves with curvature terms that are at most quadratic in $h_{\mu\nu}$ in the action [51]. The Minkowski metric will contribute no curvature terms, that is $R_{\mu\nu\alpha\rho} = 0$ for the Minkowski metric, the only contributions will come from the perturbation h. To recollect the most general action we can use is the one given in Ch. 1 and rewritten here for convenience [50, 52, 95, 96], [1]

$$S = S_{EH} + \int d^4x\sqrt{-g}\left[R_{\mu_1\nu_1\lambda_1\sigma_1}\mathcal{O}^{\mu_1\nu_1\lambda_1\sigma_1}_{\mu_2\nu_2\lambda_2\sigma_2}R^{\mu_2\nu_2\lambda_2\sigma_2}\right], \tag{5.2}$$

where S_{EH} is the Einstein-Hilbert action and $\mathcal{O}$ is a differential operator containing all the operators allowed by the diffeomorphism invariance and the the d'Alembertian, given as $\Box = g^{\mu\nu}\nabla_\mu\nabla_\nu$.

[1] Note that we can consider higher order curvature terms in the action but for this thesis we limit ourselves to the case of the quadratic curvature terms.

5.2 The linearised field equations

By expanding the $\mathcal{O}$ term to include all possible curvature terms, then applying the Bianchi identities the action in Eq. (5.2) can be rewritten as [49, 50]

$$S = \int d^4x\sqrt{g}\left[\frac{R}{2} + RF_1(\Box)R + R_{\mu\nu}F_2(\Box)R^{\mu\nu} + R_{\mu\nu\alpha\beta}F_3(\Box)R^{\mu\nu\alpha\beta}\right]. \tag{5.3}$$

The action has now been reduced to three arbitrary functions of $\mathcal{F}_i$ [2] plus the Einstein-Hilbert action. Our next step is to write the action in terms of the perturbation $h_{\mu\nu}$, and so we need to determine the values of the Ricci scalar and the Riemann tensor in the case of the linearised metric. By applying the definitions of these quantities to the perturbed Minkowski metric we can show that

$$\begin{aligned} R_{\mu\nu\lambda\sigma} =& \frac{1}{2}\left(\partial_\nu\partial_\lambda h_{\mu\sigma} + \partial_\mu\partial_\sigma h_{\nu\lambda} - \partial_\sigma\partial_\nu h_{\mu\lambda} - \partial_\mu\partial_\lambda h_{\nu\sigma}\right); \\ R_{\mu\nu} =& \frac{1}{2}\left(\partial_\rho\partial_\nu h^\rho_\mu + \partial_\rho\partial_\mu h^\rho_\nu - \partial_\mu\partial_\nu h - \Box h_{\mu\nu}\right); \\ R =& \partial_\mu\partial_\alpha h^{\alpha\mu} - \Box h. \end{aligned} \tag{5.4}$$

$$\begin{aligned} \implies S = -\int d^4x\Big[&\frac{1}{2}h_{\mu\nu}\Box\left(1 - \frac{1}{2}F_2(\Box)\Box - 2F_3(\Box)\Box\right)h^{\mu\nu} \\ &+ h^\sigma_\mu\left(-1 + \frac{1}{2}F_2(\Box)\Box + 2F_3(\Box)\Box\right)\partial_\sigma\partial_\nu h^{\mu\nu} \\ &+ \frac{1}{2}h\left(1 + 2F_1(\Box)\Box + \frac{1}{2}F_2(\Box)\Box\right)\partial_\mu\partial_\nu h^{\mu\nu} \\ &+ \frac{1}{2}h\Box\left(-2F_1(\Box)\Box - \frac{1}{2}F_2(\Box)\Box - 1\right)h \\ &+ \frac{1}{2}h^{\lambda\sigma}\frac{1}{\Box}\left(-2F_1(\Box)\Box - F_2(\Box)\Box - 2F_3(\Box)\Box\right)\partial_\sigma\partial_\lambda\partial_\mu\partial_\nu h^{\mu\nu}\Big] \end{aligned} \tag{5.5}$$

This can be rewritten as [50, 96]

$$\begin{aligned} S = -\int d^4x\Big[&\frac{1}{2}h_{\mu\nu}a(\Box)\Box h^{\mu\nu} + h^\sigma_\mu b(\Box)\partial_\sigma\partial_\nu h^{\mu\nu} + hc(\Box)\partial_\mu\partial_\nu h^{\mu\nu} + \frac{1}{2}hd(\Box)\Box h \\ &+ \frac{1}{2}h^{\lambda\sigma}\frac{f(\Box)}{\Box}\partial_\sigma\partial_\lambda\partial_\mu\partial_\nu h^{\mu\nu}\Big] \end{aligned} \tag{5.6}$$

where we have defined [50, 51]

$$\begin{aligned} a(\Box) &= 1 - \frac{1}{2}F_2(\Box)\Box - 2F_3(\Box)\Box \\ b(\Box) &= -1 + \frac{1}{2}F_2(\Box)\Box + 2F_3(\Box)\Box \\ c(\Box) &= 1 + 2F_1(\Box)\Box + \frac{1}{2}F_2(\Box)\Box \\ d(\Box) &= -1 - 2F_1(\Box)\Box - \frac{1}{2}F_2)(\Box)\Box \\ f(\Box) &= -2F_1(\Box)\Box - F_2(\Box)\Box - 2F_3(\Box)\Box. \end{aligned} \tag{5.7}$$

[2] In the functions $\mathcal{F}_i's$ there is a scale terms M_s that we have suppressed for the time being. We will reintroduce this scale variable when we have obtained the action for the IDG. At which point we will explain the significance of this scale.

At this stage we make no assumptions of the functions $a(\Box)$, $b(\Box)$, $c(\Box)$, $d(\Box)$ and $f(\Box)$, but we will later see that some specific choices of the functions are necessary to ensure consistency in our theories, and show that using the right choice of these functions allows us to obtain a renormalizable theory of gravity, which is called IDG. We only note at this stage that these definitions imply that

$$\begin{aligned} &a(\Box) + b(\Box) = 0; \\ &c(\Box) + d(\Box) = 0; \\ &b(\Box) + c(\Box) + f(\Box) = 0. \end{aligned} \tag{5.8}$$

We now have the action in its simplest form and can derive the field equations that result from varying the above action. By the principal of action we have

$$\delta S = \int d^4x \left(\frac{\delta \mathcal{L}}{\delta h_{\mu\nu}} \right) \delta h_{\mu\nu}, \tag{5.9}$$

where $\mathcal{L}$ is the Lagrangian inside given as

$$\begin{aligned} \mathcal{L} =& \frac{1}{2} h_{\mu\nu} a(\Box) \Box h^{\mu\nu} + h^{\sigma}_{\mu} b(\Box) \partial_\sigma \partial_\nu h^{\mu\nu} + h c(\Box) \partial_\mu \partial_\nu h^{\mu\nu} \\ &+ \frac{1}{2} h d(\Box) \Box h + \frac{1}{2} h^{\lambda\sigma} \frac{f(\Box)}{\Box} \partial_\sigma \partial_\lambda \partial_\mu \partial_\nu h^{\mu\nu}. \end{aligned} \tag{5.10}$$

The derivative of the Lagrangian is given as follows

$$\begin{aligned} \frac{\delta \mathcal{L}}{\delta h_{\mu\nu}} =& a(\Box) \Box h_{\mu\nu} + b(\Box) \partial_\sigma \left(\partial_\nu h^{\sigma}_{\mu} + \partial_\mu h^{\sigma}_{\nu} \right) + c(\Box) \left(\eta_{\mu\nu} \partial_\rho \partial_\sigma h^{\rho\sigma} + \partial_\mu \partial_\nu h \right) \\ &+ \eta_{\mu\nu} d(\Box) \Box h + \frac{f(\Box)}{\Box} \partial_\sigma \partial_\lambda \partial_\mu \partial_\nu h^{\sigma\lambda}. \end{aligned} \tag{5.11}$$

By the principle of least action we have that $\delta S = 0$, which implies that $\frac{\delta \mathcal{L}}{\delta h_{\mu\nu}} = 0$, giving us that in the case of a vacuum we have that

$$\begin{aligned} 0 =& a(\Box) \Box h_{\mu\nu} + b(\Box) \partial_\sigma \left(\partial_\nu h^{\sigma}_{\mu} + \partial_\mu h^{\sigma}_{\nu} \right) + c(\Box) \left(\eta_{\mu\nu} \partial_\rho \partial_\sigma h^{\rho\sigma} + \partial_\mu \partial_\nu h \right) + \eta_{\mu\nu} d(\Box) \Box h \\ &+ f(\Box) \Box^{-1} \partial_\sigma \partial_\lambda \partial_\rho \partial_\nu h^{\lambda\sigma}. \end{aligned} \tag{5.12}$$

By adding a Lagrangian for the matter part, $\mathcal{L}_m$, to the action, we obtain the following equation of motion

$$\begin{aligned} a(\Box) \Box h_{\mu\nu} + b(\Box) \partial_\sigma \left(\partial_\nu h^{\sigma}_{\mu} + \partial_\mu h^{\sigma}_{\nu} \right) + c(\Box) \left(\eta_{\mu\nu} \partial_\rho \partial_\sigma h^{\rho\sigma} + \partial_\mu \partial_\nu h \right) + \eta_{\mu\nu} d(\Box) \Box h + \\ f(\Box) \Box^{-1} \partial_\sigma \partial_\lambda \partial_\mu \partial_\nu h^{\lambda\sigma} = -\kappa \tau_{\mu\nu}, \end{aligned} \tag{5.13}$$

where $\kappa = 1/M_p^2$, M_p is the Planck mass and $\tau_{\mu\nu}$ is the stress energy tensor [51].
Our next step is to obtain the function that describes the gravitational propagator. Using this function we can show that the propagator in quadratic gravity is not necessarily ghost free, but rather that a specific choice of $a(\Box)$, $b(\Box)$, $c(\Box)$, $d(\Box)$ and $f(\Box)$ can ensure that we obtain a theory that guarantees ghost free behaviour from the propagator.

5.3 The modified gravitational propagator

In obtaining the propagator we will follow the approach as taken in Ref. [51], where we first express the field equations in the form of

$$\Pi^{-1\lambda\sigma}_{\mu\nu} h_{\lambda\sigma} = \kappa \tau_{\mu\nu}, \tag{5.14}$$

where $\Pi^{-1\lambda\sigma}_{\mu\nu}$ is the inverse propagator, and is expressed using six spin operators, $\mathcal{P}_i$. This is done such that the inverse propagator takes the form

$$\Pi^{-1} = \sum_{i=1}^{6} \mathcal{C}_1 \mathcal{P}_i, \tag{5.15}$$

where the $\mathcal{C}_i$'s in momentum space are scalars purely dependent on k^2, the momentum vector. Van Nieuwenhuizen has shown in Ref. [97–99] that the action written in Eq. (5.12) when converted to k-space can be written in terms of six projection operators

$$\begin{aligned}
\mathcal{P}^2 &= \frac{1}{2}\left(\theta_{\mu\rho}\theta_{\nu\sigma} + \theta_{\mu\sigma}\theta_{\nu\rho}\right) - \frac{1}{3}\theta_{\mu\nu}\theta_{\rho\sigma} \\
\mathcal{P}^1 &= \frac{1}{2}\left(\theta_{\mu\rho}\omega_{\nu\sigma} + \theta_{\mu\sigma}\omega_{\nu\rho} + \theta_{\nu\rho}\omega_{\mu\sigma} + \theta_{\nu\sigma}\omega_{\mu\rho}\right) \\
\mathcal{P}^0_s &= \frac{1}{3}\theta_{\mu\nu}\theta_{\rho\sigma}, \;\; \mathcal{P}^0_w = \omega_{\mu\nu}\omega_{\rho\sigma}, \\
\mathcal{P}^0_{sw} &= \frac{1}{\sqrt{3}}\theta_{\mu\nu}\omega_{\rho\sigma}, \;\; \mathcal{P}^{ws} = \frac{1}{\sqrt{3}}\omega_{\mu\nu}\theta_{\rho\sigma},
\end{aligned} \tag{5.16}$$

where $\theta_{\mu\nu} = \eta_{\mu\nu} - \frac{k_\mu k_\nu}{k^2}$ and $\omega_{\mu\nu} = \frac{k_\mu k_\nu}{k^2}$. These have been chosen since they have the following simple orthogonality relations

$$\begin{aligned}
\mathcal{P}^i_a \mathcal{P}^j_b &= \delta^{ij}\delta_{ab}\mathcal{P}^j_b, \;\; \mathcal{P}^i_{ab}\mathcal{P}^j_{cd} = \delta^{ij}\delta_{bc}\mathcal{P}^j_{ad}, \\
\mathcal{P}^i_a \mathcal{P}^j_{bc} &= \delta^{ij}\delta_{ab}\mathcal{P}^j_{ac}, \;\; \mathcal{P}^i_{ab}\mathcal{P}^j_c = \delta^{ij}\delta_{bc}\mathcal{P}^j_{ac},
\end{aligned} \tag{5.17}$$

and are complete:

$$\mathcal{P}^2 + \mathcal{P}^1_m + \mathcal{P}^0_s + \mathcal{P}^0_w = 1 \text{ and } \mathcal{P}^1_b + \mathcal{P}^1_c = 1. \tag{5.18}$$

We can understand these operators by understanding what they represent, which are the six degrees of freedom for our field. $\mathcal{P}^2$ and $\mathcal{P}^1$ represent the transverse and traceless spin-2 and spin-1 degrees of freedom [51]. Furthermore $\mathcal{P}^0_s$ and $\mathcal{P}^0_w$ represent the scalar multiplet. Finally, we have the P^0_{sw} and P^0_{ws} projection operators which, are able to mix the two scalar multiplets.
Eqs. (5.15) and (5.18) imply that Eq. (5.14) can be rewritten as

$$\sum_i^6 C_i P_i h = \kappa \left(P^2 + P^1 + P^0_s + P^0_w\right)\tau. \tag{5.19}$$

In order to solve for the projection operators we apply the operators to the actions that we have developed in Eq. (5.12). By then multiplying through by a specific projection operator, and using the orthogonality relations between each of the projectors, we will obtain solutions for each of the projection operator.

5.4 The quadratic propagator

Before we are able to represent the field equations in terms of the projection operators, we need to rewrite the field equations in Eq. (5.12) in terms of the momentum space. Using a Fourier transform we can rewrite the field equations in Eq. (5.12) into momentum space as [51, 96]

$$\begin{aligned} &a(-k^2)h_{\mu\nu} + b(-k^2)\left(k_\mu k_\alpha h^\alpha_\nu + k_\alpha k_\nu h^\alpha_\mu\right) + \frac{c(-k^2)}{k^2}\left(\eta_{\mu\nu}k_\alpha k_\beta h^{\alpha\beta} + k_\mu k_\nu h\right) \\ &+ \eta_{\mu\nu}\frac{d(-k^2)}{k^2}h + \frac{f(-k^2)}{k^4}k_\beta k_\alpha k_\mu k_\nu h^{\alpha\beta} = \kappa\frac{\tau_{\mu\nu}}{k^2}. \end{aligned} \tag{5.20}$$

So now we need to rewrite these terms in terms of the projection operators. We begin with [51, 96]

$$a(-k^2)h_{\mu\nu} = a(-k^2)\left[\mathcal{P}^2 + \mathcal{P}^1 + \mathcal{P}^0_s + \mathcal{P}^0_w\right]h_{\mu\nu}, \tag{5.21}$$

$$\begin{aligned} b(-k^2)\left(k_\mu k_\alpha h^\alpha_\nu + k_\alpha k_\nu h^\alpha_\mu\right) &= b(-k^2)k^2\left[\omega_{\alpha\mu}\eta_{\nu\rho} + \omega_{\alpha\nu}\eta_{\mu\rho}\right]h^{\alpha\rho} \\ &= b(-k^2)\frac{k^2}{2}\left[\omega_{\alpha\mu}\eta_{\nu\rho} + \omega_{\alpha\rho}\eta_{\nu\mu} + \omega_{\alpha\nu}\eta_{\mu\rho} + \omega_{\mu\nu}\eta_{\alpha\rho}\right]h^{\alpha\rho} \\ &= b(-k^2)k^2\left[\mathcal{P}^1 + 2\mathcal{P}^0_w\right]h_{\mu\nu}, \end{aligned} \tag{5.22}$$

$$\begin{aligned} \frac{c(-k^2)}{k^2}\left(\eta_{\mu\nu}k_\alpha k_\beta h^{\alpha\beta} + k_\mu k_\nu h\right) &= c(-k^2)\left[\eta_{\mu\nu}\omega_{\alpha\beta} + \omega_{\mu\nu}\eta_{\alpha\beta}\right]h^{\alpha\beta} \\ &= c(-k^2)\left[\theta_{\mu\nu}\omega_{\alpha\beta} + \omega_{\mu\nu}\omega_{\rho\sigma} + \omega_{\mu\nu}\theta_{\alpha\beta} + \omega_{\mu\nu}\omega_{\alpha\beta}\right]h^{\alpha\beta} \\ &= c(-k^2)\left[2\mathcal{P}^0_w + \sqrt{3}\left(\mathcal{P}^0_{sw} + \mathcal{P}^0_{ws}\right)\right]h_{\mu\nu}, \end{aligned} \tag{5.23}$$

$$\begin{aligned} \frac{d(-k^2))}{k^2}\eta_{\nu\mu}h &= \frac{d(-k^2)}{k^2}\left(\theta_{\mu\nu} + \omega_{\mu\nu}\right)\left(\theta_{\alpha\beta} + \omega_{\alpha\beta}\right)h^{\alpha\beta} \\ &= \frac{d(-k^2)}{k^2}\left[\theta_{\mu\nu}\theta_{\alpha\beta} + \theta_{\mu\nu}\omega_{\alpha\beta} + \omega_{\mu\nu}\theta_{\alpha\beta} + \omega_{\mu\nu}\omega_{\alpha\beta}\right]h^{\alpha\beta} \\ &= \frac{d(-k^2)}{k^2}\left[3\mathcal{P}^0_s + \mathcal{P}^0_w + \sqrt{3}\left(\mathcal{P}^0_{sw} + \mathcal{P}^0_{ws}\right)\right]h_{\mu\nu}, \end{aligned} \tag{5.24}$$

$$\begin{aligned} \frac{f(-k^2)}{k^4}k_\beta k_\alpha k_\mu k_\nu h^{\alpha\beta} &= f(-k^2)\omega_{\beta\alpha}\omega_{\mu\nu}h^{\alpha\beta} \\ &= f(-k^2)\mathcal{P}^0_w h_{\mu\nu}. \end{aligned} \tag{5.25}$$

Using these relations we can rewrite the field equations as

$$\begin{aligned} &a(-k^2)\left[\mathcal{P}^2 + \mathcal{P}^1 + \mathcal{P}^0_s + \mathcal{P}^0_w\right]h + b(-k^2)\left[\mathcal{P}^1 + 2\mathcal{P}^0_w\right]h \\ &+ c(-k^2)\left[2\mathcal{P}^0_w + \sqrt{3}\left(\mathcal{P}^0_{sw} + \mathcal{P}^0_{ws}\right)\right]h + \frac{d(-k^2)}{k^2}\left[3\mathcal{P}^0_s + \mathcal{P}^0_w + \sqrt{3}\left(\mathcal{P}^0_{sw} + \mathcal{P}^0_{ws}\right)\right]h \\ &+ f(-k^2)\mathcal{P}^0_w h = \kappa\left(\mathcal{P}^2 + \mathcal{P}^1 + \mathcal{P}^0_s + \mathcal{P}^0_w\right)\frac{\tau_{\mu\nu}}{k^2}. \end{aligned} \tag{5.26}$$

Our next step is to act on this action with each of the spin projection operators, which will give us the decoupled field equations for the different spin multiplets. We begin by multiplying Eq. (5.26) by $\mathcal{P}^2$ and using the orthogonality relations given in Eq.

(5.17)

$$a(-k^2)\mathcal{P}^2 h = \kappa \mathcal{P}^2 \tau \implies \mathcal{P}^2 h = \kappa \frac{\mathcal{P}^2}{a(-k^2)k^2}\tau. \tag{5.27}$$

Next, if we act with $\mathcal{P}^1$ on Eq. (5.26) we obtain

$$a(-k^2)\mathcal{P}^1 + b(-k^2)\mathcal{P}^1 h = \kappa \mathcal{P}^1 \frac{\tau}{k^2} \implies \left(a(-k^2) + b(-k^2)\right)\mathcal{P}^1 h = \kappa \frac{\mathcal{P}^1}{k^2}\tau, \tag{5.28}$$

but by Eq. (5.8) we know that $a + b = 0$. This implies that there are no vector degrees of freedom, and as a consequence there are no vector parts in our stress-tensor

$$\mathcal{P}^1 \tau = 0. \tag{5.29}$$

Next we look at the scalar multiplets $\mathcal{P}_s^0$ and $\mathcal{P}_w^0$ by applying each respectively we then obtain

$$\begin{aligned}
&\left(a(-k^2) + 3d(-k^2)\right)\mathcal{P}_s^0 h + \left(c(-k^2) + d(-k^2)\right)\sqrt{3}\mathcal{P}_{sw}^0 h = \kappa\left(\mathcal{P}_s^0\right)\frac{\tau_{\mu\nu}}{k^2};\\
&\left(a(-k^2) + 2b(-k^2) + 2c(-k^2) + d(-k^2) + f(-k^2)\right)\mathcal{P}_w^0 h + \Big(c(-k^2)\\
&+ d(-k^2)\Big)\sqrt{3}\mathcal{P}_{ws}^0 h = \kappa\left(\mathcal{P}_w^0\right)\frac{\tau_{\mu\nu}}{k^2}.
\end{aligned} \tag{5.30}$$

The above two equations would suggest that the scalars are coupled in some way. However, from Eq. (5.8) we know that $c + d = 0$ and so we have two decoupled equations for the scalar modes as follows

$$\begin{aligned}
&\left(a(-k^2) - 3c(-k^2)\right)\mathcal{P}_s^0 h = \kappa\left(\mathcal{P}_s^0\right)\frac{\tau_{\mu\nu}}{k^2};\\
&\left(a(-k^2) + 2b(-k^2) + 2c(-k^2) + d(-k^2) + f(-k^2)\right)\mathcal{P}_w^0 h = \kappa\left(\mathcal{P}_w^0\right)\frac{\tau_{\mu\nu}}{k^2}.
\end{aligned} \tag{5.31}$$

In the above equation it can be shown that $\kappa\mathcal{P}_w^0\tau = 0$, by using the relations in Eq. (5.8). Finally, it is easy to see that

$$\mathcal{P}_s^0 h = \kappa \frac{\mathcal{P}_s^0}{k^2\left(a(-k^2) - 3c(-k^2)\right)}\tau_{\mu\nu}. \tag{5.32}$$

Therefore, by using Eq. (5.15) and the results of the propagator component relations, we can easily show that the propagator is written as [50]

$$\Pi = \frac{\mathcal{P}^2}{ak^2} + \frac{\mathcal{P}_s^0}{(a - 3c)\,k^2}. \tag{5.33}$$

Note that if we wish to recover GR then we must have that [51]

$$a(0) = c(0) = -b(0) = -d(0) = 1. \tag{5.34}$$

This ensures that we have only the physical gravitational propagator

$$\lim_{k^2\to 0}\Pi = \frac{\mathcal{P}^2}{k^2} - \frac{\mathcal{P}_s^0}{2k^2} \equiv \Pi_{GR}, \tag{5.35}$$

where we should note that there is a negative residue for the $\mathcal{P}_s^0$ component as $k^2 = 0$ [97]. In Ref. [51] the authors show that various choices of $a(\Box)$, $b(\Box)$, $c(\Box)$, $d(\Box)$

and $f(\Box)$ provide the propagator for different gravitational theories and discuss these theories and possible pathologies in these theories.
Without loss of generality we can set $f = 0$ and then using the relations shown in Eq. (5.8) we can show that $a = -b = c = -d$ [51]. This leaves us with only one free function $a(\Box)$. We can the rewrite the propagator in the terms of only this function as

$$\Pi = \frac{1}{a(-k^2)k^2}\left(\mathcal{P}^2 - \frac{\mathcal{P}_s^0}{2}\right) = \frac{1}{a(-k^2)}\Pi_{GR}. \tag{5.36}$$

So we now need to place a set of conditions on the value of $a(\Box)$. Firstly as we wish to recover GR we need $a(0) = 1$, secondly $a(\Box)$ must have no zeros as this would result in the introduction of Weyl ghosts to the theory, so $a(\Box)$ must be some entire function [51]. Now if we choose $a(\Box)$ to be some polynomial we would obtain a theory which is finitely differential, and as seen in the case of fourth order derivative gravity this would lead to pathologies somewhere in the theory. In order to ensure that the theory is UV safe we need to choose some function that is infinitely differential. The authors in Ref. [100] have investigated whether exponential of entire functions will indeed satisfy the required conditions of the modified propagator. They have done this by looking at the form of the propagator as we have in Eq. (5.36) and then determining what the Newtonian like potentials would look like if $a(\Box)$ is an exponential entire function. Where indeed they have shown that these potentials in the case of IDG do not diverge to infinity for small values of r but do indeed return to the GR potential for large values of r. They note that the simplest choice one could make about the function is that [50]

$$a(\Box) = e^{-\frac{\Box}{M_s^2}}, \tag{5.37}$$

where M_s is the mass scale and represents the scale of non-locality. The exponential entire function introduces no new poles to the theory. Therefore there are no new dynamical degrees of freedom other than those of GR i.e. the transverse and traceless degrees of freedom. It should be noted that this is the simplest choice we could have made and that others such as Frolov et al. have shown in the Ref. [101, 102] that higher order derivatives can be used in the exponential. So as stated in the introduction our aim of this theory is to have some way of weakening the strength of the gravitational propagator as they interact at very short ranges, such that the potential, and therefore forces, between the two propagators remains finite. In this theory the radial values of M_s represents exactly the location where the interactions between two gravitational propagators weakens, at the expense of local interactions. The authors in Ref. [100] note that the limits on the value of M_s would have to be determined experimentally, where testing the deviations from GR would give us clues as to what value M_s would most likely take. Current experiments have that the bounds on the value of M_s would be between $0.004eV$ and the Plank length [103]. It should be noted that through the choices made above the action can be rewritten. Firstly we have set $a(\Box) = c(\Box)$ such that we have the following relation between $F_1(\Box)$, $F_2(\Box)$ and $F_3(\Box)$, Eq. (5.7) that

$$F_2(\Box)\Box = -2\left[F_1(\Box)\Box + F_3(\Box)\Box\right]. \tag{5.38}$$

Without a loss of generality we can set $F_3(\Box) = 0$, this means that $F_2(\Box) = -2F_1(\Box)$. Furthermore the choice made in Eq. (5.37) implies that

$$\frac{1}{2}F_2(\Box) = \frac{1 - e^{-\frac{\Box}{M_s^2}}}{\Box}, \tag{5.39}$$

this further implies that

$$F_1(\Box) = \frac{e^{-\frac{\Box}{M_s^2}} - 1}{\Box}. \tag{5.40}$$

So we are left with an action that can be written as

$$S = \int d^4x\sqrt{g}\left[R + R\frac{e^{-\frac{\Box}{M_s^2}} - 1}{\Box}R + 2R_{\mu\nu}\frac{1 - e^{-\frac{\Box}{M_s^2}}}{\Box}R^{\mu\nu}\right]. \tag{5.41}$$

5.5 Metric of a point particle in IDG

Using the action in Eq. (5.2) we can derive the metric for a static mass point source as is done in Ref. [50]. The metric in this case will have the general form of [50]

$$ds^2 = -\left(1 + 2\Phi(r)\right)dt^2 + \left(1 - 2\Psi(r)\right)dx^2, \tag{5.42}$$

where $\Phi(r)$ and $\Psi(r)$ are the two potentials, whose magnitude must be less than one to ensure that the linear approximation holds. Our task then is to determine the values of $\Phi(r)$ and $\Psi(r)$. The field equations can then be written as

$$a(\Box)\left[\Box h_{\mu\nu} - \partial_\sigma\left(\partial_\nu h^\sigma_\mu + \partial_\mu h^\sigma_\nu\right) + \eta_{\mu\nu}\partial_\rho\partial_\sigma h^{\rho\sigma} + \partial_\mu\partial_\nu h - \eta_{\mu\nu}\Box h\right] = \kappa\tau_{\mu\nu}. \tag{5.43}$$

Next we take the trace and the 00 components of the field equations, setting $\tau_{\mu\nu} = m\delta^3(r)\delta^0_\mu\delta^0_\nu$, to obtain [50]

$$4a(\nabla^2)\nabla^2\Psi = 4a(\nabla^2)\nabla^2\Phi = \kappa m\delta^3(r). \tag{5.44}$$

In the static limit and to avoid ghosts we take $a(\Box)$ such that it is an infinitely differentialable and an entire function. The simplest choice that meets this criteria is $e^{-\Box/M_s^2}$ [50, 51].[3] Furthermore note that we take $\kappa = 8\pi G$. Then we need to take the Fourier transform of Eq. (5.44), doing so we obtain the following

$$\Phi = -\frac{4\pi Gm}{r}\int\frac{dk}{k}\frac{\sin kr}{a(-k^2)}. \tag{5.45}$$

Then transforming back into the spacial coordinates we obtain the following result for the potential [50]

$$\begin{aligned}\Phi(r) &= -\frac{4\pi Gm}{r}\int\frac{dk}{k}\sin kre^{-\frac{k^2}{M_s^2}},\\ &= -\frac{Gm}{r}\mathrm{Erf}\left(\frac{rM_s}{2}\right).\end{aligned} \tag{5.46}$$

[3] If we instead take $a(\Box) = e^{\Box/M_s^2}$, we wouldn't recover the Newtonian $1/r$ law [104].

It has been shown in Ref. [50] that this potential will produce a non-singular metric if $mM_s \ll M_p^2$. It is also shown that the new metric is the same as that obtained in GR when the value of r is large and that the metric is only modified when $r \to 0$. The aim of this part of the thesis is to obtain similar potential functions for an electrically charged object, and then for an object that is rotating.

Chapter 6

Electrically charged black holes in modified gravity

A simple non-trivial extension to the Schwarzschild like metric, already developed, is the electrically charged non-rotating Reissner-Nordström type space time. The non-triviality comes from the new horizon that will be introduced due to the electric charge, called the Cauchy horizon. However before we introduce the metric for the new theory we will briefly derive the metric for the linearised Reissner-Nordström black hole space time. This will make it easier to see how the solution of the new theory differs from that of GR.

6.1 Reissner-Nordström metric in Einstein's GR

We begin with the Einstein field equations, which are given as [105]

$$R_{\mu\nu} - \frac{1}{2}g_{\mu\nu}R = 8\pi G\tau_{\mu\nu}. \tag{6.1}$$

We then plug in the values for the linear Riemann tensor and Ricci scalar, as given in Eq. (5.4), and obtain the linearised field equation to be [25]

$$\begin{aligned}\Box h_{\mu\nu} + (\eta_{\mu\nu}\partial_\rho\partial_\sigma h^{\rho\sigma} + \partial_\mu\partial_\nu h)\\ -\partial_\sigma(\partial_\nu h^\sigma_\mu + \partial_\mu h^\sigma_\nu) - \eta_{\mu\nu}\Box h = -16\pi G\tau_{\mu\nu}.\end{aligned} \tag{6.2}$$

In the case of the electrically charged space time the stress energy tensor is given as[13]

$$\tau_{\mu\nu} = \frac{1}{4\pi}\left(\eta_{\rho\nu}F_{\mu\sigma}F^{\rho\sigma} - \frac{1}{4}\eta_{\mu\nu}F_{\rho\sigma}F^{\rho\sigma}\right), \tag{6.3}$$

where $F_{\mu\nu} = \partial_\mu A_\nu - \partial_\nu A_\mu$ is the electro magnetic field strength, and A_μ is the 4-potential. For non-rotating spherically symmetric space times $F_{10} = -F_{01} = E_r$, with $E_r = \frac{Q}{r^2}$, and all other terms are zero. Finally, we know that the metric will have the form

$$ds^2 = -(1 + 2\Phi_{GR})dt^2 + (1 - 2\Psi_{GR})(dr^2 + r^2 d\Omega^2), \tag{6.4}$$

where r is the isotropic radial coordinate. We therefore need to solve for the radial two potential functions Φ_{GR} and Ψ_{GR}. By looking at the 00-component and the trace of the linearised field equations in Eq. (5.12), we obtain the following coupled equations

$$\begin{aligned}\nabla^2 h_{00} - \partial_i\partial_j h^{ij} + \nabla^2 h &= -16\pi G\tau_{00},\\ -2\nabla^2 h + 2\partial_i\partial_j h^{ij} &= -16\pi G\tau.\end{aligned} \tag{6.5}$$

Using $h = 2(\Phi - 3\Psi)$, $h_{00} = -2\Phi$ and $h_{ii} = -2\Psi$, we obtain two differential equations for the two gravitational fields Φ and Ψ:

$$\begin{aligned} \nabla^2\Phi &= 4\pi G(\tau + 2\tau_{00}), \\ \nabla^2\Psi &= 4\pi G\tau_{00}. \end{aligned} \tag{6.6}$$

Due to the anti-symmetric property of the electro magnetic tensor, the traceless component of the energy-momentum tensor is traceless, $\tau = 0$, and the 00-component is given as $\tau_{00} = Q^2/8\pi r^4$. We can now solve the two differential equations in Eq. (6.6). Note that the potential function should not change when θ or ϕ are varied and so the derivative is purely a second order derivative of the isotropic radial coordinate. This greatly simplifies the integral that we need to use. Furthermore, in the derivation of the electrically neutral non-rotating case in Ref. [50], the authors have used a Fourier transform to solve of the potentials. In this case we cannot use this trick, as the absence of the the Dirac delta means that our integrals do not converge. Instead we solve the equations as non-homogeneous second order derivative equations. The solution would therefore have to have the form of

$$\begin{aligned} \Phi(r) &= -\frac{C_1}{r} + \frac{GQ^2}{2r^2} + C_2, \\ \Psi(r) &= -\frac{C_1}{r} + \frac{GQ^2}{4r^2} + C_2, \end{aligned} \tag{6.7}$$

where C_1 and C_2 are two integration constants whose value can be fixed by imposing suitable boundary conditions. We need to ensure that the potential function vanishes as $r \to \infty$, this implies that $C_2 = 0$. Secondly, we wish to ensure that in the limit that Q goes to zero we have the Schwarzschild potential functions which is guaranteed if $C_1 = Gm$. As such that the potential functions are

$$\begin{aligned} \Phi(r) &= -\frac{Gm}{r} + \frac{GQ^2}{2r^2}, \\ \text{and } \Psi(r) &= -\frac{Gm}{r} + \frac{GQ^2}{4r^2}. \end{aligned} \tag{6.8}$$

Note that in this case the two potentials are different, in contrast to the case of the Schwarzschild solution given in Ref. [50], where both potentials are the same. As we are working the linear regime we should note that this solution is only valid if $2|\Phi| < 1$ and $2|\Psi| < 1$, so the metric breaks down when we are very close to the event horizon, which is located at $r_\pm = -Gm \pm \sqrt{G^2m^2 - GQ^2}$. Furthermore, note the solution for the event horizon implies that $Q \leq \sqrt{Gm^2}$. [1]

6.2 Linearised metric solution for an electrically charged source in IDG

Next we construct the metric for an electrically charged mass in the theory of IDG. Starting with the field equations derived in Ch. 5 see Eq. (5.13),

$$a(\Box)\left[\Box h_{\mu\nu} - \left(\partial_\mu\partial_\sigma h^\sigma_\nu + \partial_\nu\partial_\sigma h^\sigma_\mu\right) + \left(\eta_{\mu\nu}\partial_\sigma\partial_\rho h^{\sigma\rho} + \partial_\mu\partial_\nu h\right) - \eta_{\mu\nu}\Box h\right] = -\kappa\tau_{\mu\nu}, \tag{6.9}$$

[1] This is one example of the weak formulation of the *cosmic censorship conjecture*; see Refs. [106–108]

and using a metric of the same form as given in Eq. (6.4), we take the trace and then the the 00-components of the field equations to obtain

$$\begin{aligned} e^{-\nabla^2/M_s^2}\left[\nabla^2 h_{00} - \partial_i\partial_j h^{ij} + \nabla^2 h\right] &= -16\pi G\tau_{00}, \\ e^{-\nabla^2/M_s^2}\left[-2\nabla^2 h + 2\partial_i\partial_j h^{ij}\right] &= -16\pi G\tau. \end{aligned} \tag{6.10}$$

We decouple these two equations by noting that $h = 2(\Phi - 3\Psi)$, $h_{00} = -2\Phi$ and $h_{ii} = -2\Psi$. Thus we obtain two differential equations in terms of the two metric potentials Φ and Ψ

$$\begin{aligned} e^{-\nabla^2/M_s^2}\nabla^2\Phi &= 4\pi G(\tau + 2\tau_{00}), \\ e^{-\nabla^2/M_s^2}\nabla^2\Psi &= 4\pi G\tau_{00}. \end{aligned} \tag{6.11}$$

Recall that the electrically charged stress energy tensor is traceless, $\tau = 0$, while the 00-component is given by $\tau_{00} = Q^2/8\pi r^4$. So the equations in Eq. (6.11) can be rewritten as

$$\begin{aligned} e^{-\nabla^2/M_s^2}\nabla^2\Phi &= \frac{GQ^2}{r^4}, \\ e^{-\nabla^2/M_s^2}\nabla^2\Psi &= \frac{GQ^2}{2r^4}. \end{aligned} \tag{6.12}$$

By simply redefining the fields as

$$\bar{\Phi} := e^{-\nabla^2/M_s^2}\Phi, \qquad \bar{\Psi} := e^{-\nabla^2/M_s^2}\Psi, \tag{6.13}$$

the equations in Eq. (6.12) become

$$\begin{aligned} \nabla^2\bar{\Phi}(r) &= \frac{GQ^2}{r^4}, \\ \nabla^2\bar{\Psi}(r) &= \frac{GQ^2}{2r^4}. \end{aligned} \tag{6.14}$$

These equations are exactly of the same form as we had for the Reissner-Nordström case in the previous section in Eq. (6.6), so we will have the same form of the solutions,

$$\begin{aligned} \bar{\Phi}(r) &= -\frac{C_1}{r} + \frac{GQ^2}{2r^2} + C_2, \\ \bar{\Psi}(r) &= -\frac{C_1}{r} + \frac{GQ^2}{4r^2} + C_2. \end{aligned} \tag{6.15}$$

We impose the same boundary conditions as before, and obtain

$$\begin{aligned} \Phi(r) &= -Gme^{\nabla^2/M_s^2}\left(\frac{1}{r}\right) + \frac{GQ^2}{2}e^{\nabla^2/M_s^2}\left(\frac{1}{r^2}\right), \\ \Psi(r) &= -Gme^{\nabla^2/M_s^2}\left(\frac{1}{r}\right) + \frac{GQ^2}{4}e^{\nabla^2/M_s^2}\left(\frac{1}{r^2}\right). \end{aligned} \tag{6.16}$$

However, this does not necessarily reduce to the potentials obtained for the non-rotating electrically neutral case as given in Ref. [50]. This is because we have not fully accounted for the effects that the $e^{-\nabla^2/M_s^2}$ terms have on the $1/r$ and $1/r^2$ terms. Note that we can use the fact that we need to reduce to the electrically neutral case to give us to what these potentials should look like. For the $1/r$ case we use the

procedure as shown in Ref. [50] and obtain the following

$$\begin{aligned} e^{\nabla^2/M_s^2}\left(\frac{1}{r}\right) &= e^{\nabla^2/M_s^2}\int \frac{d^3k}{(2\pi)^3}\frac{4\pi}{k^2}e^{i\vec{k}\cdot\vec{r}} \\ &= \int \frac{d^3k}{(2\pi)^3}\frac{4\pi}{k^2}e^{-k^2/M_s^2}e^{i\vec{k}\cdot\vec{r}} \\ &= \frac{2}{\pi}\int_0^\infty dk\,\frac{\sin(kr)}{kr}e^{-k^2/M_s^2} \\ &= \frac{1}{r}\mathrm{Erf}\left(\frac{M_s r}{2}\right), \end{aligned} \tag{6.17}$$

where we have used the fact that $4\pi/k^2$ is the Fourier transform of $1/r$. So in the case of $Q \to 0$ we reduce to the case of the neutral metric. Using this procedure we can calculate the contribution of the $1/r^2$, where we note that the Fourier transform for $1/r^2$ is $\frac{2\pi^2}{k}\mathrm{sign}(k)$. We then have the following solution;

$$\begin{aligned} e^{\nabla^2/M_s^2}\left(\frac{1}{r^2}\right) &= \int \frac{d^3k}{(2\pi)^3}\frac{2\pi^2}{k}\mathrm{sign}(k)e^{-k^2/M_s^2}e^{i\vec{k}\cdot\vec{r}} \\ &= \int \frac{d^3k}{(2\pi)^3}\frac{2\pi^2}{k}\mathrm{sign}(k)e^{-k^2/M_s^2}e^{-2\pi ikr\cos\theta} \\ &= \int_0^\infty dk\,\frac{\sin(kr)}{r}e^{-k^2/M_s^2} \\ &= \frac{M_s}{r}\mathrm{F}\left(\frac{M_s r}{2}\right), \end{aligned} \tag{6.18}$$

where $\mathrm{F}(M_s r/2)$ is the Dawson function [109]. Which behaves in a similar way to the error function when its arguments are very small, in that the function becomes linear. Furthermore as the arguments in the function become very large the Dawson function asymptotically approaches zero. Thus, by using Eqs. (6.17, 6.18), we can now obtain the expressions for the two metric potentials in Eq. (6.16) as

$$\begin{aligned} \Phi(r) &= -\frac{Gm}{r}\mathrm{Erf}\left(\frac{M_s r}{2}\right) + \frac{GQ^2M_s}{2r}\mathrm{F}\left(\frac{M_s r}{2}\right), \\ \Psi(r) &= -\frac{Gm}{r}\mathrm{Erf}\left(\frac{M_s r}{2}\right) + \frac{GQ^2M_s}{4r}\mathrm{F}\left(\frac{M_s r}{2}\right). \end{aligned} \tag{6.19}$$

Note that $\Phi \neq \Psi$, as also happened in the GR case, see Sec. 6.1. In the case of $Q = 0$ we recover the linearised IDG metric for a static neutral point-source derived in Ref. [50], as expected. Next we need to ensure that the potential functions reduce to those of the linear Reissner-Nordström in the IR regime, that is in the region of space where $M_s r \gg 2$. For the $Gm/r\,(\mathrm{Erf}(M_s r/2))$ terms this is trivially true, since as the argument in the error function becomes large it tends towards 1. The case of the Dawson function is not so easy to see, however, by looking at the expansion of the Dawson function

$$F(x) = \frac{1}{2x} + \frac{1}{4x^3} + \frac{1}{8x^5} + \dots . \tag{6.20}$$

Note this is for when the argument x is large. We easily see that the potential function in the IDG case rapidly approaches that of the linear Reissner-Nordström case. This is shown in Fig. 6.1.

Finally, in the non-local region of space, $M_s r \leq 2$, the potentials remain small and so the metric does not break down as we approach the event horizon, as occurred with the potentials of the linear Reissner-Nordström metric. More importantly, as

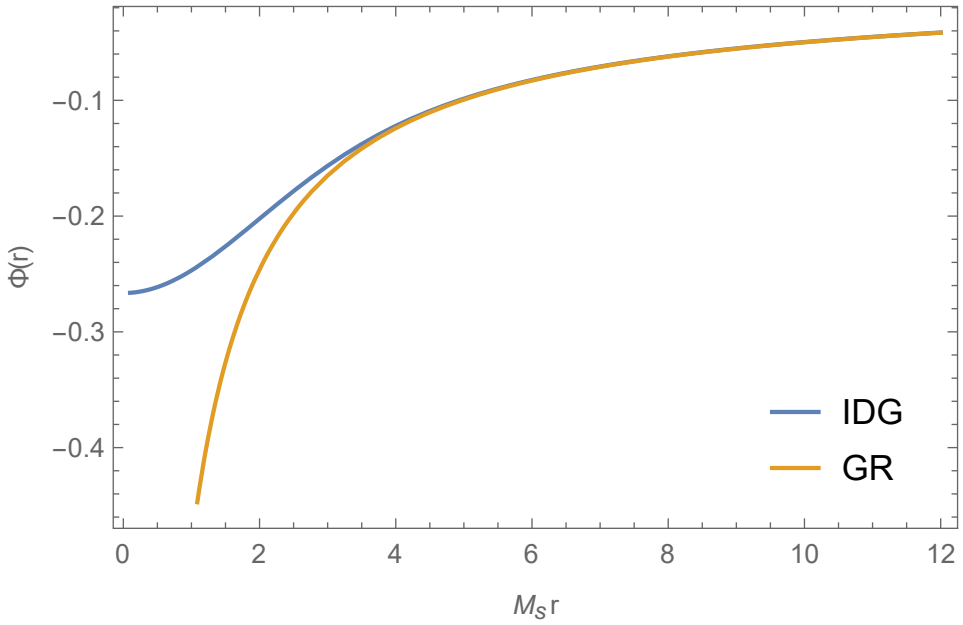

FIGURE 6.1: In the above we have shown the comparison between the potential Φ in the case of the Reissner-Nordström metric and the metric obtain from the action of IDG. We have chosen the values $G = 1, m = 1$ and $M_s = 0.5$ and take $Q = 0.5$. This figure is taken from [110]

we approach $r = 0$ the potentials approach the following constants

$$\begin{aligned}\lim_{M_s r\to 0}\Phi(r) &= -\frac{GmM_s}{\sqrt{\pi}} + \frac{1}{4}GQ^2M_s^2,\\ \lim_{M_s r\to 0}\Psi(r) &= -\frac{GmM_s}{\sqrt{\pi}} + \frac{1}{8}GQ^2M_s^2,\end{aligned} \tag{6.21}$$

because for $x \ll 1$ one has $\mathrm{Erf}(x) \sim 2x/\sqrt{\pi}$ and $\mathrm{F}(x) \sim x$. This is also shown in the Fig. 6.1, where we have chosen $G = 1, m = 1$, $M_s = 0.5$ and $Q = 0.5$. Before we move onto checking the restrictions that we must impose on our metric to ensure that it is an accurate approximation of the full metric we briefly note that the force,

$$\begin{aligned}F = \frac{\partial\Phi}{\partial r} = &-\frac{GQ^2M_sF\left(\frac{rM_s}{2}\right)}{2r^2} + \frac{GQ^2M_s^2\left(1 - rM_sF\left(\frac{rM_s}{2}\right)\right)}{4r} + \frac{GmErf\left(\frac{rM_s}{2}\right)}{r^2}\\ &- \frac{GmM_se^{-\frac{1}{4}r^2M_s^2}}{\sqrt{\pi}r},\end{aligned} \tag{6.22}$$

goes to zero linearly as r goes to zero. This vanishing force is a classical aspect of the asymptotic freedom in IDG [50].
In order for this metric to be valid we need to ensure that $2|\Phi| < 1$ and $2|\Psi| < 1$. We will work with only the Φ potential, as both potentials are essentially the same apart from a factor of a half in the electrically charged part of the potential. So by satisfying Φ we automatically satisfy Ψ. Firstly we need to ensure that in the case of $Q = 0$ we have that the potential remains less than one. So we have that

$$\frac{2Gm}{r}\frac{M_sr}{2} = GmM_s < 1. \tag{6.23}$$

Note that we know this is only a problem when r is small, so we have used the approximations for the error function when its arguments are small. The above equation implies that $mM_s < M_p^2$, where we have used that $G = 1/M_p^2$ and M_p is the Planck mass. Note also that this is the same condition as required in Ref. [50]. Next we can satisfy the weak-field inequality when the charge term is non-zero. Mathematically it is sufficient to say that in this, case as long as the sum of the two terms in less than one we are able to satisfy the weak field limit. However, in physical terms it is more correct to require that both the terms are always less than one. In fact, not having this condition in place means that it is possible for the GR action to dominate the quadratic action. That is we would lose the non singular nature of the metric at its origin [111]. As such we require that

$$\frac{GQ^2M_s}{2r}F\left(\frac{M_sr}{2}\right) \approx \frac{GQ^2M_s}{2r}\frac{M_sr}{2} < 1 \tag{6.24}$$

where in the above we have used that $F(x) \approx x$ when x is small. The above equation implies that $|Q|M_s < M_p$.

6.2.1 Comparing the IDG and the GR metrics

Recall that in the GR case we required that the condition $|Q| \leq \sqrt{G}m$, or in terms of the Planck mass $|Q| \leq \frac{m}{M_p}$ be satisfied, otherwise we would produce an extremal black hole, as it would have a naked singularity. In the IDG case we do not need this restriction, as there exists no singularity, and as such we would never violate the cosmic censorship conjecture. This limitation in GR means that we are unable to describe the gravitational effect of objects which have a charge mass ratio that violates this condition. As an example of where this may be an issue is that the electron has a charge to mass ratio that violates this condition. However, in IDG both inequalities in are allowed and provides us with two scenarios the first being

$$|Q| < \frac{m}{M_p} < \frac{M_p}{M_s}. \tag{6.25}$$

Which is the same as the GR case, and so is not as interesting as the second scenario which is

$$\frac{m}{M_p} < |Q| < \frac{M_p}{M_s}. \tag{6.26}$$

This scenario suggests that in the theory of IDG we are able to describe the gravitational effect of objects which have a charge larger than its mass in Planck units, as in the case of the electron. It should be noted that for objects the size of an electron the Compton wavelength is much larger than the Schwarzschild radius of the object, so a classical description of the their gravitational pull is not sufficient. In fact a quantum description would have to be employed to adequately describe this particle.
Finally, for the IDG metric it is possible to have a scenario where $Q^2M_s > m$. This has a rather peculiar result in that it is in the region of non-locality, $r < 2/M_s$, and it is possible to have a force that is repulsive. This repulsive force, however, occurs only within the region of non-locality and becomes attractive once again when we are outside the region of non-locality.
We now have the limits that ensure that the metric we have is guaranteed to remain linear, and have shown that the potentials return to the case of GR in the IR region

but remain non-singular all the way to $r = 0$. This does not prove that the metric is in fact non-singular, to prove that the metric is non-singular in the next section we look at the curvature terms of the metric and derive the expression for the Kretschmann scalar.

6.3 Curvature tensors

In the following we have computed the curvature tensors and invariants for the metric in Eq. (6.19). In this section however we only show the curvatures up to first order in G, since in the linear we have that $h_{\mu\nu} \sim G$. We direct the reader to App. B for the full expressions for the curvatures and the invariant quantities. The emphasis of this section will be to show that all the curvatures do in fact remain finite as $r \to 0$ for the metric given in Eq. (6.19), and that since the curvatures all remain finite, the invariants, such as the Kretschmann scalar, also remain finite. Therefore, we limit our analysis to the region of non-locality namely $r < 2/M_s$.
We begin our analysis with the Riemann tensor. In this case most of the components go to zero as r tends to zero. The only component that does not got to zero is

$$\mathcal{R}_{0101} \sim \frac{1}{12} G M_s^3 \left(\frac{2m}{\sqrt{\pi}} - Q^2 M_s \right). \tag{6.27}$$

As an aside we note that in the case where $Q = 0$ we recover the same Riemann tensor limit as for the non-rotating electrically neutral case given in Refs. [50, 112], furthermore, for the linear Reissner-Nordström metric all the non-zero Riemann tensor components tend to infinite in this limit. Using the Riemann tensor we can obtain the Ricci tensor, then checking the same limit we find that the only non-zero components are:

$$\begin{aligned} \mathcal{R}_{00} &\sim \frac{1}{4} G M_s^3 \left(\frac{2m}{\sqrt{\pi}} - Q^2 M_s \right), \\ \mathcal{R}_{11} &\sim \frac{1}{12} G M_s^3 \left(\frac{6m}{\sqrt{\pi}} - Q^2 M_s \right). \end{aligned} \tag{6.28}$$

Again in the appropriate limit these results are consistent with the electrically neutral case. The Ricci scalar is determined to be

$$\mathcal{R} \sim \frac{G m M_s^3}{\sqrt{\pi}}. \tag{6.29}$$

Finally, we can notice that all components of the Weyl tensor tend to zero in the non-local region, as we take $M_s r \to 0$:

$$\mathcal{C}_{\mu\nu\rho\sigma} \sim 0, \tag{6.30}$$

which implies that the static metric of a charged source becomes *conformally-flat* in the UV regime, $r < 2/M_s$. In fact, in the short distance regime, the metric in Eq. (6.19) can be approximated to

$$ds^2 \approx -(1 - \frac{2GmM_s}{\sqrt{\pi}} + \frac{GQ^2M_s^2}{2})dt^2 + (1 + \frac{2GmM_s}{\sqrt{\pi}} - \frac{GQ^2M_s^2}{4})(dr^2 + r^2 d\Omega^2), \tag{6.31}$$

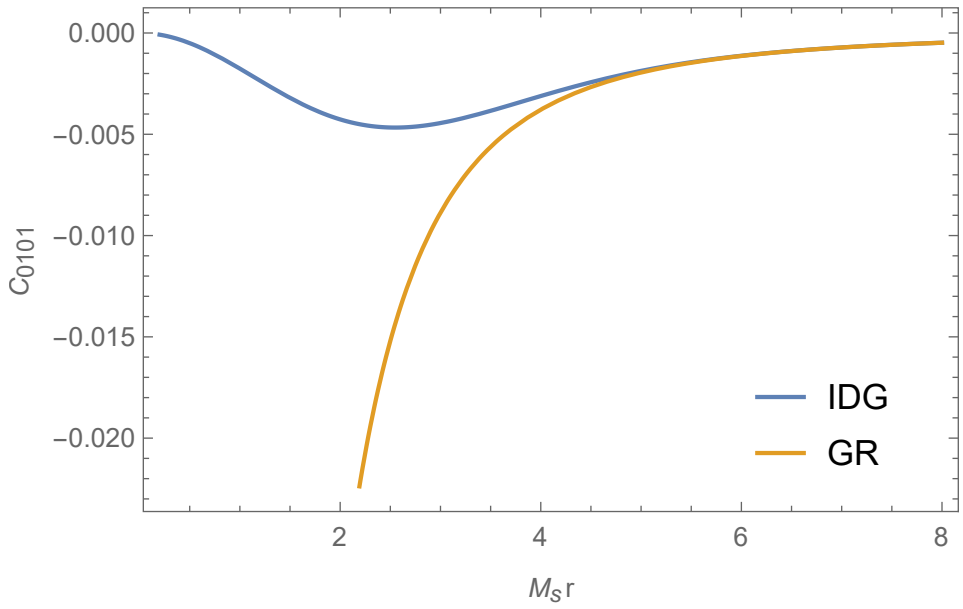

FIGURE 6.2: Here we have plotted the 0101 Weyl tensor component for both the linearised Reissner-Nordström metric and the charged metric obtained from the action of IDG. We have set $M_p = 1$, $m = 1$, $M_s = 0.5$ and $Q = 0.5$. In these units the Schwarzschild radius is $r_{sch} = 2$. This figure is taken from [110].

which can be put in a conformally-flat form by introducing a *conformal time*, τ, through the following coordinate transformation

$$\tau = \sqrt{\frac{1 - \frac{2GmM_s}{\sqrt{\pi}} + \frac{GQ^2M_s^2}{2}}{1 + + \frac{2GmM_s}{\sqrt{\pi}} - \frac{GQ^2M_s^2}{4}}}\, t; \tag{6.32}$$

such that the metric in the non-local region reads

$$\begin{aligned} ds^2 &= \left(1 + \tfrac{2GmM_s}{\sqrt{\pi}} - \tfrac{GQ^2M_s^2}{4}\right)\left[-d\tau^2 + dr^2 + r^2 d\Omega^2\right] \\ &= F^2 \eta, \end{aligned} \tag{6.33}$$

where η is the Minkowski metric and $F^2 \equiv 1 + \frac{2GmM_s}{\sqrt{\pi}} - \frac{GQ^2M_s^2}{4} > 0$ is the conformal factor. In Fig. 6.2 we have plotted the component $\mathcal{C}_{0101}$ of the Weyl tensor for both the charged case in *ghost-free* IDG and Reissner-Nordström in GR.

Fig. 6.2 shows that unlike in GR where the linearised approximation would break down for $r \leq 2$, in the case of *ghost-free* IDG we smoothly approach $r = 0$, provided $mM_s < M_p^2$ and $|Q|M_s < M_p$.
Finally we have computed all the curvature invariants squared. Their full expressions are shown in App. B, while in this section we will present their values in the non-local region. In the non-local regime, $r < 2/M_s$, the Kretschmann scalar $\mathcal{K} = \mathcal{R}_{\mu\nu\rho\sigma}\mathcal{R}^{\mu\nu\rho\sigma}$ tends to the following finite constant value:

$$\mathcal{K} \sim \frac{G^2M_s^6\left(10m^2 - 6\sqrt{\pi}mQ^2M_s + \pi Q^4M_s^2\right)}{6\pi}. \tag{6.34}$$

In Fig. 6.3 we have plotted the Kreschmann scalar for both the IDG theory, the

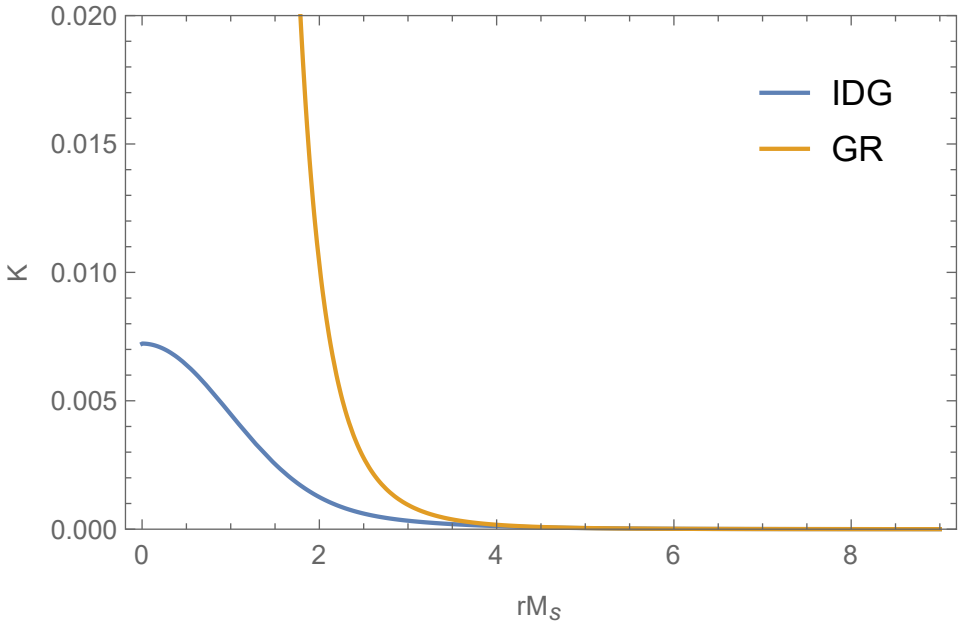

FIGURE 6.3: In the above plot we have used $M_p = 1$, $m = 1$, $M_s = 0.5$ and $Q = 0.5$. The plot shows that in the case of IDG the Kretschmann scalar does indeed remain finite as r tends to zero. This figure is taken from [110].

expression is given in App. B Eq. (B.8), and the linearised Reissner-Nordström metric.

We see from Fig. 6.3 that in the case of *ghost-free* IDG we can smoothly approach $r = 0$, provided $mM_s < M_p^2$ and $|Q|M_s < M_p$. From these two plots it is obvious that the presence of non-locality helps to avoid the curvature-singularities at the origin. Moreover, in the non-local region, the non-zero components of the Ricci scalar squared and the Ricci tensor squared are given by the following finite constant values

$$\mathcal{R}^2 \sim \frac{G^2 m^2 M_s^6}{\pi}, \tag{6.35}$$

$$\mathcal{R}_{\mu\nu}\mathcal{R}^{\mu\nu} \sim \frac{G^2 M_s^6 \left(12m^2 - 6\sqrt{\pi} m Q^2 M_s + \pi Q^4 M_s^2\right)}{12\pi}. \tag{6.36}$$

While the Weyl tensor squared vanishes for $r < 2/M_s$

$$\mathcal{C}_{\mu\nu\rho\sigma}\mathcal{C}^{\mu\nu\rho\sigma} \sim 0. \tag{6.37}$$

For completeness, it can be checked that the squared curvatures satisfy the following identity [13]:

$$\mathcal{C}_{\mu\nu\rho\sigma}\mathcal{C}^{\mu\nu\rho\sigma} = \frac{\mathcal{R}^2}{3} - 2\mathcal{R}_{\mu\nu}\mathcal{R}^{\mu\nu} + \mathcal{K}. \tag{6.38}$$

Needless to say, all the curvature invariants for the case of a point-charge source in *ghost free* IDG reduce to those of the uncharged case, $Q = 0$, as obtained in Ref. [112]. To sum up this chapter we make some brief concluding remarks. We note that we are indeed able to produce a metric in a charged space time in IDG using the action as given in Eq. (5.12) [50]. We are also able to ensure that this metric is accurate in the linear limit given that the conditions $mM_s < M_P^2$ and $|Q|M_s < M_p$ are met.

More importantly we have shown that invariant functions such as the Kretschmann scalar, are indeed singularity free, as none of these invariants become infinite in the limit $r \to 0$. Finally, we have also shown that the new metric, and all curvature and invariant terms, reduce to the metric obtained for a non-rotating electrically neutral object.

Chapter 7

Rotating black holes in IDG

In this chapter we begin with the Kerr metric from GR. This is so that we can familiarise ourselves with the important differences between the non-rotating case and the Kerr case. These will be crucial for guiding us towards finding the equivalent rotating metric in IDG. For the IDG metric we will begin with the field equations given in Eq. (5.12), and as we have done previously, we will check the potential functions for the rotating metric and the curvature tensors of the rotating metric, to ensure that they are indeed non-singular.

7.1 The Kerr metric

In rational polynomial coordinates the Kerr metric is given as [113, 114]

$$\begin{aligned} ds^2 = &-\left(1-\frac{2mr}{r^2+a^2\chi^2}\right)dt^2 - \frac{4mar\left(1-\chi^2\right)}{r^2+a^2\chi^2}dtd\varphi + \frac{r^2+a^2\chi^2}{r^2-2mr+a^2}dr^2 \\ &+\left(r^2+a^2\chi^2\right)\frac{d\chi^2}{1-\chi^2} + \left(1-\chi^2\right)\left(r^2+a^2+\frac{2ma^2r\left(1-\chi^2\right)}{r^2+a^2\chi^2}\right)d\varphi^2, \end{aligned} \tag{7.1}$$

where $\chi = \cos\theta$ is a transformation parameter used to convert the metric back into standard Boyer-Lindquist coordinates, while m is the mass and $J = am$ is the angular momentum, with a being the rotation parameter. In non-rotating black holes we have two regions of interest. Firstly we have the region of space outside of the black hole, or outside of the event horizon. Secondly we have the region of space inside the event horizon. This is the region of space where it is no longer possible for particle to escape the gravitational pull of the black hole. This is due to the the fact that at the event horizon, all lightlike paths point towards the centre of the black hole. This means that the only path a particle can take is towards the centre of the black hole. In the case of the rotating black hole, however, we have more than two regions of interest, so we briefly discuss them here as they will help in our derivation of the rotating metric in IDG and will allow us to perform a better comparison between the rotating black holes in IDG and GR. The first two regions we will briefly look at are the event horizons, namely the inner and outer event horizons. They are described by the equations $r_\pm = m \pm \sqrt{m^2-a^2}$, where r is the Boyer-Lindquist radial coordinate, which transforms to the Cartesian coordinate system as follows $x = \sqrt{r^2+a^2}\sin\theta\cos\phi$, $y = \sqrt{r^2+a^2}\sin\theta\sin\phi$ and $z = r\cos\theta$. So this region of space is topologically spherical, however, geometrically the region is elongated at its equator, which is due to the rotational parameter a, see Ref. [114] for a more in depth discussion.
Next we consider a new region called the ergosurfaces, given by the equation $r_E^\pm = m \pm \sqrt{m^2-a^2\cos^2\theta}$. The area enclosed by the outer ergosphere and the outer event

horizon is called the ergoregion. This is the region of space where an observer could still move radial away from the black hole, but cannot remain at the same angular location, since the effects of the frame dragging are too great and the observer is dragged along with the rotating black hole.
Finally, we will look a the singularity contained within the black hole. Unlike the non-rotating case this singularity is not a central singular region in the the black hole, instead it is a thin ring with the location given as [107]

$$x^2 + y^2 = a^2 \text{ and } z = 0. \tag{7.2}$$

Note that the ring is located perpendicularly to the rotation of the black hole. In all the cases above it should be clear that as $a \to 0$ we return to the case of the Schwarzschild black hole, as the event horizon returns to a geometrically spherical surface, and the ring singularity becomes the central point singularity. Finally, it should be noted that in the above we infer the restriction $a \leq m$, otherwise we have none physical solutions to the locations of these important regions.

7.2 The linearised rotating metric in IDG

Before we show the general form of the metric we need to first determine what the stress-tensor looks like. In the static cases of the stress-energy tensors we assumed that the tensor was all zeros except the τ_{00}, which had a Dirac delta function $\delta(r)$ so that we had a singularity at the location $r = 0$. We keep this in mind for the case of the rotating metric, but use the fact that the singularity is distributed about a ring with radius a, and set the energy tensor components to be

$$\tau_{00} = m\delta(z)\frac{\delta(x^2 + y^2 - a^2)}{\pi}, \quad \tau_{0i} = \tau_{00}v_i. \tag{7.3}$$

Note that the factor π in the denominator comes from the fact that $\delta(x, y) \equiv \delta(x)\delta(y) = \pi\delta(x^2 + y^2)$ [109], and v_i is the tangential velocity whose magnitude can be expressed as $v = \omega a$. Assuming that the rotation happens around the z-axis, we have $v_x = -y\omega$, $v_y = x\omega$, $v_z = 0$. Here ω is the angular velocity. Note that this choice of the stresss-energy tensor, in analogy with the static case, is compatible with the fact that in order for the Einstein equations and the Kerr metric to be defined in the entire spacetime we need a non-vanishing stress-energy tensor at the ring. In fact, by using the theory of distribution [115], it was rigorously shown that the stress-energy tensor for a Kerr metric has a structure similar to the one we have written in Eq. (7.3). For example, the (00)-component of the Einstein tensor in the case of the Kerr metric is $G_{00} \sim m\delta(z)\delta(x^2 + y^2 - a^2)$ [115]. A general linearised metric, which can describe the spacetime in the presence of a rotating source can be written in isotropic coordinates, as

$$ds^2 = -(1 + 2\Phi)dt^2 + 2\vec{h} \cdot d\vec{x}dt + (1 - 2\Psi)d\vec{x}^2, \tag{7.4}$$

where $h_{00} = -2\Phi < 1$, $h_{ij} = -2\Psi\delta_{ij} < 1$ and $h_{0i} \equiv h_i < 1$ to ensure that we are in the the weak-field and the slow rotation regime. Note that the metric components depend on the isotropic radius, r, which should not be confused with the Boyer-Lindquist radial coordinate used above. As before, we consider the 00-components and the trace of the field equations given in Eq. (5.12), furthermore, we also consider the $0x$ and the $0y$-components of the stress energy tensor, so as to include the off

diagonal terms. We then need to solve the following set of equations

$$\begin{aligned} &a(\Box)\left[2\nabla^2 h_{00} - \partial_\sigma\partial_\rho h^{\sigma\rho}\right] = -\kappa\tau_{00};\\ &-2a(\Box)\left[\nabla^2 h - 2\partial_\sigma\partial_\rho h^{\sigma\rho}\right] = -\kappa\tau;\\ &a(\Box)\left[\nabla h_{0x} - \partial_x\partial_\sigma h_0^\sigma\right] = -\kappa\tau_{0x};\\ &a(\Box)\left[\nabla h_{0y} - \partial_y\partial_\sigma h_0^\sigma\right] = -\kappa\tau_{0y}. \end{aligned} \tag{7.5}$$

In this case $\tau = -m\delta(z)\frac{\delta(x^2+y^2-a^2)}{\pi}$ and $h = 2(\Phi - 3\Psi)$. Applying these relations and simplifying we obtain the following:

$$\begin{aligned} e^{-\nabla^2/M_s^2}\nabla^2\Phi(\vec{r}) = e^{-\nabla^2/M_s^2}\nabla^2\Psi(\vec{r}) &= 4Gm\delta(z)\delta(x^2+y^2-a^2),\\ e^{-\nabla^2/M_s^2}\nabla^2 h_{0x}(\vec{r}) &= -16Gm\omega y\delta(z)\delta(x^2+y^2-a^2),\\ e^{-\nabla^2/M_s^2}\nabla^2 h_{0y}(\vec{r}) &= 16Gm\omega x\delta(z)\delta(x^2+y^2-a^2). \end{aligned} \tag{7.6}$$

Note that we have used $a(\Box) = e^{-\nabla^2/M_s^2}$ in the above. To solve the differential equations in Eq. (7.6) we can go to the Fourier space and then anti-transform back to coordinate space.

7.3 Smearing out the ring singularity at the linearised level

We begin by calculating the potential functions Φ and Ψ. To begin we first calculate the Fourier transform of the ring singularity distribution as shown in Eq. (7.3):

$$\mathcal{F}[\delta(z)\delta(x^2+y^2-a^2)] = \int dxdydz\delta(z)\delta(x^2+y^2-a^2)e^{ik_x x}e^{ik_y y}e^{ik_z z}. \tag{7.7}$$

It can be computed by performing the integral in cylindrical coordinates: $x = \rho\cos\varphi$, $y = \rho\sin\varphi$, $z = z$. Our integrals then transforms as follows,

$$\begin{aligned} \mathcal{F}[\delta(z)\delta(x^2+y^2-a^2)] &= \int_{-\infty}^{\infty} dz\delta(z)e^{ik_z z}\int_0^\infty d\rho\rho\delta(\rho^2-a^2)\int_0^{2\pi} d\varphi e^{ik_x\rho\cos\varphi}e^{ik_y\rho\sin\varphi}\\ &= \int_{-\infty}^{\infty} dz\delta(z)e^{ik_z z}\int_0^\infty d\rho\rho\delta(\rho^2-a^2)2\pi I_0\left(\sqrt{-\rho^2\left(k_x^2-k_y^2\right)}\right)\\ &= \int_{-\infty}^{\infty} dz\delta(z)e^{ik_z z}\int_0^\infty d\rho^2\delta(\rho^2-a^2)\pi I_0\left(\sqrt{-\rho^2\left(k_x^2-k_y^2\right)}\right)\\ &= \pi I_0\left(ia\sqrt{k_x^2+k_y^2}\right), \end{aligned} \tag{7.8}$$

where I_0 is a modified Bessel function, which is also defined in terms of the Bessel function $I_0(x) = J_0(ix)$. We then transform back to space-time coordinates. From Eq. (7.5) we have that the transformation back to radial coordinates is as follows

$$\Phi(\vec{r}) = -4\pi Gm\int\frac{d^3k}{(2\pi)^3}\frac{e^{-k^2/M_s^2}}{k^2}I_0\left(ia\sqrt{k_x^2+k_y^2}\right)e^{ik_x x}e^{ik_y y}e^{ik_z z}, \tag{7.9}$$

where $d^3k = dk_x dk_y dk_z$ and $k^2 = k_x^2 + k_y^2 + k_z^2$. In general it is not possible to solve this integral, however, we can determine if the ring singularity is still present by checking whether the potential functions diverge as they did in the case of the GR

potentials. This simplifies the above integrals as we now restrict ourselves to the case when $z = 0$, as this puts us in the plane in which the ring should be present. Using cylindrical coordinates, that is $k_x = \zeta \cos\phi$, $k = \zeta \sin\phi$ and $k_z = k_z$, we can rewrite the integral in Eq. (7.9) as

$$\begin{aligned}\Phi(\rho) &= -4\pi G m \int_0^\infty d\zeta \int_0^{2\pi} d\varphi \int_0^\infty dk_z \frac{1}{(2\pi)^3} \frac{e^{-\frac{\left(k_z^2+\zeta^2\right)}{M_s^2}}}{k_z^2+\zeta^2} I_0\left(ia\zeta\right) e^{i\zeta\cos\varphi x} e^{i\zeta\sin\varphi y} e^{ik_z z} \\ &= -\frac{Gm}{4\pi^2} \int_0^\infty d\zeta \int_0^{2\pi} d\varphi J_0\left(a\zeta\right) \mathrm{Erfc}\left(\frac{\zeta}{M_s}\right) e^{i\zeta\cos\varphi x} e^{i\zeta\sin\varphi y} \\ &= -Gm \int_0^\infty d\zeta J_0\left(ia\zeta\right) J_0\left(i\zeta\rho\right) \mathrm{Erfc}\left(\frac{\zeta}{M_s}\right),\end{aligned} \tag{7.10}$$

where J_0 is the Bessel function and Erfc(x) is the complimentary error function [109]. Note that for large values of x the Erfc(x)function goes to zero, and as $x \to 0$ the Erfc(x) $\to 1$ linearly. It is not possible to solve this integral analytically, however numerically we can show that at the position $x^2 + y^2 = a^2$ the potential does not diverge, see Fig. 7.1. We can recover the GR limit of this potential function if we let the region of non-locality vanish, that is if we let $M_s \to \infty$, then the potential becomes

$$\Phi_{GR}(\rho) = -Gm \int_0^\infty d\zeta J_0\left(ia\zeta\right) J_0\left(i\zeta\rho\right). \tag{7.11}$$

A comparison between this potential and the potential for IDG is given in Fig. 7.1. Notice also that the potential in the GR case diverges at the ring singularity as expected, whereas the potential for the IDG metric does not diverge, and its absolute value remains less than one. This is what we have expected to be physically that is, the IDG smears out a ring distribution very similarly to the case of a point source [49, 50, 112, 117]. We also note that the multipole expansion is a good approximation for the potential function for $\rho > a$. In the figure above we can trust the linear approximation all the way up to $\rho = 0$, where to ensure that this is always the case we must have that $2\Phi(0) < 1$. in this case we can analytically solve the integral, as it reduces to

$$\begin{aligned}\Phi(0) &= -Gm \int_0^\infty d\zeta J_0\left(ia\zeta\right) \mathrm{Erfc}\left(\frac{\zeta}{M_s}\right) \\ &= -\frac{Gm}{a} \mathrm{Erf}\left(\frac{M_s a}{2}\right).\end{aligned} \tag{7.12}$$

In the case that $\mathrm{Erf}\left(M_s a/2\right) < 1$ we need that $a > 2Gm$ in order to ensure that the weak field approximation is always true. However, in the case that $a < 2Gm$, the weak-field inequality is satisfied as long as

$$a < \frac{2}{M_s} \quad \left(\text{radius of the ring} < \text{scale of nonlocality}\right). \tag{7.13}$$

This suggests that ghost-free IDG can indeed avoid the ring-type singularity.

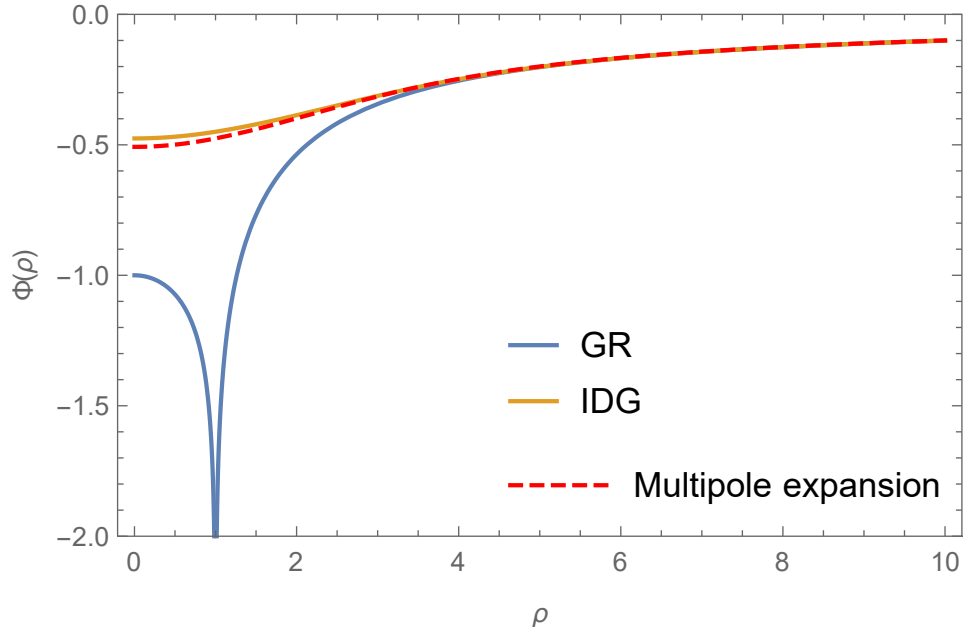

FIGURE 7.1: In the above we have shown the comparison for the Φ component in the GR case, shown in blue, the IDG case, shown in orange and obtained by numerically integrating Eq. 7.25. Finally the red dashed line represents the potential obtained by performing the multipole expansion. In the above we have set $G = 1$, $m = 0.5$, $a = 1$ and $M_s = 0.9$. This figure is taken from [116].

7.3.1 Computing h_{0i} components for a rotating ring

This is not the full solution, as up to now we have only calculated the potential function for a static ring. In order to introduce the rotation we must include the h_{0i}. We proceed as before, in that we first perform a Fourier transform on the functions h_{0i}, and then transform back into coordinate space. In general these transforms can be written as

$$\mathcal{F}[j\,\delta(z)\delta(x^2+y^2-a^2)] = \int dxdydz\; j\,\delta(z)\delta(x^2+y^2-a^2)e^{ik_x x}e^{ik_y y}e^{ik_z z}, \tag{7.14}$$

where $j = x,\ y$ depending on whether we are investigating h_{0y} or h_{0x}. As we have done in Eq. (7.8), we perform the integration in cylindrical coordinates. For the h_{0x} component we have the following integration

$$\begin{aligned}
\mathcal{F}[x\,\delta(z)\delta(x^2+y^2-a^2)] &= \int_{-\infty}^{\infty} dz\delta(z)e^{ik_z z}\int_0^{\infty} d\rho\rho^2\delta(\rho^2-a^2)\int_0^{2\pi} d\varphi e^{ik_x\rho\cos\varphi}e^{ik_y\rho\sin\varphi}\cos\varphi \\
&= \int_0^{\infty} d\rho\rho^2\delta(\rho^2-a^2)\left(\frac{2\pi k_x}{\sqrt{k_x^2+k_y^2}}I_1\left(i\rho\sqrt{k_x^2+k_y^2}\right)\right) \\
&= \pi\frac{k_x}{\sqrt{k_x^2+k_y^2}}\int_0^{\infty} d(\rho^2)\rho\delta(\rho^2-a^2)I_1\left(i\rho\sqrt{k_x^2+k_y^2}\right) \\
&= \pi a\frac{k_x}{\sqrt{k_x^2+k_y^2}}I_1\left(ia\sqrt{k_x^2+k_y^2}\right),
\end{aligned} \tag{7.15}$$

similarly for the h_{0y} component where we obtain the following result

$$\mathcal{F}[y\delta(z)\delta(x^2+y^2-a^2)] = \pi a \frac{k_y}{\sqrt{k_x^2+k_y^2}} I_1\left(ia\sqrt{k_x^2+k_y^2}\right), \tag{7.16}$$

with I_1 being the modified Bessel function. We now transform back into coordinate space where the components h_{0i} are then integrated as follows:

$$\begin{aligned} h_{0j}(\vec{r}) &= \frac{2Gm\omega a}{\pi^3}\int_0^\infty d\zeta \int_0^{2\pi} d\phi \int_0^\infty dk_z \frac{e^{-(k_z^2+\rho^2)/M_s^2}}{k_z^2+\rho^2}\frac{\zeta\cos\phi}{\zeta} I_1\left(ia\zeta\right) e^{i(\zeta\cos\phi x} e^{i\zeta\sin\phi y} \\ &= 16Gm\omega a \int \frac{d^3k}{(2\pi)^3}\frac{e^{-k^2/M_s^2}}{k^2}\frac{k_j}{\sqrt{k_x^2+k_y^2}} I_1\left(ia\sqrt{k_x^2+k_y^2}\right) e^{ik_x x} e^{ik_y y} e^{ik_z z}, \end{aligned} \tag{7.17}$$

where $j = x,\ y$. Again, in general these integrals cannot be solved analytically, so as we have done in Eq. (7.10) we set $z = 0$ and obtain the following for the cross terms,

$$\begin{aligned} h_{0x}(\vec{r}) &= \int dk^2 \pi a \frac{k_x}{\sqrt{k_x^2+k_y^2}} I_1\left(ia\sqrt{k_x^2+k_y^2}\right) \times \\ &\quad 16Gm\omega a \int \frac{d^3k}{(2\pi)^3}\frac{e^{-k^2/M_s^2}}{k^2}\frac{k_j}{\sqrt{k_x^2+k_y^2}} I_1\left(ia\sqrt{k_x^2+k_y^2}\right) e^{ik_x x} e^{ik_y y} e^{ik_z z} \\ &= \frac{Gma\omega}{8\pi^2}\int_0^\infty d\zeta \int_0^{2\pi} e^{\frac{2\zeta^2}{M_s^2}} e^{ix\zeta\cos\phi + iy\zeta\sin\phi}\frac{\cos\phi}{\zeta} I_1(ia\zeta)\mathrm{Erfc}\left(\frac{\zeta}{M_s}\right) \\ &= \frac{Gma\omega}{8\pi^2}\int_0^\infty d\zeta e^{\frac{2\zeta^2}{M_s^2}} I_1(i\zeta\rho) I_1(ia\zeta)\mathrm{Erfc}\left(\frac{\zeta}{M_s}\right). \end{aligned} \tag{7.18}$$

For the case of h_{0y} we obtain the result

$$h_{0y}(x,y) = -4Gm\omega a\frac{x}{\rho}\int_0^\infty d\zeta I_1(ia\zeta) I_1(i\zeta\rho)\mathrm{Erfc}\left(\frac{\zeta}{M_s}\right), \tag{7.19}$$

where $\rho = \sqrt{x^2+y^2}$ is the radial cylindrical coordinate in the plane $z = 0$. Since $\theta = \pi/2$, we have $x = \rho\cos\varphi$ and $y = \rho\sin\varphi$ thus all the radial dependence and the singularity structure are taken into account by the integrals. Next we can show that the GR limit is obtained when we let $M_s \to \infty$, since $\mathrm{Erfc}(\zeta/M_s)$ goes to one, such that the integral becomes

$$H_{GR}(\rho) := \int_0^\infty d\zeta I_1(ia\zeta) I_1(i\zeta\rho). \tag{7.20}$$

The integrals in Eq.(7.18), (7.19) and (7.20) cannot be solved analytically but, we can numerically calculate them to show that there is no singularity in the IDG case. This has been done in Fig. 7.2.

As we had in the case of the potential Φ and Ψ in the GR limit for the h_{0i} components we see that we have a singularity forming at the location $\rho = a$, however in the case of IDG this does not occur, and the values remains finite. In fact in the case

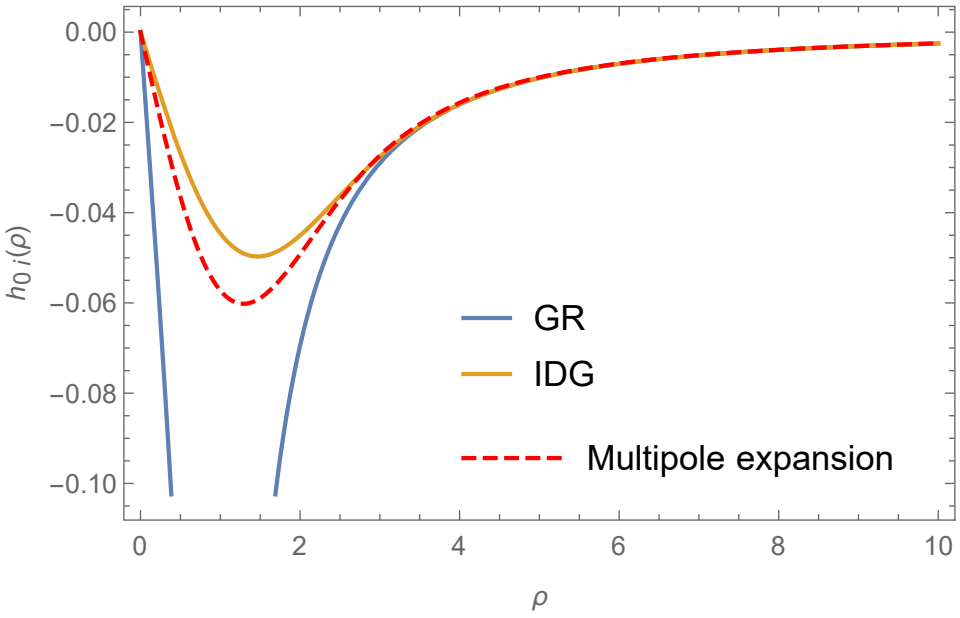

FIGURE 7.2: In this plot we have shown the results of the numerical computation for the integrals in Eq. (7.20) and the behaviour of the same function in the case of the multipole expansion in Eq.(7.24). The blue line corresponds to the behaviour of the function H_{GR}, and so of the cross-term in GR; the orange line to the behaviour of the function H_{IDG}, and so of the cross-term in IDG; while the dashed red line represents the cross-term in the case of the multipole expansion. For convenience we have chosen $a = 1$ and $M_s = 1.5$. We can notice that the metric components h_{0i} blow up in GR for $\rho = a = 1$, while they are finite in IDG; moreover, the metric coming from the multipole expansion is a very good approximation outside the source, i.e. for $\rho > a$. This figure is taken from [116].

of IDG H remain finite everywhere, it is always less than 1, so we can trust our linear approximation all the way up to $\rho = 0$. As in the case of the static metrics in the IDG smears out the ring singularity. At the origin we note that the cross terms and the metric approaches conformal-flatness as it becomes the solution of the static metric [112].
In the IR regime, that is the case of $\rho \gg a$, we see that the rotational metric components for both IDG and GR match very well. In fact at these large distances we recover the Lense-Thirring metric, which is a weak field approximation of the Kerr metric [118]

$$ds^2 = -\left(1 - \frac{2Gm}{r}\right) dt^2 + \frac{4GJ}{r^3}(ydxdt - xdydt) + \left(1 + \frac{2Gm}{r}\right)(dr^2 + r^2 d\Omega^2). \tag{7.21}$$

To exactly recover the Lense-Thirring metric at large distances, we need to identify $J = ma^2\omega$, which is nothing but the relation $J = I\omega$, where $I = ma^2$ is the moment of inertia of the delta-Dirac ring distribution. Note that the relation $J = am$ does not hold, but the angular momentum is related to the parameter a through the momentum of inertia of the source.

7.4 Rotating metric outside the source: multipole expansion in IDG

We want to find a more general metric for the rotating metric in IDG, which is outside of the region of nonlocality and where we have not assumed the large distance limit. In this limit the metric given in Eq. (7.4) is valid, the h_{00} and h_{ii} components will be the same as those obtained in the static case. Though for the off diagonal terms we will need to use a multipole expansion for $\mathrm{Erf}\left(M_s|\vec{r}-\vec{r}'|/2\right)/|\vec{r}-\vec{r}'|$,

$$\begin{aligned}\frac{1}{|\vec{r}-\vec{r}'|}\mathrm{Erf}\left(\frac{M_s|\vec{r}-\vec{r}'|}{2}\right) =& \frac{1}{r}\mathrm{Erf}\left(\frac{M_s r}{2}\right) \\ &+\left[\frac{1}{r^3}\mathrm{Erf}\left(\frac{M_s r}{2}\right)-\frac{M_s}{\sqrt{\pi}r^2}e^{-\frac{M_s^2 r^2}{4}}\right]\sum_{j=1}^{3}x^j x'^j+\cdots;\end{aligned} \tag{7.22}$$

which recovers the GR case in the large distance regime, $M_s r \gg 2$, as expected. This expansion holds true for $r > r' \sim a$, which would be regions outside of the source. By using Eq. (7.22), we can now compute the h_{0i} components

$$\begin{aligned}h_{0i}(\vec{r}) &= 4G\int d^3r'\frac{T_{0i}(\vec{r}')}{|\vec{r}-\vec{r}'|}\mathrm{Erf}\left(\frac{M_s|\vec{r}-\vec{r}'|}{2}\right) \\ &= 2G\left[\frac{1}{r^3}\mathrm{Erf}\left(\frac{M_s r}{2}\right)-\frac{M_s}{\sqrt{\pi}r^2}e^{-\frac{M_s^2 r^2}{4}}\right](\vec{r}\times\vec{J})_i.\end{aligned} \tag{7.23}$$

We can move from Cartesian to isotropic coordinates, so that the $d\varphi dt$ component of the metric will be given by:

$$2\vec{h}\cdot d\vec{x}dt = -4GJ\left[\frac{1}{r}\mathrm{Erf}\left(\frac{M_s r}{2}\right)-\frac{M_s}{\sqrt{\pi}}e^{-\frac{M_s^2 r^2}{4}}\right]\sin^2\theta d\varphi dt, \tag{7.24}$$

which in the regime $M_s r \gg 2$ recovers the GR result, as expected. Moreover, by expressing $J = I\omega = ma^2\omega$ and imposing $|h_{0i}| \sim GmM_s^2\omega a^2 < 1$, we notice that the slow rotation regime means $\omega < 1/a$, when we also require $GmM_s < 1$ and $aM_s < 1$. Note that by recasting the cross-term in terms of the angular momentum and imposing the linearised regime we obtain $|h_{0i}| \sim GM_s^2 J < 1$, which also means; $J < (M_p/M_s)^2$. From the last inequality, since $M_s \leq M_p$, the angular momentum J may also exceed one in IDG. The linearised spacetime metric in Eq. (7.4) outside the source, $r > a$, in the case of IDG reads:

$$\begin{aligned}ds^2 = &-\left(1-\frac{2Gm}{r}\mathrm{Erf}\left(\frac{M_s r}{2}\right)\right)dt^2+\left(1+\frac{2Gm}{r}\mathrm{Erf}\left(\frac{M_s r}{2}\right)\right)(dr^2+r^2d\Omega^2) \\ &-4GJ\left[\frac{1}{r}\mathrm{Erf}\left(\frac{M_s r}{2}\right)-\frac{M_s}{\sqrt{\pi}}e^{-\frac{M_s^2 r^2}{4}}\right]\sin^2\theta d\varphi dt.\end{aligned} \tag{7.25}$$

From Fig. 7.1 and 7.2, it is clear that the metric constructed by using the multipole expansion is a very good approximation to describe the spacetime outside the source, $r > a$; while in the regime $M_s r \gg 2$, we recover the GR predictions, indeed Eq. (7.25) reduces to the Lense-Thirring metric [118] in Eq. (7.21). Thus, in the case of ghost-free IDG, for a rotating source we have found a hierarchy of scales: the radius of the source a, the Schwarzschild radius $r_{\mathrm{sch}} = 2Gm$ and the scale of non-locality $r_{NL} \sim 2/M_s$, which have to satisfy the following set of inequalities to preserve the

linearity:

$$r_{NL} \sim \frac{2}{M_s} > r_{\rm sch} = \frac{2m}{M_p^2} > a\,. \tag{7.26}$$

As long as the inequality in Eq. (7.26) holds, the spacetime metric is valid all the way from $r = \infty$ up to $r = 0$, and it turns out to be free from any curvature singularity, and also devoid of any horizons. Furthermore, since in our case, the h_{00} component is always bounded below unity, there is no ergo-region, as first pointed out in [116]. As a brief conclusion to this chapter we have successfully obtained a metric that can describe a rotating object in the theory of IDG by using the same technique as used by Biswar et al. [50]. This being said the notable difference between our work and that of Biswar et al., is that we have had to first determine the metric produced by a delta ring singularity. We then determine that this metric is indeed non-singular at all its points. Furthermore this metric (in the appropriate limit) matches that of the GR metric, as shown in Fig. 7.1. Secondly, we have determined the metric as produced by a rotating delta-Dirac ring, and again shown that it satisfies the required condition, as shown in Fig. 7.2. We have also shown that the linear limit of this metric is correct, given that the conditions $mM_s < M_p^2$ and $a < 2/M_s$ are met. Note that this last condition means that the ring singularity must be contained within the region of non-locality.

Chapter 8

Conclusions

8.1 QNMs for spin-3/2 fields

We note that we have successfully obtained the effective potentials for spin-3/2 fields near a Reissner-Nordström black holes, as well as for a Schwarzschild black hole in (A)dS space times. The results are given in Chs. 3 and 4 respectively. Where we have obtained these potentials using the eigenvalues for spinors and spinor-vectors on the S^N. This makes obtaining the effective potentials for space times of a dimension larger than 4 much simpler, when compared to using the Newman-Penrose method. We note that the effective potential for the Reissner-Nordström black hole is dependant purely on the radial coordinate, similar to the case of the Schwarzschild black hole. However this is not true for the effective potential of the (A)dS space time. In this case we are able to obtain a pure radial dependence only in the limit that the cosmological constant Λ is very small. This is unsurprising since we expect in this limit to recover the Schwarzschild potential function obtained in Ref. [74]. Furthermore the dependence on the ω term would suggest that the scenario in the case of the (A)dS space time behaves like a potential box, this is similarly noted in Ref. [91]. This is seen when taking the higher dimensional effective potentials to radial infinity. Where it is observed that the function tends to infinity. The exception to this is for the 4 dimensional case where the function tends to a non-zero finite number in the radial limit of infinity.
We can also note that the effective potential for the TT-eigenmodes is simpler than that of the non-TT eigenmodes. This may explain the stability issues seen when plotting the potential function and when obtaining the QNMs for each case. For the Reissner-Nordström and the dS potential we notice that the maximum of the potential is directly related to the number of the dimensions in the space time. A similar behaviour is seen for the effective potential of the higher dimensional Schwarzschild metric obtained in Ref. [74]. This increase in the maximum of the potential would suggest that the black holes with a larger number of dimensions will produce QNMs with a higher frequency. It is further noted that in these two cases increasing the value of the electrical charge, or increasing the value of cosmological constant, results in a potential function with larger maximal values.
However since the effective potential for the AdS space does not behave like a potential barrier we do not see this behaviour. We observe that in this case the gradient of the potential function decreases for an increase in the number of dimensions. Suggesting that the field is approaching some sort of potential barrier as is moves away from the black hole. The form of the potentials also suggests that in this case the fields will always fall into the black hole and not propagate away to infinity.
For the Reissner-Nordström black hole we were able to obtain the QNMs associated with the black hole using the well known WKB method and the improved AIM. The results are given in Figs. 3.6 and 3.8 where we can see that the frequency of the

QNMs is directly related to the number of dimensions in the space time. We also observe that as the number of dimensions increases so to does the imaginary part of the QNMs. This would imply that although QNMs coming from higher dimensional black hole would be more energetic they would also be more difficult to observe as they would decay much quicker.The results suggest two relations between the QNMs and the quantum numbers l and n, firstly they show that changes in the quantum number l result in direct changes to the frequency of the QNMs. Secondly they show that the quantum number n has a more pronounced effect on the QNMs as it changes both the real and imaginary parts of the QNMs. With higher values of n giving lower values for the real part and larger values for the imaginary part of the QNM. So much so that fields with larger values of l and n may have QNMs with a lower frequency and higher damping term than fields with smaller values of both l and n. Finally we note that the electrical charge of the black hole has a direct relation on the values of the QNMs. With QNMs produced from black hole with larger values of Q being more energetic. While the imaginary part increases in this case it does not increase as much as the real value does.
Fig. 3.6 shows that the AIM method agrees very strongly with the WKB method to 6th order. Both these methods however do not always agree with the WKB method to third order, which appears to be more stable when obtaining QNMs for black holes in the extremal limits of Q and for large values of the number of space time dimensions. This can easily be seen in Fig. 3.6 for the case of 9 dimensions and $Q = 0.5$. In this case the QNMs for the low values of l do not agree at all between the WKB method to 3rd order and the WKB to 6th order and for the improved AIM. The values obtained for the QNMs in this case suggested that the most trustworthy method for the QNMs for the low valued l mode fields would be the WKB method to 3rd order.
In the case of the AdS space time we were unable to use the WKB method and AIM to solve for the QNMs and instead we needed to use a method developed by Horowitz and Hubeny in Ref. [91]. This method sets the AdS curvature radius to one and then compares black holes of various sizes by changing the mass of the black holes. As such the QNMs are much larger than those obtained for previous works, however this is expected to be due to the change of scale. This does mean however that we cannot comment on how the results compare to the Schwarzschild case in Ref. [74]. However we can note that as is expected QNMs from black holes with more mass are more energetic, but also decay faster. In terms of comparing the number of dimensions to the QNMs we observe the same behaviour as in the previous results, namely more energetic modes with higher damping terms. This is consistent with the results obtained in Ref. [91].
So in conclusion in the first part of this thesis we have shown that using the eigenvalues of spinors and spinor-vectors on an S^N we can obtain higher dimensional effective potentials for spin-3/2 fields. Then using well established numerical methods we are able to obtain QNMs associate to the black holes for the spin-3/2 fields. Where finally using the approach outlined by Unruh in Ref. [83] we can also obtain the absorption probabilities associated to the QNMs.

8.2 Metrics in IDG

We have shown that we can indeed obtain a metric for both electrically charged and rotating objects in the theory of IDG. In the case of the electrically charged metric

we can ensure that the metric does not have a $1/r$ divergence, as is seen in the case of the metric from pure GR. The linearity condition that we impose in this case is given in Eq. (6.23). Taking $r \to 0$ implies that $|Q|\, M_s < M_p$ to ensure the condition is met. The other condition that must be ensured is that $mM_s < M_p^2$ so as to ensure the metric remains linear in the limit that $Q \to 0$ [50]. Given that this condition is met we ensured that the metric remains finite all the way to $r \to 0$, as is shown in Fig. 6.1. Furthermore, as is shown in Figs. 6.2 and 6.3, when this condition is met the Weyl and scalar curvature terms also remain finite for the entire metric. A consequence of the lack of a singularity existing in the metric means that the we are no longer required to ensure that $Q \leq (m/M_p)$. In the case of the Reissner-Nordström metric violating this condition would result in a naked singularity being present in the space. Finally using the comparisons shown in Figs. 6.1, 6.2 and 6.3 we can see that in the IR limit this metric is exactly the same as its GR equivalent. Where divergence between the GR and IDG metric only occurs in the UV regime. As such we have a theory that indeed only alters the UV behaviour of gravity while leaving the IR region unchanged from the GR predictions.

For the rotating metric in IDG we have shown that we can indeed remove the ring singularity seen in the Kerr metric. As in the case of the non-rotating metric and the electrically charged metric this is only guaranteed if the linearity conditions are met. In the case of the rotating metric this is $a > 2Gm$, however if this is not the case then we must ensure that $a < 2/M_s$. If these conditions are met then as is shown in Figs. 7.1 and 7.2 the metric can indeed be non-singular. Furthermore in the IR limit the metric is once again indistinguishable from its GR equivalent. Showing again that the theory of IDG only modifies the behaviour of gravity in the UV regime while leaving the gravitational interactions in the IR limit unchanged from the observed behaviour from GR.

As extensions to the work considered in this thesis one could look at the QNMs for spin-3/2 fields near rotating black holes. As this would introduce a range of new interesting phenomena that would have to be considered. As the rotation of the black hole may greatly affect the energy of the emitted QNMs. Furthermore an investigation of QNMs in the theory of IDG may provide some interesting results. An initial investigation of these QNMs could provide some results on the stability of the metrics that have been derived in the above. Any deviation of results in the IDG theory could provide some interest in further investigating the theory of IDG as a modified alternative to the standard theory of gravity.

List of publications

- Ch. 3 is based on the paper: Chen, C. H., Cho, H. T., Cornell, A. S., Harmsen, G., Ngcobo, X. (2018).
  Quasinormal modes and absorption probabilities of spin-3/2 fields in D-dimensional Reissner-Nordström black hole spacetimes.
  Physical Review D, **97(2)**, 024038. arXiv:1710.08024 **[gr-qc]**

- Ch. 4 is based on the paper: Chen, C-H., Cho, H. T., Cornell, A. S., Harmsen, G.
  "Quasinormal modes of spin-3/2 fields in D-dimensional (A)dS spaces",
  Preprint arXiv:1907.11856 **[gr-qc]**

- Ch. 6 is based on the paper: Buoninfante, Luca, Gerhard Harmsen, Shubham Maheshwari, and Anupam Mazumdar.
  "Nonsingular metric for an electrically charged point-source in ghost-free infinite derivative gravity."
  Physical Review D **98**, no. 8 (2018): 084009. arXiv:1804.09624 **[gr-qc]**

- Ch. 7 is based on the paper: Buoninfante, Luca, Alan S. Cornell, Gerhard Harmsen, Alexey S. Koshelev, Gaetano Lambiase, João Marto, and Anupam Mazumdar.
  "Towards nonsingular rotating compact object in ghost-free infinite derivative gravity."
  Physical Review D **98**, no. 8 (2018): 084041. arXiv:1807.08896 **[gr-qc]**

- Ch. 7 Cornell, Alan S., Gerhard Harmsen, Gaetano Lambiase, and Anupam Mazumdar.
  "Rotating metric in nonsingular infinite derivative theories of gravity."
  Physical Review D **97**, no. 10 (2018): 104006. arXiv:1710.02162 **[gr-qc]**

Appendix A

Gamma Matrices

During the derivation of the Super covariant derivative and subsequently the derivation of the radial equations we have used the Dirac gamma matrices some of their identities. As such we will briefly go over these matrices and show some useful identities. The gamma matrices are a set of γ_i, where $i = 0, 1, 2, ..., N-1$, $N \times N$ matrices with a specific anti-commutation relation that ensures they generate the $\mathcal{C}^{\updownarrow}_{\downarrow 1,N-1}(R)$ Clifford algerbra, where N represents the total number of space time dimensions. That is they must obey the relation [119]

$$\gamma^{\mu}, \gamma^{\nu} = 2\eta^{\mu\nu}\mathbb{I}_N. \tag{A.1}$$

Furthermore if N is even we can construct another matrix as follows[119]

$$\gamma_N = i^{N/2-1} \prod_{i=0}^{N-1} \gamma^i, \tag{A.2}$$

in some literature this is called the Hermitian chiral matrix.
For our work the identities we will need involve the anti-symmetric gamma matrix relations given as follows

$$\begin{aligned}
\gamma^a\gamma^b &= \gamma^{ab} + g^{ab} \\
\gamma^a\gamma^b\gamma^c &= \gamma^{abc} + \gamma^a g^{bc} - \gamma^b g^{ac} + \gamma^c g^{ab} \\
\gamma^a\gamma^b\gamma^c\gamma^d &= \gamma^{abcd} + \left(\gamma^{ab}g^{cd} - \gamma^{ac}g^{bd} + \gamma^{ad}g^{bc}\right) + \left(\gamma^{bc}g^{ad} - \gamma^{bd}g^{ac} + \gamma^{cd}g^{ab}\right) \\
&\quad + \left(g^{ab}g^{cd} - g^{ac}g^{bd} + g^{ad}g^{bc}\right) \\
\gamma^a\gamma^b\gamma^c\gamma^d\gamma^e &= \gamma^{abcde} + \left(\gamma^{abc}g^{de} - \gamma^{abd}g^{ce} + \gamma^{abe}g^{cd} + \gamma^{acd}g^{be} - \gamma^{ace}g^{bd}\right. \\
&\quad \left. + \gamma^{ade}g^{bc} - \gamma^{bcd}g^{ae} + \gamma^{bce}g^{ad} - \gamma^{bde}g^{ac} + \gamma^{cde}g^{ab}\right) \\
&\quad + \left(\left(g^{bc}g^{de} - g^{bd}g^{ce} + g^{be}g^{cd}\right)\gamma^a - \left(g^{cd}g^{ea} - g^{ce}g^{da} + g^{ca}g^{de}\right)\gamma^b\right. \\
&\quad \left. + \left(g^{de}g^{ab} - g^{da}g^{eb} + g^{db}g^{ea}\right)\gamma^c - \left(g^{ea}g^{bc} - g^{eb}g^{ac} + g^{ec}g^{ab}\right)\gamma^d\right. \\
&\quad \left. + \left(g^{ab}g^{cd} - g^{ac}g^{bd} + g^{ad}g^{bc}\right)\gamma^e\right)
\end{aligned} \tag{A.3}$$

Using the above identities we can easily, although tedious, obtain the following results

$$\gamma^a\gamma_a = D \tag{A.4}$$

$$\gamma^a\gamma_{ab} = (D-1)\,\gamma_b \tag{A.5}$$

$$\gamma^a\gamma_{abc} = (D-2)\gamma_{bc} \tag{A.6}$$

$$\gamma^{ab}\gamma_b = (D-1)\gamma^a \tag{A.7}$$

$$\gamma^{ab}\gamma_{bc} = (D-2)\gamma^a_{\ c} + (D-1)g^a_{\ c} \tag{A.8}$$

$$\gamma^{ab}\gamma_{bcd} = (D-3)\gamma^a_{\ cd} - (D-2)(\gamma_c g^a_{\ d} - \gamma_d g^a_{\ c}) \tag{A.9}$$

$$\gamma^{abc}\gamma_c = (D-2)\gamma^{ab} \tag{A.10}$$

$$\gamma^{abc}\gamma_{cd} = (D-3)\gamma^{ab}_{\ d} + (D-2)(\gamma^a g^b_{\ d} - \gamma^b g^a_{\ d}) \tag{A.11}$$

$$\begin{aligned}\gamma^{abc}\gamma_{cef} =&(D-4)\gamma^{ab}_{\ ef} - (D-3)\left(\gamma^a_{\ e}g^b_{\ f} - \gamma^a_{\ f}g^b_{\ e} - \gamma^b_{\ e}g^a_{\ f} + \gamma^b_{\ f}g^a_{\ e}\right)\\ &- (D-2)(g^a_{\ e}g^b_{\ f} - g^a_{\ f}g^b_{\ e}).\end{aligned} \tag{A.12}$$

$$\gamma^{gefa}\gamma_a = (D-3)\gamma^{gef} \tag{A.13}$$

$$\gamma^{gacb}\gamma_{be} = (D-4)\,\gamma^{gac}_{\ \ \ e} + (D-3)\left(\gamma^{ga}g^c_e - \gamma^{gc}g^a_e + \gamma^{ac}g^g_e\right) \tag{A.14}$$

$$\begin{aligned}\gamma^{gacb}\gamma_{bef} =& (D-5)\,\gamma^{gac}_{\ \ \ ef}\\ &- (D-4)\left(\gamma^{ga}_{\ \ e}g^c_f - \gamma^{ga}_{\ \ f}g^c_e + \gamma^{gc}_{\ \ f}g^a_e - \gamma^{gc}_{\ \ e}g^a_f + \gamma^{ac}_{\ \ e}g^g_f - \gamma^{ac}_{\ \ f}g^g_e\right)\\ &- (D-3)\left(\gamma^g\left(g^a_e g^c_f - g^a_f g^c_e\right) - \gamma^a\left(g^c_f g^g_e - g^c_e g^g_f\right) + \gamma^c\left(g^g_e g^a_f - g^a_e g^g_f\right)\right)\end{aligned} \tag{A.15}$$

There are further relations we may need to consider which are nessecary for the calculation of the super covariant derivative. We have given there results below.

$$\gamma^{\lambda\mu\nu}[\mathcal{D}, \gamma_{\nu\rho\sigma}F^{\rho\sigma}] = 2(D-3)\gamma^\lambda_\nu\nabla_\mu F^{\mu\nu} - (D-3)\gamma_{\mu\nu}\nabla^\lambda F^{\mu\nu} + 2(D-2)\nabla_\mu F^{\mu\lambda}.$$

$$\gamma^{\lambda\mu\nu}[\gamma_\mu, \gamma_{nu}] = -2(D-2)(D-1)\gamma^\lambda.$$

$$\gamma^{\lambda\mu\nu}[\gamma_\mu, \gamma^\rho F_{\nu\rho}] = -2(D-3)\gamma^{\lambda\nu\rho}F_{\nu\rho} + 2(D-2)\gamma^\nu F^\lambda_\nu.$$

$$\gamma^{\lambda\mu\nu} = -2(D-4)(D-3)\gamma^\lambda_{\rho\sigma}F^{\rho\sigma} + 4(D-3)(D-2)\gamma_\rho F^{\rho\lambda}$$

$$\gamma^{\lambda\mu\nu}[\gamma^\rho F_{\mu\rho}, \gamma^\sigma F_{\nu\sigma}] = -2\gamma^{\lambda\mu\nu\rho\sigma}F_{\mu\nu}F_{\rho\sigma} - 4\gamma_{\mu\nu\rho}F^{\mu\rho}F^{\nu\lambda} - 2\gamma^\lambda F_{\rho\sigma}F^{\rho\sigma} - 4\gamma^\mu F_{\mu\nu}F^{\nu\lambda}.$$

$$\gamma^{\lambda\mu\nu}[\gamma^\alpha F_{\mu\alpha}, \gamma_{\nu\rho\sigma}F^{\rho\sigma}] = -2(D-5)\gamma^{\lambda\mu\nu}_{\ \ \ \rho\sigma}F_{\mu\nu}F^\rho + 6(D-4)\gamma^\mu_{\ \rho\sigma}F^{\rho\sigma}F_\mu^{\ \lambda}.$$

$$\begin{aligned}\gamma^{\lambda\mu\nu}[\gamma_{\mu\alpha\beta}F^{\alpha\beta}, \gamma_{\nu\rho\sigma}F^{\rho\sigma}] =& -2(D^2-11D+26)\gamma^\lambda_{\ \alpha\beta\rho\sigma}F^{\alpha\beta}F^{\rho\sigma} + 8(D-6)(D-3)\gamma_{\rho\alpha\beta}F^{\alpha\beta}F^{\rho\lambda}\\ &+ 4(D-4)(D-3)\gamma^\lambda F_{\rho\sigma}F^{\rho\sigma} - 16(D-3)\gamma_\rho F^{\rho\sigma}F_\sigma^{\ \lambda}.\end{aligned}$$

Appendix B

Full expressions of the curvature tensors

In this appendix we show the full expressions for all curvature tensors and invariants for the IDG linearized static metric for a charged point-source derived in Eqs. (6.19). Furthermore we recall that $F(x)$ is the Dawson function and $\mathrm{Erf}(x)$ is the error function.

The Ricci scalar is given by[110]:

$$\mathcal{R} = \frac{GmM_s^3 e^{-\frac{1}{4}r^2M_s^2}}{\sqrt{\pi}}; \tag{B.1}$$

the non-zero components of the Riemann tensor:

$$\begin{aligned}
\mathcal{R}_{0101} =& \frac{1}{8}G\left[M_s^3\left(\frac{2Q^2\mathrm{F}\left(\frac{rM_s}{2}\right)}{r}+\frac{4me^{-\frac{1}{4}r^2M_s^2}}{\sqrt{\pi}}\right)+\frac{8M_s\left(Q^2\mathrm{F}\left(\frac{rM_s}{2}\right)+\frac{2mre^{-\frac{1}{4}r^2M_s^2}}{\sqrt{\pi}}\right)}{r^3}\right.\\
&\left.+Q^2rM_s^5\mathrm{F}\left(\frac{rM_s}{2}\right)-\frac{16m\mathrm{Erf}\left(\frac{rM_s}{2}\right)}{r^3}-\frac{4Q^2M_s^2}{r^2}-Q^2M_s^4\right],\\
\mathcal{R}_{0303} =& \mathcal{R}_{0202}\sin^2(\theta)\\
=& \frac{1}{4}G\sin^2(\theta)\left[M_s\left(-\frac{2Q^2\mathrm{F}\left(\frac{rM_s}{2}\right)}{r}-\frac{4me^{-\frac{1}{4}r^2M_s^2}}{\sqrt{\pi}}\right)\right.\\
&\left.-Q^2rM_s^3\mathrm{F}\left(\frac{rM_s}{2}\right)+\frac{4m\mathrm{Erf}\left(\frac{rM_s}{2}\right)}{r}+Q^2M_s^2\right],\\
\mathcal{R}_{1313} =& \mathcal{R}_{1212}\sin^2(\theta)\\
=& \frac{1}{16}G\sin^2(\theta)\left[M_s\left(\frac{4Q^2\mathrm{F}\left(\frac{rM_s}{2}\right)}{r}+\frac{16me^{-\frac{1}{4}r^2M_s^2}}{\sqrt{\pi}}\right)+Q^2r^3M_s^5\mathrm{F}\left(\frac{rM_s}{2}\right)\right.\\
&\left.-\frac{16m\mathrm{Erf}\left(\frac{rM_s}{2}\right)}{r}+\frac{8mr^2M_s^3e^{-\frac{1}{4}r^2M_s^2}}{\sqrt{\pi}}-Q^2r^2M_s^4-2Q^2M_s^2\right],\\
\mathcal{R}_{2323} =& \frac{1}{4}Gr\sin^2(\theta)\left[M_s\left(-2Q^2\mathrm{F}\left(\frac{rM_s}{2}\right)-\frac{8mre^{-\frac{1}{4}r^2M_s^2}}{\sqrt{\pi}}\right)-Q^2r^2M_s^3\mathrm{F}\left(\frac{rM_s}{2}\right)\right.\\
&\left.+8m\mathrm{Erf}\left(\frac{rM_s}{2}\right)+Q^2rM_s^2\right];
\end{aligned} \tag{B.2}$$

the non-zero components of the Ricci tensor:

$$\begin{aligned}
\mathcal{R}_{00} = & \frac{1}{8}GM_s^3\left[\frac{Q^2\left(r^2M_s^2-2\right)\mathrm{F}\left(\frac{rM_s}{2}\right)}{r}+\frac{4me^{-\frac{1}{4}r^2M_s^2}}{\sqrt{\pi}}-Q^2M_s\right],\\
\mathcal{R}_{11} = & \frac{1}{4}GM_s\left[M_s\left(\frac{2mM_se^{-\frac{1}{4}r^2M_s^2}}{\sqrt{\pi}}+\frac{Q^2}{r^2}\right)-\frac{Q^2\left(r^2M_s^2+2\right)\mathrm{F}\left(\frac{rM_s}{2}\right)}{r^3}\right],\\
\mathcal{R}_{22} = & \frac{1}{16}GM_s\left[\frac{Q^2\left(r^4M_s^4+4\right)\mathrm{F}\left(\frac{rM_s}{2}\right)}{r}+M_s\left(\frac{8mr^2M_se^{-\frac{1}{4}r^2M_s^2}}{\sqrt{\pi}}-Q^2r^2M_s^2-2Q^2\right)\right],\\
\mathcal{R}_{33} = & \frac{1}{16}G\sin^2(\theta)M_s\left[\frac{Q^2\left(r^4M_s^4+4\right)\mathrm{F}\left(\frac{rM_s}{2}\right)}{r}\right.\\
& \left.+M_s\left(\frac{8mr^2M_se^{-\frac{1}{4}r^2M_s^2}}{\sqrt{\pi}}-Q^2r^2M_s^2-2Q^2\right)\right];
\end{aligned} \tag{B.3}$$

the non-zero components of the Weyl tensor:

$$\begin{aligned}
\mathcal{C}_{0101} = & \frac{1}{48}G\left[M_s^3\left(\frac{12Q^2\mathrm{F}\left(\frac{rM_s}{2}\right)}{r}+\frac{16me^{-\frac{1}{4}r^2M_s^2}}{\sqrt{\pi}}\right)+\frac{M_s\left(36Q^2\mathrm{F}\left(\frac{rM_s}{2}\right)+\frac{96mre^{-\frac{1}{4}r^2M_s^2}}{\sqrt{\pi}}\right)}{r^3}\right.\\
& \left.+3Q^2rM_s^5\mathrm{F}\left(\frac{rM_s}{2}\right)-\frac{96m\mathrm{Erf}\left(\frac{rM_s}{2}\right)}{r^3}-\frac{18Q^2M_s^2}{r^2}-3Q^2M_s^4\right],\\
\mathcal{C}_{0303} = & -\mathcal{C}_{1313}=\mathcal{C}_{0202}\sin^2(\theta)=-\mathcal{C}_{1212}\sin^2(\theta)\\
= & \frac{1}{96}G\sin^2(\theta)\left[4rM_s^3\left(-3Q^2\mathrm{F}\left(\frac{rM_s}{2}\right)-\frac{4mre^{-\frac{1}{4}r^2M_s^2}}{\sqrt{\pi}}\right)\right.\\
& +M_s\left(-\frac{36Q^2\mathrm{F}\left(\frac{rM_s}{2}\right)}{r}-\frac{96me^{-\frac{1}{4}r^2M_s^2}}{\sqrt{\pi}}\right)\\
& \left.-3Q^2r^3M_s^5\mathrm{F}\left(\frac{rM_s}{2}\right)+\frac{96m\mathrm{Erf}\left(\frac{rM_s}{2}\right)}{r}+3Q^2r^2M_s^4+18Q^2M_s^2\right],\\
\mathcal{C}_{2323} = & \frac{1}{48}Gr\sin^2(\theta)\left[4r^2M_s^3\left(-3Q^2\mathrm{F}\left(\frac{rM_s}{2}\right)-\frac{4mre^{-\frac{1}{4}r^2M_s^2}}{\sqrt{\pi}}\right)\right.\\
& +M_s\left(-36Q^2\mathrm{F}\left(\frac{rM_s}{2}\right)-\frac{96mre^{-\frac{1}{4}r^2M_s^2}}{\sqrt{\pi}}\right)\\
& \left.-3Q^2r^4M_s^5\mathrm{F}\left(\frac{rM_s}{2}\right)+96m\mathrm{Erf}\left(\frac{rM_s}{2}\right)+3Q^2r^3M_s^4+18Q^2rM_s^2\right].
\end{aligned} \tag{B.4}$$

We will now show the expressions for the curvature invariants. The Ricci scalar squared is given by:

$$\mathcal{R}^2=\frac{G^2m^2M_s^6e^{-\frac{1}{2}r^2M_s^2}}{\pi}; \tag{B.5}$$

the Ricci tensor squared:

$$\begin{aligned}\mathcal{R}_{\mu\nu}\mathcal{R}^{\mu\nu} = \; & \frac{G^2 M_s^2}{128\pi r^6}\Bigg[\mathrm{F}\left(\frac{rM_s}{2}\right)\Bigg(32\sqrt{\pi}mQ^2r^7M_s^6e^{-\frac{1}{4}r^2M_s^2} - 64\sqrt{\pi}mQ^2r^5M_s^4e^{-\frac{1}{4}r^2M_s^2} \\ & -6\pi Q^4r^7M_s^7 + 4\pi Q^4r^5M_s^5 - 24\pi Q^4r^3M_s^3 - 48\pi Q^4rM_s\Bigg) \\ & +\pi Q^4\left(3r^8M_s^8 - 8r^6M_s^6 + 24r^4M_s^4 + 32r^2M_s^2 + 48\right)\mathrm{F}\left(\frac{rM_s}{2}\right)^2 \\ & +M_s^4\left(128m^2r^6e^{-\frac{1}{2}r^2M_s^2} + 4\pi Q^4r^4\right) - 32\sqrt{\pi}mQ^2r^6M_s^5e^{-\frac{1}{4}r^2M_s^2} \\ & +3\pi Q^4r^6M_s^6 + 12\pi Q^4r^2M_s^2\Bigg];\end{aligned} \tag{B.6}$$

the Weyl tensor squared:

$$\begin{aligned}\mathcal{C}_{\mu\nu\rho\sigma}\mathcal{C}^{\mu\nu\rho\sigma} = \; & \frac{G^2e^{-\frac{1}{2}r^2M_s^2}}{192\pi r^6}\Bigg[-4r^2M_s^3\left(3\sqrt{\pi}Q^2e^{\frac{1}{4}r^2M_s^2}\mathrm{F}\left(\frac{rM_s}{2}\right) + 4mr\right) \\ & -12M_s\left(3\sqrt{\pi}Q^2e^{\frac{1}{4}r^2M_s^2}\mathrm{F}\left(\frac{rM_s}{2}\right) + 8mr\right) \\ & -3\sqrt{\pi}Q^2r^4M_s^5e^{\frac{1}{4}r^2M_s^2}\mathrm{F}\left(\frac{rM_s}{2}\right) + 96\sqrt{\pi}me^{\frac{1}{4}r^2M_s^2}\mathrm{Erf}\left(\frac{rM_s}{2}\right) \\ & +18\sqrt{\pi}Q^2rM_s^2e^{\frac{1}{4}r^2M_s^2} + 3\sqrt{\pi}Q^2r^3M_s^4e^{\frac{1}{4}r^2M_s^2}\Bigg]^2;\end{aligned} \tag{B.7}$$

and the Kretschmann invariant:

$$
\begin{aligned}
\mathcal{K} = \; & \frac{e^{-\frac{1}{2}r^2M_s^2}G^2}{32\pi r^6}\Bigg[3e^{\frac{1}{2}r^2M_s^2}\pi Q^4 r^8 \mathrm{F}\left(\frac{rM_s}{2}\right)^2 M_s^{10} - 6e^{\frac{1}{2}r^2M_s^2}\pi Q^4 r^7 \mathrm{F}\left(\frac{rM_s}{2}\right) M_s^9 \\
& + \Bigg(32e^{\frac{1}{4}r^2M_s^2} m\sqrt{\pi}Q^2 \mathrm{F}\left(\frac{rM_s}{2}\right) r^7 + 3e^{\frac{1}{2}r^2M_s^2}\pi Q^4 r^6 \\
& + 8e^{\frac{1}{2}r^2M_s^2}\pi Q^4 \mathrm{F}\left(\tfrac{rM_s}{2}\right)^2 r^6\Bigg) M_s^8 \\
& - 4e^{\frac{1}{4}r^2M_s^2}\sqrt{\pi}Q^2 r^5\left(7e^{\frac{1}{4}r^2M_s^2}\sqrt{\pi}\mathrm{F}\left(\frac{rM_s}{2}\right) Q^2 + 8mr\right) M_s^7 \\
& + 4r^4\Bigg(18e^{\frac{1}{2}r^2M_s^2}\pi \mathrm{F}\left(\frac{rM_s}{2}\right)^2 Q^4 + 5e^{\frac{1}{2}r^2M_s^2}\pi Q^4 + 32e^{\frac{1}{4}r^2M_s^2} m\sqrt{\pi} r \mathrm{F}\left(\frac{rM_s}{2}\right) Q^2 \\
& + 24m^2r^2\Bigg) M_s^6 \\
& - 24e^{\frac{1}{4}r^2M_s^2}\sqrt{\pi}Q^2 r^3\left(8mr + e^{\frac{1}{4}r^2M_s^2}\sqrt{\pi}\mathrm{F}\left(\frac{rM_s}{2}\right)\left(5Q^2 + 4mr\mathrm{Erf}\left(\frac{rM_s}{2}\right)\right)\right) M_s^5 \\
& + 4r^2\Bigg(40e^{\frac{1}{2}r^2M_s^2}\pi \mathrm{F}\left(\frac{rM_s}{2}\right)^2 Q^4 + 15e^{\frac{1}{2}r^2M_s^2}\pi Q^4 + 144e^{\frac{1}{4}r^2M_s^2} m\sqrt{\pi} r \mathrm{F}\left(\frac{rM_s}{2}\right) Q^2 \\
& + 24e^{\frac{1}{2}r^2M_s^2} m\pi r \mathrm{Erf}\left(\frac{rM_s}{2}\right) Q^2 + 128m^2r^2\Bigg) M_s^4 \\
& - 16e^{\frac{1}{4}r^2M_s^2}\sqrt{\pi} r\Bigg(3e^{\frac{1}{4}r^2M_s^2}\sqrt{\pi}\mathrm{F}\left(\frac{rM_s}{2}\right)\left(5Q^2 + 8mr\mathrm{Erf}\left(\frac{rM_s}{2}\right)\right) Q^2 \\
& + 4mr\left(9Q^2 + 8mr\mathrm{Erf}\left(\frac{rM_s}{2}\right)\right)\Bigg) M_s^3 + 48\Bigg(5e^{\frac{1}{2}r^2M_s^2}\pi \mathrm{F}\left(\frac{rM_s}{2}\right)^2 Q^4 \\
& + 24e^{\frac{1}{4}r^2M_s^2} m\sqrt{\pi} r \mathrm{F}\left(\frac{rM_s}{2}\right) Q^2 + 4mr\left(3e^{\frac{1}{2}r^2M_s^2}\pi \mathrm{Erf}\left(\frac{rM_s}{2}\right) Q^2 + 8mr\right)\Bigg) M_s^2 \\
& - 384e^{\frac{1}{4}r^2M_s^2} m\sqrt{\pi}\left(3e^{\frac{1}{4}r^2M_s^2}\sqrt{\pi}\mathrm{F}\left(\frac{rM_s}{2}\right) Q^2 + 8mr\right)\mathrm{Erf}\left(\frac{rM_s}{2}\right) M_s \\
& + 1536e^{\frac{1}{2}r^2M_s^2} m^2\pi \mathrm{Erf}\left(\tfrac{rM_s}{2}\right)^2\Bigg].
\end{aligned}
\tag{B.8}
$$

In the case $Q = 0$, we would recover all curvature tensors and invariants for the case of a neutral point-source obtained in Ref. [120], as expected.

Bibliography

1. Einstein, A. On the General Theory of Relativity. *Sitzungsber. Preuss. Akad. Wiss. Berlin (Math. Phys.)* **1915.** [Addendum: Sitzungsber. Preuss. Akad. Wiss. Berlin (Math. Phys.)1915,799(1915)], 778–786 (1915).
2. Øyvind, G. & Hervik, S. *Einstein's General Theory of Relativity: With Modern Applications in Cosmology* (Springer, 2007).
3. Pais, A. *Subtle is the Lord: The Science and the Life of Albert Einstein: The Science and the Life of Albert Einstein* (Oxford University Press, USA, 1982).
4. Liesenborgs, J. *GravitationalLensingScenario* <http://en.citizendium.org/wiki/File:GravitationalLensingScenario.png> (1999).
5. Sauer, T. Nova Geminorum 1912 and the origin of the idea of gravitational lensing. *Archive for history of exact sciences* **62,** 1–22 (2008).
6. Soldner, J. On the deflection of a light ray from its rectilinear motion, by the attraction of a celestial body at which it nearly passes by. *Berliner Astronomisches Jahrbuch,* 161–172 (1804).
7. Dyson, F. W., Eddington, A. S. & Davidson, C. IX. A determination of the deflection of light by the sun's gravitational field, from observations made at the total eclipse of May 29, 1919. *Philosophical Transactions of the Royal Society of London. Series A, Containing Papers of a Mathematical or Physical Character* **220,** 291–333 (1920).
8. Will, C. M. The confrontation between general relativity and experiment. *Astrophysics and Space Science* **283,** 543–552 (2003).
9. Shomer, A. A pedagogical explanation for the non-renormalizability of gravity. *arXiv preprint arXiv:0709.3555* (2007).
10. Hawkins, S & Ellis, G. Singularities in homogeneous world models. *Physics Letters* **17,** 246–247 (1965).
11. Hawking, S. W. Occurrence of singularities in open universes. *Physical Review Letters* **15,** 689 (1965).
12. Schwarzschild, K. "U about the gravitational field of a mass point according to Einstein's theory. *Sessions of the Royal Prussian Academy of Sciences (Berlin), 1916, pages 189-196* (1916).
13. Misner, C. W., Thorne, K. S., Wheeler, J. A. & Kaiser, D. I. *Gravitation* (Princeton University Press, 2017).
14. Penrose, R. The question of cosmic censorship. *Journal of Astrophysics and Astronomy* **20,** 233–248 (1999).
15. Misner, C. W. Feynman quantization of general relativity. *Reviews of Modern Physics* **29,** 497 (1957).
16. Carlip, S., Chiou, D.-W., Ni, W.-T. & Woodard, R. Quantum gravity: A brief history of ideas and some prospects. *International Journal of Modern Physics D* **24,** 1530028 (2015).

17. Clifton, T., Ferreira, P. G., Padilla, A. & Skordis, C. Modified gravity and cosmology. *Physics reports* **513,** 1–189 (2012).
18. Kiefer, C. in *Towards quantum gravity* 158–187 (Springer, 2000).
19. Van Nieuwenhuizen, P. Supergravity. *Physics Reports* **68,** 189–398 (1981).
20. Aaboud, M. *et al.* Search for supersymmetry in final states with two same-sign or three leptons and jets using 36 fb- 1 of TeV pp collision data with the ATLAS detector. *Journal of High Energy Physics* **2017,** 84 (2017).
21. Aaboud, M. *et al.* Search for squarks and gluinos in final states with jets and missing transverse momentum using 36 fb- 1 of s= 13 TeV p p collision data with the ATLAS detector. *Physical Review D* **97,** 112001 (2018).
22. Durkee, M. New approaches to higher-dimensional general relativity. *arXiv preprint arXiv:1104.4414* (2011).
23. Stelle, K. Renormalization of higher-derivative quantum gravity. *Physical Review D* **16,** 953 (1977).
24. Abbott, B. P. *et al.* Observation of gravitational waves from a binary black hole merger. *Physical review letters* **116,** 061102 (2016).
25. Carroll, S. M. An introduction to general relativity: spacetime and geometry. *Addison Wesley* **101,** 102 (2004).
26. DeWitt, C. M. & Rickles, D. *The role of gravitation in physics: Report from the 1957 Chapel Hill Conference* (epubli, 2011).
27. Taylor, J. H. & Weisberg, J. M. A new test of general relativity-Gravitational radiation and the binary pulsar PSR 1913+ 16. *The Astrophysical Journal* **253,** 908–920 (1982).
28. Castelvecchi, D. & Jokes, A. Einstein's gravitational waves found at last. *Nature news* (2016).
29. Michelson, A. A. & Morley, E. W. On the Relative Motion of the Earth and of the Luminiferous Ether. *Sidereal Messenger, vol. 6, pp. 306-310* **6,** 306–310 (1887).
30. Willke, B., Collaboration, L. S., *et al.* Observation of gravitational waves from a binary black hole merger–dawn of a new astronomy. *Symmetry: Culture and Science* **29,** 257–264 (2018).
31. Regge, T. & Wheeler, J. A. Stability of a Schwarzschild singularity. *Physical Review* **108,** 1063 (1957).
32. Vishveshwara, C. V. Scattering of Gravitational Radiation by a Schwarzschild Black-hole. *Nature* **227,** 936–938 (1970).
33. Arnold, P. & Szepietowski, P. Spin 1/2 quasinormal mode frequencies in Schwarzschild-AdS spacetime. *Phys. Rev.* **D88,** 086002 (2013).
34. Cardoso, V. Quasinormal modes and gravitational radiation in black hole spacetimes. *arXiv preprint gr-qc/0404093* (2004).
35. Chen, C.-H., Cho, H., Cornell, A., Harmsen, G & Naylor, W. Gravitino fields in Schwarzschild black hole spacetimes. *arXiv preprint arXiv:1504.02579* (2015).
36. Camporesi, R. & Higuchi, A. On the eigenfunctions of the Dirac operator on spheres and real hyperbolic spaces. *Journal of Geometry and Physics* **20,** 1–18 (1996).
37. Konoplya, R. Quasinormal behavior of the D-dimensional Schwarzschild black hole and the higher order WKB approach. *Physical Review D* **68,** 024018 (2003).

38. Konoplya, R. & Zhidenko, A. Quasinormal modes of black holes: From astrophysics to string theory. *Reviews of Modern Physics* **83,** 793 (2011).
39. Cho, H. T. Dirac quasinormal modes in Schwarzschild black hole spacetimes. *Physical Review D* **68,** 024003 (2003).
40. Cho, H., Cornell, A., Doukas, J. & Naylor, W. Asymptotic iteration method for spheroidal harmonics of higher-dimensional Kerr-(A) dS black holes. *Physical Review D* **80,** 064022 (2009).
41. Cho, H., Cornell, A., Doukas, J. & Naylor, W. Black hole quasinormal modes using the asymptotic iteration method. *Classical and Quantum Gravity* **27,** 155004 (2010).
42. Cho, H.-T., Cornell, A. S., Doukas, J., Huang, T. R. & Naylor, W. A New Approach to Black Hole Quasinormal Modes: A Review of the Asymptotic Iteration Method. *Advances in Mathematical Physics* **2012,** 281705 (2012).
43. Polchinski, J. An introduction to the bosonic string. *String Theory* **1,** 402 (1994).
44. Kiefer, C. *Quantum Gravity* (Oxford university press, 2012).
45. Kiefer, C. Quantum gravity: general introduction and recent developments. *Annalen der Physik* **15,** 129–148 (2006).
46. Dowker, F. Causal sets and the deep structure of spacetime. *A. Ashtekar (ed.)* **100,** 445–467 (2005).
47. Henson, J. The causal set approach to quantum gravity. To be published in'Approaches to Quantum Gravity-Towards a new understanding of space and time (2006).
48. Padmanabhan, T. Emergent gravity paradigm: recent progress. *Modern Physics Letters A* **30,** 1540007 (2015).
49. Biswas, T., Mazumdar, A. & Siegel, W. Bouncing universes in string-inspired gravity. *Journal of Cosmology and Astroparticle Physics* **2006,** 009 (2006).
50. Biswas, T., Gerwick, E., Koivisto, T. & Mazumdar, A. Towards singularity-and ghost-free theories of gravity. *Physical Review Letters* **108,** 031101 (2012).
51. Biswas, T., Koivisto, T. & Mazumdar, A. Nonlocal theories of gravity: the flat space propagator. *arXiv preprint arXiv:1302.0532* (2013).
52. Biswas, T. & Talaganis, S. String-inspired infinite-derivative theories of gravity: A brief overview. *Modern Physics Letters A* **30,** 1540009 (2015).
53. Boos, J., Frolov, V. P. & Zelnikov, A. Gravitational field of static p-branes in linearized ghost-free gravity. *Physical Review D* **97,** 084021 (2018).
54. Boos, J., Frolov, V. P. & Zelnikov, A. Quantum scattering on a delta potential in ghost-free theory. *Physics Letters B* **782,** 688–693 (2018).
55. Gording, B. & Schmidt-May, A. Ghost-free infinite derivative gravity. *Journal of High Energy Physics* **2018,** 44 (2018).
56. Clifton, T. Parametrized post-Newtonian limit of fourth-order theories of gravity. *Physical Review D* **77,** 024041 (2008).
57. Eddington, A. *The mathematical theory of relativity Cambridge Univ* 1923.
58. Weyl, H. A new extension of the relativity theory. *Annalen der Physik* **364,** 101–133 (1919).
59. Utiyama, R. & DeWitt, B. S. Renormalization of a classical gravitational field interacting with quantized matter fields. *Journal of Mathematical Physics* **3,** 608–618 (1962).

60. Sotiriou, T. P. & Faraoni, V. f (R) theories of gravity. *Reviews of Modern Physics* **82,** 451 (2010).
61. Buchdahl, H. A. Non-linear Lagrangians and cosmological theory. *Monthly Notices of the Royal Astronomical Society* **150,** 1–8 (1970).
62. Lovelock, D. The Einstein tensor and its generalizations. *Journal of Mathematical Physics* **12,** 498–501 (1971).
63. Lovelock, D. The four-dimensionality of space and the Einstein tensor. *Journal of Mathematical Physics* **13,** 874–876 (1972).
64. Modified gravity and cosmology. *Physics Reports* **513.** Modified Gravity and Cosmology, 1 –189. ISSN: 0370-1573 (2012).
65. M 'e moires on the differential e equations, relating to the problem of isop ee , author = Ostrogradsky, Michael, journal = Mem. Acad. St. Petersburg, volume = 6, pages 385 to -517 = 1850 year =.
66. Kuz'min, Y. V. Finite nonlocal gravitation. *Yadernaya Fizika* **50,** 1630–1635 (1989).
67. Tomboulis, E. Superrenormalizable gauge and gravitational theories. *arXiv preprint hep-th/9702146* (1997).
68. Kokkotas, K. D. & Schmidt, B. G. Quasi-normal modes of stars and black holes. *Living Rev. Rel* **2,** 262 (1999).
69. Weinberg, S. *The quantum theory of fields* (Cambridge university press, 1995).
70. Rarita, W. & Schwinger, J. On a theory of particles with half-integral spin. *Physical Review* **60,** 61 (1941).
71. Steane, A. M. An introduction to spinors. *arXiv preprint arXiv:1312.3824* (2013).
72. Cartan, E. *The Theory of Spinors, edition Hermann* 1966.
73. Chen, C. & Cho, H. CH Chen, HT Cho, AS Cornell, G. Harmsen, and W. Naylor, Chin. J. Phys. 53, 110101 (2015). *Chin. J. Phys.* **53,** 110101 (2015).
74. Chen, C.-H., Cho, H., Cornell, A. & Harmsen, G. Spin-3/2 fields in D-dimensional Schwarzschild black hole spacetimes. *Physical Review D* **94,** 044052 (2016).
75. Newman, E. & Penrose, R. An approach to gravitational radiation by a method of spin coefficients. *Journal of Mathematical Physics* **3,** 566–578 (1962).
76. Del Castillo, G. T. & Silva-Ortigoza, G. Rarita-Schwinger fields in the Kerr geometry. *Physical Review D* **42,** 4082 (1990).
77. Del Castillo, G. T. & Silva-Ortigoza, G. Spin-3 2 perturbations of the Kerr-Newman solution. *Physical Review D* **46,** 5395 (1992).
78. Griffiths, D. J. & Harris, E. G. *Introduction to quantum mechanics* (Prentice Hall New Jersey, 1995).
79. Harmsen, G. E. *Quasi-normal Modes for Spin-3/2 Fields* in *Journal of Physics: Conference Series* **645** (2015), 012003.
80. Iyer, S. & Will, C. M. Black-hole normal modes: A WKB approach. I. Foundations and application of a higher-order WKB analysis of potential-barrier scattering. *Physical Review D* **35,** 3621 (1987).
81. Ciftci, H., Hall, R. L. & Saad, N. AIM eigenvalue problems. *Journal of Physics A: Mathematical and General* **36,** 11807 (2003).
82. Hawking, S. W. Black hole explosions? *Nature* **248,** 30 (1974).

83. Unruh, W. Absorption cross section of small black holes. *Physical Review D* **14,** 3251 (1976).
84. Cho, H. & Lin, Y. WKB analysis of the scattering of massive Dirac fields in Schwarzschild black-hole spacetimes. *Classical and Quantum Gravity* **22,** 775 (2005).
85. Liu, J. T., Zayas, L. A. P. & Yang, Z. Small treatise on spin-3/2 fields and their dual spectral functions. *Journal of High Energy Physics* **2014,** 1–38 (2014).
86. Kodama, H. & Ishibashi, A. A master equation for gravitational perturbations of maximally symmetric black holes in higher dimensions. *Progress of theoretical physics* **110,** 701–722 (2003).
87. Chandrasekhar, S. & Thorne, K. S. *The mathematical theory of black holes* 1985.
88. Carter, B. Global structure of the Kerr family of gravitational fields. *Physical Review* **174,** 1559 (1968).
89. Chen, C.-H., Cho, H., Cornell, A., Harmsen, G & Ngcobo, X. Quasinormal modes and absorption probabilities of spin-3/2 fields in D-dimensional Reissner-Nordström black hole spacetimes. *Physical Review D* **97,** 024038 (2018).
90. Cho, H., Cornell, A. S., Doukas, J. & Naylor, W. Split fermion quasinormal modes. *Physical Review D* **75,** 104005 (2007).
91. Horowitz, G. T. & Hubeny, V. E. Quasinormal modes of AdS black holes and the approach to thermal equilibrium. *Physical Review D* **62,** 024027 (2000).
92. Brady, P. R., Chambers, C. M., Laarakkers, W. G. & Poisson, E. Radiative falloff in Schwarzschild–de Sitter spacetime. *Physical Review D* **60,** 064003 (1999).
93. Barreto, A. S. & Zworski, M. Distribution of resonances for spherical black holes. *Mathematical Research Letters* **4,** 103–122 (1997).
94. Gibbons, G. W. in *Mathematical and quantum aspects of relativity and cosmology* 102–142 (Springer, 2000).
95. Alvarez-Gaume, L., Kehagias, A., Kounnas, C., Lüst, D. & Riotto, A. Aspects of quadratic gravity. *Fortschritte der Physik* **64,** 176–189 (2016).
96. Buoninfante, L. Ghost and singularity free theories of gravity. *arXiv preprint arXiv:1610.08744* (2016).
97. Van Nieuwenhuizen, P. On ghost-free tensor lagrangians and linearized gravitation. *Nuclear Physics B* **60,** 478–492 (1973).
98. Iwasaki, Y. Consistency condition for propagators. *Physical Review D* **2,** 2255 (1970).
99. Van Dam, H. & Veltman, M. Massive and mass-less Yang-Mills and gravitational fields. *Nuclear Physics B* **22,** 397–411 (1970).
100. Edholm, J., Koshelev, A. S. & Mazumdar, A. Behavior of the Newtonian potential for ghost-free gravity and singularity free gravity. *Physical Review D* **94,** 104033 (2016).
101. Boos, J., Frolov, V. P. & Zelnikov, A. On thermal field fluctuations in ghost-free theories. *Physics Letters B* **793,** 290–296 (2019).
102. Boos, J., Frolov, V. P. & Zelnikov, A. Probing the vacuum fluctuations in scalar ghost-free theories. *Physical Review D* **99,** 076014 (2019).
103. Kapner, D. *et al.* Tests of the gravitational inverse-square law below the dark-energy length scale. *Physical Review Letters* **98,** 021101 (2007).

104. Talaganis, S., Biswas, T. & Mazumdar, A. Towards understanding the ultraviolet behavior of quantum loops in infinite-derivative theories of gravity. *Classical and Quantum Gravity* **32,** 215017 (2015).

105. Einstein, A. *et al.* The foundation of the general theory of relativity. *Annalen der Physik* **49,** 769–822 (1916).

106. Penrose, R. "Golden Oldie": Gravitational Collapse: The Role of General Relativity. *General Relativity and Gravitation* **34,** 1141–1165 (2002).

107. Hawking, S. W. & Ellis, G. F. R. *The large scale structure of space-time* (Cambridge university press, 1973).

108. Wald, R. M. in *Black Holes, Gravitational Radiation and the Universe* 69–86 (Springer, 1999).

109. Arfken, G. B. & Weber, H. J. *Mathematical methods for physicists* 1999.

110. Buoninfante, L., Harmsen, G., Maheshwari, S. & Mazumdar, A. Nonsingular metric for an electrically charged point-source in ghost-free infinite derivative gravity. *Physical Review D* **98,** 084009 (2018).

111. Buoninfante, L., Koshelev, A. S., Lambiase, G., Marto, J. & Mazumdar, A. Conformally-flat, non-singular static metric in infinite derivative gravity. *Journal of Cosmology and Astroparticle Physics* **2018,** 014 (2018).

112. Buoninfante, L., Koshelev, A. S., Lambiase, G. & Mazumdar, A. Classical properties of non-local, ghost-and singularity-free gravity. *Journal of Cosmology and Astroparticle Physics* **2018,** 034 (2018).

113. Kerr, R. P. Gravitational field of a spinning mass as an example of algebraically special metrics. *Physical review letters* **11,** 237 (1963).

114. Visser, M. The Kerr spacetime: A brief introduction. *arXiv preprint arXiv:0706.0622* (2007).

115. Balasin, H. & Nachbagauer, H. Distributional energy–momentum tensor of the Kerr–Newman spacetime family. *Classical and Quantum Gravity* **11,** 1453 (1994).

116. Cornell, A. S., Harmsen, G., Lambiase, G. & Mazumdar, A. Rotating metric in nonsingular infinite derivative theories of gravity. *Physical Review D* **97,** 104006 (2018).

117. Buoninfante, L., Koshelev, A. S., Lambiase, G., Marto, J. & Mazumdar, A. Conformally-flat, non-singular static metric in infinite derivative gravity. *Journal of Cosmology and Astroparticle Physics* **2018,** 014 (2018).

118. Thirring, H. On the effect of rotating distant masses in Einstein's theory of gravitation, Phys. Z. 19 (1918) 33-39 [German translation: On the effect of rotating distant masses in Einstein's theory of gravitation]. *gene. Rel. Grav* **16,** 712–725 (1984).

119. Peskin, M. & Schroeder, D. An introduction to quantum field theory Westview Press. *Boulder, Colorado* (1995).

120. Buoninfante, L., Koshelev, A. S., Lambiase, G. & Mazumdar, A. Classical properties of non-local, ghost-and singularity-free gravity. *Journal of Cosmology and Astroparticle Physics* **2018,** 034 (2018).

Dutch summary

In dit proefschrift heb ik de toegestane quasi-normale modi (QNM's) van spin-3/2 velden in de buurt van de hogere dimensionale Reissner-Nordström en Schwarzschild zwarte-gaten in de hogere dimensionale (anti-) de Sitter ((A) dS) ruimte onderzocht. Verder onderzoek ik een theorie van de gemodificeerde zwaartekracht genaamd "infinite derivative gravity", waar deze theorie hoopt een aantal van de pathologieën op te lossen die in algemene relativiteit worden gezien.
Om te beginnen zal ik het gedeelte van mijn werk over QNM's samenvatten. Dit werk wordt behandeld in hoofdstukken 2, 3 en 4 van het proefschrift. Merk op dat QNM's een vorm van energiedissipatie zijn die weg van een verstoord object straalt in de vorm van een gedempte golf. Ze kunnen worden beschouwd als normale modi die in de loop van de tijd vervallen, zoals je zou zien met een gitaarsnaar die zijn amplitude in de loop van de tijd vermindert, nadat hij is getrapt. Ze kunnen worden beschreven door de volgende vergelijking

$$\Psi(r,t) = e^{-i\omega t}\phi(r)\,. \tag{B.9}$$

Hier is ω een complex getal waarbij het reële deel de frequentie van de QNM beschrijft en het denkbeeldige deel de hoeveelheid demping die de QNM ervaart. Verder beschrijft $\Psi(r,t)$ de golffunctie van ons spin-3/2 velden. Om te begrijpen hoe ze zich zullen gedragen terwijl ze zich vanuit het zwarte gat voortplanten, moeten we hun bewegingsvergelijkingen kennen. De bewegingsvergelijkingen worden gegeven door de Rarita-Schwinger-vergelijkingen geschreven als

$$\gamma^{\mu\nu\lambda}\nabla_\nu\Psi_\lambda = 0. \tag{B.10}$$

In de bovenstaande $\gamma^{\mu\nu\lambda}$ is de anti-symmetrische gamma-matrix, ∇_ν is een covariante afgeleide en Ψ_λ is onze golf-functie voor het veld spin-3/2. Met behulp van deze bewegingsvergelijkingen kunnen we het effectieve potentieel bepalen voor de spin-3/2-velden in de buurt van de zwarte gaten die we onderzoeken. Met behulp van de benaderingen Wentzel–Kramers–Brillouin en de methode "Improved Asymptotic Iterative Method" (AIM) zijn we in staat om de numerieke waarden voor ω te verkrijgen (B.9). In dit proefschrift beschouwen we hogere dimensionale Reissner-Nordström zwarte gaten, dat wil zeggen elektrisch geladen, niet-roterende zwarte gaten, die in dit proefschrift meer dan 4 ruimtetijddimensies kunnen hebben. Zodra we de numerieke waarden hebben van de QNM's vergelijken we ze met die verkregen voor het geval van de hogere dimensionale Schwarzschild (niet-roterende elektrisch neutrale) zwarte gaten. Hierdoor kunnen we begrijpen wat het effect van de elektrische lading op de uitgestoten QNM's heeft. Op basis van de resultaten kunnen we om te bepalen dat zwarte gaten met grotere elektrische ladingen meer energieke QNM's produceren, die ook meer gedempt zijn. Ten tweede beschouwen we zwarte gaten met een hogere dimensionale Schwarzschild die zich in AdS-ruimtetijden bevinden. Dit zijn ruimtetijden met een scalaire term die een constante kromming beschrijft op al zijn punten, wat onafhankelijk is van de hoeveelheid massa die zich op dat punt bevindt. In dit geval merken we op welk effect de (A)dS-kromming scalar heeft op de toegestane QNM's. We hebben geconstateerd dat de grotere De kromming van de ruimte hoe energieker de QNM's zijn, maar dat ze ook last hebben van hogere dempende voorwaarden.
In het tweede deel van het proefschrift onderzoeken we de metrics verkregen met behulp van de theorie van oneindige afgeleide zwaartekracht. Dit onderwerp wordt behandeld in de hoofdstukken 5, 6 en 7. De algemene relativiteitstheorie is een

uitstekende theorie voor het beschrijven van zwaartekrachtinteracties op lange afstand, zoals de banen van planeten, evenals het beschrijven van de kromming van ruimtetijd nabij een zwart gat. De theorie heeft echter een paar pathologieën voor interacties op zeer korte afstand. In dit geval kunnen de zwaartekrachten extreem groot worden vanwege een $1/r$ potentiaalfunctie. In extreme gevallen, zoals die bij de oerknal of in het midden van zwarte gaten, kunnen deze zwaartekrachten oneindig worden. De theorie van oneindige afgeleide zwaartekracht probeert deze pathologieën te verwijderen door de zwaartekrachttheorie aan te passen in de korte interactielimiet. Het doet dit door hogere-orde kromtetermen te introduceren, waarvan het cumulatieve effect is dat ze de zwaartekracht verminderen in de interacties op korte afstand. Als zodanig worden de metrieken die de ruimtetijd in de buurt van of in een zwart gat beschrijven gewijzigd om deze verzwakking van de kracht aan te tonen. In zowel het geval van het elektrisch geladen object als het roterende object hebben we metrieken verkregen die geen gebied bevatten dat tot in het oneindige neigt. Wat nog belangrijker is, deze gewijzigde beschrijvingen van ruimtetijd rond de objecten keren terug naar die voorspeld door algemene relativiteit in de grote r-limiet.

Biography

Gerhard Erwin Harmsen was born on the 21st of August 1992, in Randburg South Africa. He holds a Bachelors of science in Physics (2014) and a masters of science in physics (2016) from the university of the Witwatersrand, Johannesburg, South Africa. His masters thesis was titled "Quasinormal modes for spin-3/2 particles in N-dimensional Schwarzschild black hole space times". It was completed under the supervision of Prof. Alan S. Cornell. Following his masters he was awarded the opportunity to pursue a dual degree with the university of Groningen. He was supervised by Prof. Alan S. Cornell (University of the Witwatersrand) and Prof. Anupam Mazumdar (University of Groningen).